

**Organocatalytic anionic polymerization of  
*o*-phthaldialdehyde and *n*-butyraldehyde**

**by**

**Inge Weideman**

Thesis presented in partial fulfilment of the requirements for  
the degree of Master of Science (Polymer Science)

at

Stellenbosch University

Supervisor: Dr. Rueben Pfukwa

Co-Supervisor: Prof. Bert Klumperman

Department of Chemistry and Polymer Science

Faculty of Science

March 2017

## **Declaration**

By submitting this thesis electronically, I declare that the entirety of the work contained therein is my own, original work, that I am the sole author thereof (save to the extent explicitly otherwise stated), that reproduction and publication thereof by Stellenbosch University will not infringe any third party rights and that I have not previously in its entirety or in part submitted it for obtaining any qualification.

.....

Inge Weideman

.....

March 2017

Copyright ©2017 Stellenbosch University

All rights reserved

## **Abstract**

Self-immolative polymers (SIPs) can be defined as polymers that are capable of complete head-to-tail depolymerization upon cleavage of an end-cap from the polymer chain-end in response to a trigger/stimulus. The use of SIPs has emerged as an alternative strategy in designing smart materials that are capable of responding to selective signals and provide an amplified response since the depolymerization process converts the entire polymer into its monomeric units and other small molecule products that can play a role in the amplified response. The incorporation of these polymers also offers the opportunity to alter the properties of a material after it has been prepared since the depolymerization of the SIP can cause a change in the shape, internal structure and/or surface properties of the material.

Poly(phthaldialdehyde) (PPA), a well-known SIP, has been successfully prepared via non-organometallic catalyst based anionic polymerization in recent years. However, the methods that have been reported require expensive reagents and delicate experimental conditions. Hence, a new facile method for the non-organometallic anionic polymerization of PA was introduced and optimized in this work. The effect of a range of phosphazene and amine base catalysts were investigated. The results showed 1,8-diazabicyclo[5.4.0]undec-7-ene with a catalyst to initiator ratio of four to be the ideal catalytic system. It was further determined that the optimum experimental conditions for the DBU catalyzed system consisted of a 1.0 M monomer concentration, tetrahydrofuran as solvent and a reaction time of ten minutes. It was also shown that carboxylic acids can be used to initiate the polymerization reaction, which has thus far only been achieved using primary alcohols. The optimized method for the preparation of PPA was applied to the preparation of polystyrene-poly(phthaldialdehyde) block copolymers (BCPs). Hydroxyl end-functional polystyrene was prepared via activator regenerated by electron transfer atom transfer radical polymerization to serve as macroinitiator for the BCP reaction. Analysis of these BCPs, revealed that they had been prepared with narrow molecular weight distributions and a good agreement between the theoretical and experimentally obtained molecular weights.

A systematic study was carried out to optimize the preparation of poly(butylaldehyde) (PBA), a SIP that has to date only been prepared using organometallic catalysts, by non-organometallic catalyst based anionic polymerization. The results of the study showed the phosphazene base catalyst  $P_2$ -*t*-Bu with a catalyst to initiator ratio of 1 to 1 to be the ideal catalytic system for the preparation of PBA. Further investigation revealed a monomer concentration of 1.0 M, a

## *Abstract*

---

nonpolar solvent such as pentane and a reaction time of ten minutes to be the optimum experimental conditions for the phosphazene base catalytic system.

## **Opsomming**

Self-immolatië polimere (SIPe) word gedefinieer as polimere wat in staat is daartoe om van kop-tot-stert te depolimeriseer na die verwydering van die polimeerketting se eind-groep weens blootstelling aan 'n sneller/stimulus. Die gebruik van SIPe het na vore gekom as 'n alternatiewe strategie vir die ontwerp van slim materiale wat in staat is daartoe om te reageer op 'n spesifieke sein en ook 'n versterkte reaksie te bied, aangesien die depolimerisasie proses lei tot die afbreek van die polimeer na sy monomeriese eenhede en ander klein molekules wat 'n rol kan speel in die versterkte reaksie. Die insluiting van hierdie polimere bied ook die geleentheid om die eienskappe van die materiaal te verander nadat dit voorberei is, aangesien die depolimerisasie van die SIP die vorm, interne struktuur en/of oppervlak eienskappe van die materiaal kan teweeg bring.

Poli(phthalaldehyd) (PPA), 'n bekende SIP, is relatief onlangs voorberei deur nie-organometaal anioniese polimerisasie. Die metodes wat berig is hiervoor, vereis egter duur reagentse en delikate eksperimentele toestande. Dus word 'n eenvoudiger metode vir die nie-organometaal anioniese polimerisasie van PPA in hierdie bekendgestel en geoptimeer. Die effek van 'n verskeidenheid fosfor en amien bevattende katalisators was ondersoek. Die resultate het getoon dat 1,8-diazabicyclo[5.4.0]undec-7-ene (DBU) met 'n katalisator tot inisieerder verhouding van 4 tot 1 die ideale katalitiese sisteem is. Dit is verder bepaal dat die optimale eksperimentele toestande vir die DBU gekataliseerde stelsel bestaan uit 'n monomeer konsentrasie van 1.0 M, tetrahydrofuraan as oplosmiddel en 'n reaksie tyd van 10 minute. Die optimale metode vir die voorbereiding van PPA is toegepas vir die voorbereiding van polistireen-poli(phthalaldehyd) blokkopolimere (BKPe). Hidroksiel eind-funksionele polistireen is voorberei om te dien as makroinisieerder vir die ketting groei reaksie. Analise van die BKPe het gewys dat die hulle voorberei is met smal molekulêre gewig verspreiding en 'n goeie ooreenkoms tussen die geteikende en eksperimentele molêre massas.

'n Sistematiese studie is uitgevoer om die optimale toestande vir die nie-organometaal anioniese polimerisasie van butielaldehyd te bepaal. Poli(butielaldehyd) (PBA) is 'n SIP wat tot dusvêr slegs voorberei is met organometaal kataliste. Die resultate van die studie het aangedui dat die fosfor bevattende katalis  $P_2-t-Bu$  met 'n katalisator tot inisieerder verhouding van 1 tot 1 die ideale katalitiese sisteem is. Dit is verder bepaal dat 'n monomeer konsentrasie van 1.0 M, pentaan as oplosmiddel en 'n reaksie tyd van 10 minute lei tot die beste resultate vir die spesifieke sisteem.

## *Acknowledgements*

---

### **Acknowledgements**

I gratefully acknowledge my supervisor, Dr. Rueben Pfukwa. Thank you for your guidance, support and never-ending optimism. You have taught me so much more than just chemistry.

To Prof. Bert Klumperman for giving me a chance as an undergraduate student and for his continued support ever since. Your knowledge and insight never ceases to amaze me.

The National Research Foundation of South Africa is kindly acknowledged for funding.

Elsa Malherbe for NMR assistance and Dawie de Villiers for TGA assistance.

Dr. Helen Pfukwa and Zanelle Victor for their assistance with SEC analysis.

I gratefully acknowledge the members of the Free Radical Research Group and Polymer Science Department, past and present. I would like to especially thank Nathalie Bailly for her mentorship and introducing me to the world of Polymer Science. To Stefan and Andre, thank you for your friendship and all of the memorable moments that we have shared.

On a more personal note, I would like to thank my family. To my parents for raising me to believe that anything is possible if you work hard, trust in the Lord and never give up. Thank you for leading by example every day. Your belief in me has enabled me to achieve more than I would have ever dreamed possible. To Kirk, thank you for your love, support and encouragement. You were by my side when this journey began, through every challenge and every success. I would not have wanted to complete it with anyone else.

Finally, I want to thank God for His undeserving blessings, presence and guidance.

## **Table of Contents**

<b>Declaration.....</b>	<b>i</b>
<b>Abstract.....</b>	<b>ii</b>
<b>Opsomming.....</b>	<b>iv</b>
<b>Acknowledgements.....</b>	<b>v</b>
<b>Table of contents.....</b>	<b>iv</b>
<b>List of Figures.....</b>	<b>xi</b>
<b>List of Tables.....</b>	<b>xiv</b>
<b>List of Schemes.....</b>	<b>xvi</b>
<b>List of Symbols.....</b>	<b>xviii</b>
<b>List of Abbreviations.....</b>	<b>xix</b>
<b>Chapter 1.....</b>	<b>1</b>
<b>General information and objective.....</b>	<b>1</b>
<b>1.1 Introduction.....</b>	<b>1</b>
<b>1.2 Objective of this work.....</b>	<b>2</b>
<b>1.3 Layout of thesis.....</b>	<b>2</b>
1.3.1 Chapter 1. Introduction.....	2
1.3.2 Chapter 3. Historical and theoretical background.....	2
1.3.3 Chapter 3. The metal free organocatalyzed anionic polymerization of <i>o</i> -phthaldialdehyde.....	3
1.3.4 Chapter 4. Preparation of polystyrene- <i>b</i> -poly(phthaldialdehyde) copolymers.....	3
1.3.5 Chapter 5. The metal free organocatalyzed anionic polymerization of <i>n</i> -butyraldehyde.....	3
1.3.6 Chapter 6. Conclusions and future outlook.....	3
<b>References.....</b>	<b>4</b>
<b>Chapter 2.....</b>	<b>5</b>

***Index***

---

<b>2.1 The history and development of self-immolative systems.....</b>	<b>5</b>
<b>2.2 Current classes of self-immolative polymers.....</b>	<b>7</b>
<b>2.3 Methods of synthesis.....</b>	<b>12</b>
<b>2.4 Potential triggers.....</b>	<b>14</b>
<b>2.5 Potential applications.....</b>	<b>18</b>
<b>2.6 Polyaldehydes as SIPs.....</b>	<b>20</b>
<b>2.7 Polyaldehyde homopolymers.....</b>	<b>22</b>
<b>References.....</b>	<b>24</b>
<b>Chapter 3.....</b>	<b>29</b>
<b>3.1 Introduction.....</b>	<b>29</b>
<b>3.2 Experimental.....</b>	<b>31</b>
3.2.1 Materials.....	31
3.2.2 Methods.....	32
3.2.2.1 NMR.....	32
3.2.2.2 SEC.....	32
3.2.2.3 TGA.....	32
3.2.3 Polymer Synthesis.....	32
3.2.3.1 General polymerization procedure.....	32
3.2.3.1.1 Anionic polymerization: Phosphazene base catalysts.....	33
3.2.3.1.2 Anionic polymerization: Amine base catalysts.....	33
<b>3.3 Results and Discussion.....</b>	<b>34</b>
3.3.1 Systematic study of the influence of experimental parameters.....	34
3.3.1.1 Effect of the catalyst type.....	34
3.3.1.2 Monomer concentration.....	41
3.3.1.3 Reaction time.....	43
3.3.1.4 Solvent.....	43
3.3.1.5 Molecular weight.....	44



***Index***

3.3.2 UV-labile end-caps.....	45
3.3.3 Carboxylic acids as initiators for the anionic polymerization of PA.....	48
3.3.4 Investigation of polymer microstructure.....	49
3.3.5 Investigation of the self-immolative nature of PPA.....	51
3.3.6 Thermal analysis.....	53
<b>3.4 Conclusions.....</b>	<b>53</b>
<b>References.....</b>	<b>54</b>
<b>Chapter 4.....</b>	<b>57</b>
<b>4.1 Introduction.....</b>	<b>57</b>
<b>4.2 Experimental.....</b>	<b>59</b>
4.2.1 Materials.....	59
4.2.2 Methods.....	60
4.2.3 Preparation of the macroinitiator: Polystyrene.....	60
4.2.3.1 Preparation of polystyrene by ARGET ATRP.....	60
4.2.3.1.1 Synthesis of the ligand: tris [2-(dimethylamino) ethyl] amine (Me <sub>6</sub> TREN).....	60
4.2.3.1.2 General polymerization procedure.....	60
4.2.3.1.3 Debromination of ARGET ATRP-made polystyrene.....	61
4.2.3.2 Preparation of polystyrene by RAFT-mediated polymerization.....	61
4.2.3.2.1 Synthesis of 2-(((butylthio)carbonothioyl)thio)-2-methylpropanoic acid.....	61
4.2.3.2.2 General polymerization procedure.....	62
<b>4.3 Preparation of polystyrene-<i>b</i>-polyphthaldialdehyde.....</b>	<b>62</b>
4.3.1 General polymerization procedure.....	62
<b>4.4 Results and discussion.....</b>	<b>63</b>
4.4.1 Synthesis of polystyrene by ARGET ATRP.....	63
4.4.1.1 Control over molecular weight distribution and end- Group functionality.....	65
4.4.1.2 Debromination of ARGET ATRP.....	67

**Index**

4.4.2 Synthesis of polystyrene by RAFT-mediated polystyrene.....	68
4.4.2.1 Control over molecular weight distribution and end- group functionality.....	68
4.4.3 Synthesis of PS- <i>b</i> -PPA.....	69
4.4.3.1 Control over the mole ratios of each monomer.....	73
<b>4.5 Conclusions.....</b>	<b>75</b>
<b>References.....</b>	<b>76</b>
<b>Chapter 5.....</b>	<b>77</b>
<b>5.1 Introduction.....</b>	<b>77</b>
<b>5.2 Experimental.....</b>	<b>78</b>
5.2.1 Materials.....	78
5.2.2 Methods.....	78
5.2.3 Polymer Synthesis.....	78
5.2.3.1 General polymerization procedure.....	78
5.2.3.1.1 Anionic polymerization: Phosphazene base catalysts.....	78
5.2.3.1.2 Anionic polymerization: Amine base catalysts.....	78
<b>5.3 Results and discussion.....</b>	<b>79</b>
5.3.1 Systematic study of the influence of experimental parameter.....	79
5.3.1.1 Effect of the catalyst type.....	79
5.3.1.2 Monomer concentration .....	82
5.3.1.3 Reaction Time.....	83
5.3.1.4 Solvent.....	84
5.3.1.5 Molecular weight.....	85
5.3.2 Investigation of polymer microstructure.....	87
5.3.3 The self-immolative nature of PBA.....	90
5.3.4 Thermal Analysis.....	91
<b>5.4 Conclusions.....</b>	<b>92</b>

## ***Index***

---

<b>References.....</b>	<b>93</b>
<b>Chapter 6.....</b>	<b>94</b>
<b>Conclusions and outlook.....</b>	<b>94</b>

## List of Figures

Figure 2.1. Preparation of PPA that depolymerizes upon exposure to palladium.....	16
Figure 3.1. Phosphazene base catalysts $P_1$ - <i>t</i> -Bu, $P_2$ - <i>t</i> -Bu and $P_4$ - <i>t</i> -Bu.....	30
Figure 3.2. Amine base catalysts DBU and TBD.....	31
Figure 3.3. An overlay of the SEC traces of PPA prepared with $P_4$ - <i>t</i> -Bu with different catalyst:initiator.....	37
Figure 3.4. An overlay of the SEC traces of PPA prepared with $P_1$ - <i>t</i> -Bu with different catalyst:initiator.....	37
Figure 3.5. SEC traces for DBU catalyzed anionic polymerization of PA with different catalyst:initiator.....	40
Figure 3.6. $^1\text{H}$ NMR spectrum ( $\text{CDCl}_3$ ) of PPA prepared with DBU as catalyst, a with catalyst:initiator of 4:1, monomer concentration of 0.5 M, THF as solvent and reaction time of ten minutes.....	41
Figure 3.7. An overlay of the SEC traces for the $P_1$ - <i>t</i> -Bu catalyzed anionic polymerization of PA with different monomer concentrations.....	42
Figure 3.8. An overlay of the SEC traces for the DBU catalyzed anionic polymerization of PA with different monomer concentrations.....	42
Figure 3.9. An overlay of the SEC traces for PPA polymers prepared with different $M_n^{\text{Target}}$ .....	45
Figure 3.10. Graph showing the relationship between the $M_n^{\text{Theoretical}}$ and $M_n^{\text{SEC}}$ . The solid red line acts as a representation of an ideal system with a 100% conversion.....	45
Figure 3.11. An overlay of the UV-vis spectra for 4,5-dimethoxy-2-nitrobenzyl carbonochloridate (green), PPA prepared with 4,5-dimethoxy-2-nitrobenzyl carbonochloridate as quenching agent (red) and PPA prepared with acetic anhydride as quenching agent (blue).....	47
Figure 3.12. An overlay of the SEC trace comparing the UV (red) and the DRI (blue) signals of PPA prepared with 4,5-dimethoxy-2-nitrobenzyl carbonochloridate as quenching agent.....	47

**Index**

Figure 3.13. An overlay of the SEC traces for the anionic polymerization of PA with a carboxylic acid as initiator (entry 1, 3 and 5, Table 3.8).....	49
Figure 3.14. $^1\text{H}$ NMR spectrum ( $\text{CDCl}_3$ ) of PPA prepared with linoleic acid as initiator (entry 3, Table 3.8).....	49
Figure 3.15. $^1\text{H}$ NMR spectrum ( $\text{CDCl}_3$ ) of PPA prepared with DBU as catalyst, a with catalyst:initiator of 4:1, monomer concentration of 1.0 M, THF as solvent and reaction time of ten minutes.....	51
Figure 3.16. An overlay of the $^1\text{H}$ NMR spectra ( $\text{CDCl}_3$ ) of PPA, prepared under the optimum conditions determined in this work, taken over a two month period: (a) no degradation, (b) some degradation, (c) complete degradation.....	52
Figure 3.17. TGA thermogram of PPA prepared with DBU as catalyst, a with catalyst:initiator of 4:1, monomer concentration of 1.0 M, THF as solvent and reaction time of ten minutes.....	53
Figure 4.1. Schematic representation of a cylinder-forming block copolymer thin film and the corresponding nanoporous thin film obtained via selective etching of the minority domains.....	58
Figure 4.2. The $^1\text{H}$ NMR spectrum ( $\text{CDCl}_3$ ) of polystyrene (entry 2, Table 5.1) prepared via ARGET ATRP.....	66
Figure 4.3. An overlay of the $^1\text{H}$ NMR spectra ( $\text{CDCl}_3$ ) of polystyrene (entry 2 Table 4.1) (a) before and (b) after debromination.....	67
Figure 4.4. The $^1\text{H}$ NMR spectrum ( $\text{CDCl}_3$ ) of polystyrene prepared by RAFT-mediated polymerization.....	69
Figure 4.5. An overlay of the $^1\text{H}$ NMR spectra ( $\text{CDCl}_3$ ) of the (a) polystyrene macroinitiator (entry 2 Table 4.1) following debromination, (b) polyphthaldialdehyde homopolymer and (c) PS- <i>b</i> -PPA copolymer (entry 1, Table 4.3).....	72
Figure 4.6. An overlay of the SEC traces of the PS macroinitiator (entry 2, Table 4.1) and that of the PS- <i>b</i> -PPA copolymer (entry 1, Table 4.3).	74
Figure 4.7. An overlay of the SEC traces of the PS macroinitiator (entry 2, Table 4.1) and that of the PS- <i>b</i> -PPA copolymer (entry 3, Table 4.3).....	74

***Index***

Figure 4.8. An overlay of SEC traces of the PS macroinitiator (entry 2, Table 4.1) and that of the PS- <i>b</i> -PPA copolymer (entry 5, Table 4.3).....	75
Figure 5.1. An overlay of the SEC traces of PBA prepared with P <sub>4</sub> - <i>t</i> -Bu with different catalyst:initiator.....	81
Figure 5.2. An overlay of the SEC traces of PBA prepared with P <sub>2</sub> - <i>t</i> -Bu with different catalyst:initiator.....	81
Figure 5.3. <sup>1</sup> H NMR spectrum (CDCl <sub>3</sub> ) of PBA prepared with P <sub>2</sub> - <i>t</i> -Bu as catalyst, a with catalyst:initiator of 1:1, monomer concentration of 1.0 M, pentane as solvent and reaction time of ten minutes.....	82
Figure 5.4. An overlay of the SEC traces for the P <sub>2</sub> - <i>t</i> -Bu catalyzed anionic polymerization of BA with different monomer concentrations.....	83
Figure 5.5. An overlay of the SEC traces for the kinetic study of BA.....	84
Figure 5.6. An overlay of the SEC traces for PBA polymers prepared with different $M_n^{\text{Target}}$ .....	86
Figure 5.7. Graph showing the relationship between the theoretical molecular weight and that determined by SEC. The solid red line acts as a representation of an ideal system with a 100% conversion.....	87
Figure 5.8. Triad configurational sequences of a polymer backbone.....	87
Figure 5.9. <sup>13</sup> C NMR spectrum (CDCl <sub>3</sub> ) of entry 1 in Table 5.4. ....	89
Figure 5.10. <sup>1</sup> H NMR spectrum (CDCl <sub>3</sub> ) focusing on the chemical shift region 69-96 ppm of Figure 5.10.....	89
Figure 5.11. An overlay of the <sup>1</sup> H NMR spectra (CDCl <sub>3</sub> ) of PBA, prepared under the optimum conditions determined in this work, taken over a two month period: (a) no degradation, (b) some degradation, (c) complete degradation.....	91
Figure 5.12. TGA thermogram of PBA prepared with P <sub>2</sub> - <i>t</i> -Bu as catalyst, a with catalyst:initiator of 1:1, monomer concentration of 1.0 M, pentane as solvent and reaction time of ten minutes.....	92

## List of Tables

Table 2.1. Triggers that induce depolymerization of self-immolative polymers.....	15
Table 3.1. Results for the anionic polymerization of PA with P <sub>1</sub> - <i>t</i> -Bu, P <sub>2</sub> - <i>t</i> -Bu and P <sub>4</sub> - <i>t</i> -Bu phosphazene base catalysts with different catalyst:initiator.....	36
Table 3.2. Results for the TBD- and DBU catalyzed anionic polymerization of PA with different catalyst:initiator.....	39
Table 3.3. Results for the anionic polymerization of PA with different monomer concentrations.....	41
Table 3.4. Results for the kinetic study of both the P <sub>1</sub> - <i>t</i> -Bu and DBU catalyzed polymerization of PA.....	43
Table 3.5. Results for the anionic polymerization of PA in THF and DCM.....	44
Table 3.6. Summary of the results obtained for the preparation of PPA with different $M_n^{\text{Target}}$ .....	44
Table 3.7. Results for the anionic polymerization of PA with 4,5-dimethoxy-2-nitrobenzyl carbonochloridate as quenching agent.....	46
Table 3.8. Results for the DBU catalyzed anionic polymerization of PA from different initiating groups.....	48
Table 4.1. Results for the ARGET ATRP of styrene.....	65
Table 4.2. Results for the RAFT-mediated polymerization of PA with 2-(((butylthio)carbonothioyl)thio)-2-methylpropanoic acid as RAFT agent.....	69
Table 4.3. Results for the preparation of different PS- <i>b</i> -PPA copolymers.....	70
Table 5.1. Results for the anionic polymerization of BA with P <sub>2</sub> - <i>t</i> -Bu and P <sub>4</sub> - <i>t</i> -Bu phosphazene base catalysts with different catalyst:initiator.....	80
Table 5.2. Results for the P <sub>2</sub> - <i>t</i> -Bu catalyzed anionic polymerization of PA with different monomer concentrations.....	82
Table 5.3. Results for the kinetic study of the P <sub>2</sub> - <i>t</i> -Bu catalyzed anionic polymerization of BA.....	83

***Index***

---

Table 5.4. Results for the P <sub>2</sub> - <i>t</i> -Bu catalyzed anionic polymerization of BA in various solvents.....	85
Table 5.5. Partial molar heats of mixing for <i>iso</i> -butyraldehyde in various solvents.	85
Table 5.6. Summary of the results obtained for the preparation of PBA with different $M_n^{\text{Target}}$ .....	86



## **List of Schemes**

Scheme 2.1. Mechanism of self-immolation of (a) spacer molecules, (b) dendrimers and (c) polymers.....	6
Scheme 2.2. Mechanism for self-immolation via the formation of azquinone.....	8
Scheme 2.3. Mechanism for self-immolation via the formation of quinone.....	9
Scheme 2.4. Undesired cyclization of the activated 2-mercaptoethanol based monomer that prevents polymerization from occurring.....	9
Scheme 2.5. Mechanism of self-immolation via cyclization.....	10
Scheme 2.6. Undesired cyclization of the activated monomer.....	10
Scheme 2.7. Mechanism of self-immolation via a combination of cyclization and 1,6-elimination.....	11
Scheme 2.8. Mechanism of self-immolation of poly(aldehydes).....	12
Scheme 2.9. (a) The application of poly(benzyl carbamate) in sensory applications. (b) the application of comb polymers in sensory applications.....	19
Scheme 2.10. (a) The cationic and (b) anionic polymerization of aldehydes.....	21
Scheme 3.1. The anionic polymerization of aldehydes in the presence of the phosphazene base catalyst P <sub>4</sub> - <i>t</i> -Bu.....	30
Scheme 3.2. The anionic polymerization of <i>o</i> -phthaldialdehyde.....	34
Scheme 3.3. Preparation of PPA with 4,5-dimethoxy-2-nitrobenzyl carbonochloridate as quenching agent.....	46
Scheme 3.4. A mixture of the trans and cis stereoisomers of PPA, following the anionic polymerization of PA.....	50
Scheme 3.5. The depolymerization of PPA into its monomeric units.....	52
Scheme 4.1. Synthesis route for the preparation of PS- <i>b</i> -PPA, reported by Vogt and coworkers.....	59
Scheme 4.2. The ARGET ATRP mechanism.....	63
Scheme 4.3. The ARGET ATRP of styrene.....	64
Scheme 4.4. The debromination of PS prepared via ARGET ATRP.....	67

***Index***

---

Scheme 4.5. Insertion of the monomeric units into the C-S bond of the trithiocarbonate RAFT agent, 2-(((butylthio)carbonothioyl)thio)-2-methylpropanoic acid. ....	68
Scheme 4.6. Insertion of the monomeric units into the C-S bond of the trithiocarbonate RAFT agent, 2-(((butylthio)carbonothioyl)thio)-2-methylpropanoic acid.....	71
Scheme 5.1. The anionic polymerization of <i>n</i> -butyraldehyde.....	79
Scheme 5.2. Depolymerization of PBA into its monomeric units.....	90

**List of Symbols**

$f$	Chain-end functionality
$\varepsilon$	Dielectric constant
$T_c$	Ceiling temperature (°C)
$S$	Entropy (kJ/K.mol)
$H$	Enthalpy (kJ/mol)
$G$	Gibbs free energy (kJ/mol)
$pK_a$	Logarithmic acid dissociation constant
$m$	Meso
$Mr_{initiator}$	Molecular weight of initiator (g/mol)
$Mr_{monomer}$	Molecular weight of monomer (g/mol)
$M_n^{NMR}$	Number average molecular weight by NMR (g/mol)
$M_n^{SEC}$	Number average molecular weight by SEC (g/mol)
$M_n^{Target}$	Targeted number average molecular weight (g/mol)
$M_n^{Theoretical}$	Theoretical number average molecular weight (g/mol)
$H_m^{mix}$	molar heat of mixing (kJ/mol)
$\bar{D}$	dispersity
$k_p$	Propagation rate constant
$r$	racemic
$T$	Temperature (°C)

## **List of Abbreviations**

ARGET ARTP	Activators regenerated by electron transfer atom transfer radical polymerization
BCP	Block copolymer
Cat	Catalyst
DBU	1, 8-diazabicyclo [5.4.0] undec-7-ene
DMAP	4-Dimethylaminopyridine
DCM	Dichloromethane
DEE	Diethyl ether
EO	Ethylene oxide
HEBIB	2-hydroxyethyl 2- bromoisobutyrate
IR	Infrared
Init	Initiator
BA	<i>n</i> -butyraldehyde
NIR	Near-infrared spectroscopy
NMR	Nuclear magnetic resonance
PA	<i>o</i> -phthaldialdehyde
PBA	Poly(butyraldehyde)
PEO	Poly(ethylene oxide)
PEG <sub>x</sub>	Poly(ethylglyoxylate)
PMG <sub>x</sub>	Poly(glyoxylate)
PPA	Poly(phthaldialdehyde)
PS	Polystyrene
SI	Self-immolative
SID	Self-immolative dedrimer
SIP	Self-immolative polymer

***Index***

---

SEC	Size exclusion chromatography
P <sub>4</sub> - <i>t</i> -Bu	3- <i>t</i> -butylimino-1,1,1,5,5,5-hexakis(dimethylamino)-3-[tris(dimethylamino)phosphoranylidene]amino}-1 $\Lambda$ 5,3 $\Lambda$ 5,5 $\Lambda$ 5-1,4-triphosphazadiene
P <sub>1</sub> - <i>t</i> -Bu	<i>tert</i> -butylimino-tris(dimethylamino)phosphorane,
P <sub>2</sub> - <i>t</i> -Bu	1- <i>tert</i> -butyl-2,2,4,4,4-pentakis(dimethylamino)-2 $\Lambda$ 5,4 $\Lambda$ 5-catenadi(phosphazene)
TGA	Thermogravimetric analysis
TBD	1, 5, 7-triazabicyclo [4.4.0] dec-5-ene
Me <sub>6</sub> TREN	tris [2-(dimethylamino) ethyl] amine
UV-vis	Ultraviolet visible

# **Chapter 1**

## **General information and objective**

### **1.1 Introduction**

Self-immolative polymers (SIPs) are an interesting class of stimuli-responsive materials, which completely disassemble into their monomeric units when exposed to a stimulus which cleaves the polymer end-cap.<sup>1</sup> The use of self-immolative polymers has emerged as a new strategy for designing smart materials that have dual capabilities of responding to a stimulus and providing an amplified response.<sup>2, 3</sup> Incorporating a SIP in a material offers the opportunity of altering the properties of the material after it has been prepared, as depolymerization of the self-immolative component can change its shape, internal structure and surface properties.<sup>4</sup>

From this group of fascinating polymers, those that depolymerize via acetal chemistry, specifically polyaldehydes, have attracted much attention in recent years. Polyaldehydes distinguish themselves from other SIPs in that their ceiling temperatures ( $T_c$ ), the temperature above which a polymer is thermodynamically unstable, are close to and even below room temperature. As a result, polyaldehydes have been characterized by having poor thermal stability and the ability to depolymerize in a fast, quantitative and controllable manner at room temperature. First thought to be an inherent disadvantage, modern polymer technologies have begun to exploit this behaviour for selective and amplified decomposition in a broad range of applications.<sup>5</sup> Polyaldehydes have already been shown to be useful in applications such as photolithography and nanopatterning.<sup>5</sup> The incorporation of polyaldehydes in BCPs to create even more versatile materials with additional functionality has opened up a broader range for further opportunities.

Organometallic catalyst based anionic polymerization has been the traditional method for the preparation of polyaldehydes following the introduction of the method by Vogl in the 1960s.<sup>11</sup> The metal based process has however been associated with many synthetic difficulties. These difficulties include the need for delicate experimental conditions, long reaction times and limited solubility of the monomer in most common solvents.<sup>6</sup> To overcome these issues, the non-organometallic catalyst-based polymerization of *o*-phthaldialdehyde (PA) using phosphazene base catalysts were attempted.<sup>6</sup> The results from these polymerization reactions showed that the application of these non-organometallic catalysts allowed for a diminished

## Chapter 1

---

reaction time and the preparation of well-defined poly(phthaldialdehyde) (PPA) with tailored molecular weights. However, the use of phosphazene base catalysts has not eliminated the issue of delicate experimental conditions as the air and moisture sensitivity of these catalysts requires for it to be handled in a glovebox. In addition, these catalysts are very expensive. The challenge still remains therefore to simplify the method for the non-organometallic catalyst based polymerization of aldehydes.

### 1.2 Objective of this work

The primary objective of this work is to carry out a systematic study to investigate the effect of several experimental parameters on the metal free organo-catalyzed anionic polymerization of aldehydes, exemplified by *o*-phthaldialdehyde (PA) and *n*-butyraldehyde (BA). PPA is by far the most intensively studied self-immolative polyaldehyde with various applications.<sup>7</sup> Polybutyraldehyde (PBA), on the other hand, is a relatively unknown polymer with few having investigated its potential methods of synthesis and applications. The incorporation of PPA into BCPs has started to attract attention in recent years.<sup>6, 8-10</sup> However, the methods by which these BCPs are prepared have been restricted to alkyne-azide coupling reactions or chain extension with the aldehyde monomer from hydroxyl chain-end functional macroinitiators, under delicate experimental conditions.<sup>6, 8</sup> In this work, a simpler method for the preparation of polystyrene-*b*-poly(phthaldialdehyde) copolymers is introduced. It is also shown that chain extension with the aldehyde monomer can occur from a number of different initiating groups. All polymers prepared here, is subsequently characterized by SEC, NMR spectroscopy and TGA. The details of this work is briefly outlined below.

### 1.3 Layout of thesis

#### 1.3.1 Chapter 1. Introduction

This chapter gives a brief insight into self-immolative polymers, what they entail and how they can be applied. It also provides a short outline of the details of this work.

#### 1.3.2 Chapter 2. Historical and theoretical background

Chapter 2 contains an overview of self-immolative polymers. The history thereof, the chemistry involved in their synthesis and degradation, what advantages they hold as well as current and potential future applications are discussed. The well-known self-immolative

## Chapter 1

---

polymer PPA is discussed in more detail. Short comings in current literature reports that focus on the preparation of SIPs and how they may be overcome is also mentioned.

### **1.3.3 Chapter 3. The metal free organocatalyzed anionic polymerization of *o*-phthaldialdehyde**

The optimization for the preparation of PPA by non-organometallic catalyst based anionic polymerization is described. The effect of several experimental parameters including the type of the catalyst, catalyst to initiator ratio, monomer concentration, reaction time and the nature of the solvent, on the polymerization of PA, is investigated. Initiation of the polymerization reaction from a range of different initiating groups, other than the traditionally used primary alcohol, is shown. The microstructure of PPA, prepared under the optimized conditions determined in this work, is also assessed. The subsequently synthesized polymers are characterized by SEC, NMR spectroscopy and TGA.

### **1.3.4 Chapter 4. Preparation of polystyrene-*b*-poly(phthaldialdehyde) copolymers**

The synthetic procedures for the preparation of various polystyrene (PS) macroinitiators by both ARGET ATRP and RAFT is described. The preparation of PS-*b*-PPA copolymers via chain extension of the various macroinitiators is also described here. The subsequently synthesized macroinitiators and BCPs are characterized by SEC and NMR spectroscopy.

### **1.3.5 Chapter 5. The metal free organocatalyzed anionic polymerization of *n*-butyraldehyde**

The non-organometallic catalyst based anionic polymerization of *n*-butyraldehyde is described here. The effect of the catalyst type, catalyst to initiator ratio, monomer concentration, reaction time and the nature of the solvent on the polymerization of BA is investigated. The subsequently synthesized polymers are characterized by SEC, NMR spectroscopy and TGA.

### **1.3.6 Chapter 6. Conclusions and future outlook**

This chapter briefly describes the achievements in this work. It also gives recommendations for future work.



## Chapter 1

---

### References

- (1) Dilauro, A. M.; Zhang, H.; Baker, M. S.; Wong, F.; Sen, A.; Phillips, S. T. *Macromolecules* **2013**, 46, 7257–7265.
- (2) Phillips, S. T.; Dilauro, A. M. *ACS Macro Lett.* **2014**, 3, 298–304.
- (3) Chen, E. K. Y.; McBride, R. A.; Gillies, E. R. *Macromolecules* **2012**, 45, 7364–7374.
- (4) Seo, W.; Phillips, S. T. *J. Am. Chem. Soc.* **2010**, 132, 9234–9235.
- (5) Köstler, S.; Zechner, B.; Trathnigg, B.; Fasl, H.; Kern, W.; Ribitsch, V. *J. Polym. Sci. A Polym. Chem.* **2009**, 47, 1499–1509.
- (6) De Winter, J.; Dove, A. P.; Knoll, A.; Gerbaux, P.; Dubois, P.; Coulembier, O. *Polym. Chem.* **2014**, 5, 706–711.
- (7) Vogt, A. P.; De Winter, J.; Krolla-Sidenstein, P.; Geckle, U.; Coulembier, O.; Barner-Kowollik, C. *J. Mater. Chem. B* **2014**, 2, 3578–3791.
- (8) Pessoni, L.; De Winter, J.; Surin, M.; Hergué, N.; Delbosc, N.; Lazzaroni, R.; Dubois, P.; Gerbaux, P.; Coulembier, O. *Macromolecules* **2016**, 49, 3001–3008.
- (9) Kaitz, J. A.; Diesendruck, C. E.; Moore, J. S. *Macromolecules* **2013**, 46, 8121–8128.
- (10) Kaitz, J. A.; Moore, J. S. *Macromolecules* **2014**, 47, 5509–5513.
- (11) Vogl, O. *J. Polym. Sci. A Polym. Chem.* 1964, 2, 4607–4620.

## **Chapter 2**

### **2.1 The history and development of self-immolative systems:**

The field of polymer science have evolved such that synthetic polymers are now approaching the same level of complexity and sophistication as their natural counterparts both in architecture and function.<sup>1-4</sup> The techniques used to generate these polymers from artificial building blocks have become highly sophisticated and has resulted in a wide range of polymeric materials with seemingly unlimited potential.<sup>5-7</sup> However, with the emphasis mostly on the hierarchical self-assembly of these materials, much less attention has been given to their controlled degradation. This is surprising when one considers that natural polymers are assembled and disassembled with remarkable ease. There are still progress to be made, therefore, in designing synthetic polymers that are assembled and degraded in an equally facile manner.

A promising proposition involves an approach that makes use of a unique group of polymers, commonly referred to as self-immolative polymers (SIPs).<sup>8</sup> SIPs can be programmed, through their method of synthesis, depolymerize in a head-to-tail fashion when exposed to an environmental trigger.<sup>8, 9, 10</sup> SIPs are ideally thermodynamically stable until the functional group, commonly referred to as an end-cap, is cleaved. Upon removal of the end-cap, depolymerization occurs continuously and completely to generate the monomeric units and additional small molecule products. The application of SIPs offers the opportunity to alter the structure, surface properties or stability of a material after it has been prepared. Adding even more value to this group of polymers, is the idea that they can be designed in such a way that the products of depolymerization process can serve a secondary function.<sup>11, 12, 14</sup> One such an example is the preparation of programmable core-shell microcapsules with polymeric shell walls composed of SIP networks.<sup>38</sup> Upon exposure to an environmental trigger, the shell degrades and the core contents is released.<sup>38</sup> These microcapsules are of interest in drug delivery, fragrance release and self-healing materials.<sup>38</sup>

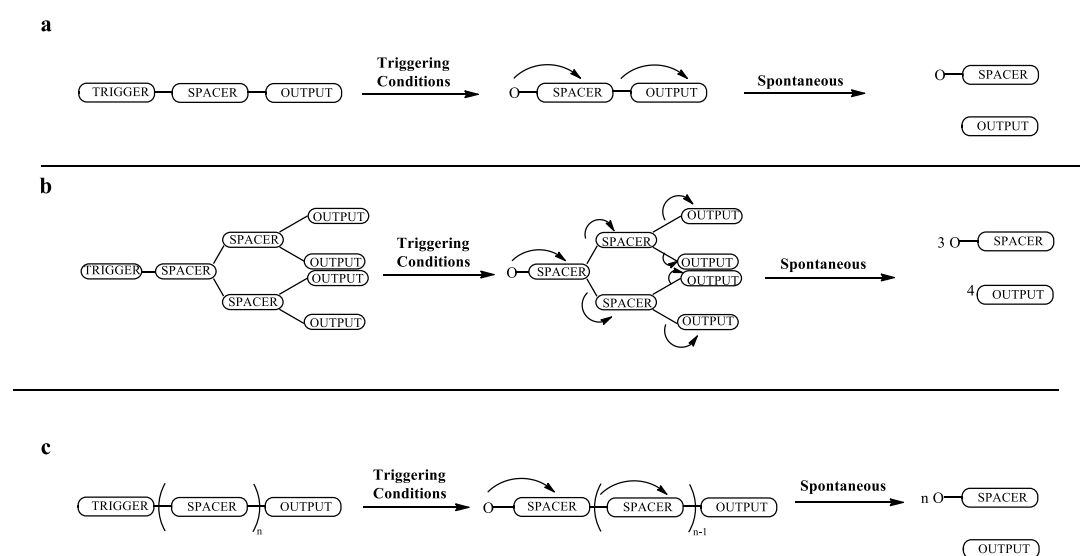
The inspiration for self-immolative polymers can be traced back to their small predecessors. In 1981, Katzenel-Lenbogen developed a SI spacer, applied in prodrug chemistry.<sup>79, 9</sup> The spacer is flanked by a triggering moiety and an output molecule.<sup>79, 9</sup> Upon the introduction of a stimulus, a reactive functional group is revealed. This is then followed by a series of intramolecular reactions to release a drug (output molecule) in its active form (Scheme 2.1a).<sup>8</sup>

## Chapter 2

<sup>79, 9</sup> This idea was then expanded into the development of SI materials where, in addition to the end-cap, these materials comprised of multiple SI spacer units that were covalently linked in an iterative manner.<sup>8, 9</sup> Here, the introduction of a stimulus cleaves the end-cap so that the spacer units may undergo a series of intramolecular reactions resulting in the complete degradation of the material (Scheme 2.1b).<sup>8</sup> The first SI macromolecules were prepared in 2003 by three separate groups and were referred to as self-immolative dendrimers (SIDs).<sup>13-15</sup>

SIDs were believed to be promising systems for the simultaneous release of multiple drug molecules.<sup>8</sup> However, the preparation of these dendrimers were found to be time consuming and the number of output molecules that could be incorporated on the dendrimer were limited as a result of steric hindrance.<sup>11</sup>

SIPs were developed in an attempt to overcome these shortcomings.<sup>11</sup> In contrast to SID, these polymers could be prepared by a simple one-pot synthesis method and contain any number of output molecules.<sup>9</sup> These unique polymers have since been developed to include a number of designs and architectures.<sup>16</sup> SIPs undergo head-to-tail depolymerization upon the removal of the stimulus-responsive end-cap (Scheme 2.1c).<sup>8, 9, 10</sup> This particular mechanism of degradation holds a number of advantages: (i) it allows for the amplification of a stimulus, in that only one triggering event is required to achieve complete degradation; (ii) the stimulus with which to trigger degradation can be adjusted to better suit the application simply by changing the identity of the triggering moiety; (iii) the degradation kinetics can be controlled by adjusting the chemical composition and length of the polymer backbone.<sup>16</sup>



**Scheme 2.1. Mechanism of self-immolation of (a) spacer molecules, (b) dendrimers and (c) polymers.<sup>9</sup>**

## Chapter 2

---

The first example of a linear polymer capable of complete head-to-tail depolymerization upon exposure to a stimulus was reported in 2008.<sup>12, 16</sup> Since then four additional classes of SIP have been established.<sup>17</sup>

### 2.2 Current classes of self-immolative polymers:

The key requirements for a polymer to be recognised as SI is that it must be capable of depolymerizing completely, predictably and continuously in response to a stimulus.<sup>8</sup> Other attractive attributes include fast rates of depolymerization but also chemical and thermal stability in the absence of a stimulus. There are still a number design challenges that require further investigation in order to overcome them. These include: the incompatibility of SIPs with other materials, limited number of repeating units that SIPs can be extended to, insolubility in most common solvents and issues related to the properties of the products of depolymerization.<sup>17, 18</sup>

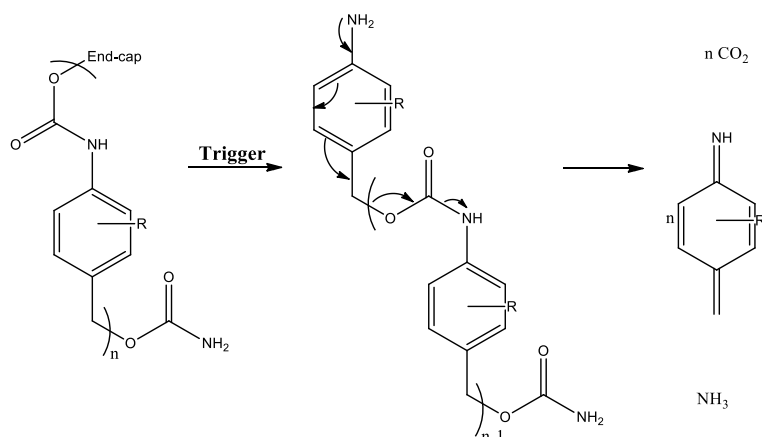
There are currently five classes of SIPs. Those that depolymerize via: (i) the formation of azaquinone or (ii) quinonemethide, (iii) cyclization reactions, (iv) a combination of (i), (ii) and (iii) and finally, (v) acetal chemistry.<sup>17</sup> The SIPs belonging to each of these four classes differ substantially in their rate of depolymerization as well as their thermal and chemical stability. They are also vastly different in the ease with which they can be synthesized and manipulated to fabricate a responsive material. SIPs all share the common trait of being inherently unstable, even though their thermal and chemical stability can be improved by end-capping to allow for their processing and application.<sup>17</sup> Removal of the end-cap reveals a functional group, unique to each class of SIP, that initiates the depolymerization process.<sup>17</sup> Brief descriptions of the polymers belonging to each of these classes are given below.

#### (i) Depolymerization via formation of azaquinone: poly(benzyl carbamate)

Poly(benzyl carbamate) were the first linear SIPs to be reported in literature.<sup>12</sup> The Shabat group reported the use of a polycarbamate, based on 4-aminophenyl alcohol derivatives, that depolymerized solely via 1,6-elimination reactions in response to an enzyme catalyzed end-cap cleavage.<sup>19</sup> However, further investigation into this class of SIPs have revealed that they typically contain less than twenty repeat units and suffer from slow rates of depolymerization in polar solvents or any environment with a dielectric constant lower than that of water.<sup>17</sup>

## Chapter 2

After the end-cap is cleaved, depolymerization follows via the repetitive and sequential decarboxylation and 1,6-azaquinone methide elimination reactions as shown in Scheme 2.2 below.<sup>12, 19</sup> This proposed mechanism of depolymerization, suggests that the release of each repeat unit proceeds through a less aromatic transition state (i.e. azaquinone methide) than the aromatic repeat unit.<sup>17</sup> This path presumably results in a large thermodynamic penalty for depolymerization, resulting in a slow rate of azaquinone-mediated depolymerization.<sup>17</sup>

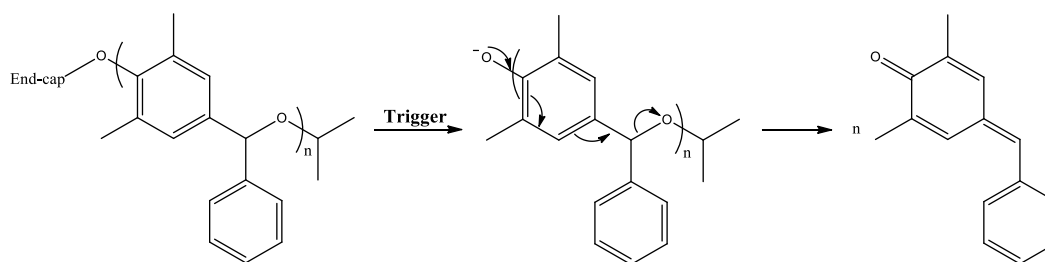


**Scheme 2.2. Mechanism for self-immolation via the formation of azaquinone.<sup>17</sup>**

### (ii) Depolymerization via formation of azaquinone: poly(benzyl ether)

In response to the need for better performing SIPs, Olah *et al.* attempted to design a new class of SIP that would be chemically and thermally robust, could be manipulated easily and could be stored for prolonged periods of time.<sup>18</sup> Their design incorporated an ether linkage between repeating units rather than more sensitive carbonates, thiocarbonates or carbamates.<sup>18</sup> In doing so they managed to design a SIP that was both chemically and thermally stable, easily handled and manipulated, that could be polymerized up to long linear polymers and was capable of rapid depolymerization.<sup>18</sup> Poly(benzyl ether) was found to depolymerize within minutes after cleaving the end-cap upon treatment of the polymer with a base.<sup>18</sup> As with poly(benzyl carbamate), depolymerization occurs via a cascade of 1,6-elimination reactions (Scheme 2.3). However, in this case the transition state is that of a quinone methide and not an azaquinonemethide.<sup>18</sup>

## Chapter 2

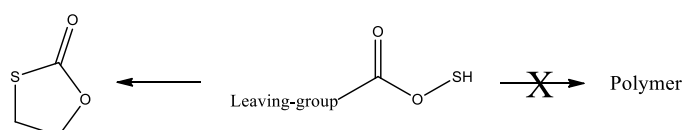


**Scheme 2.3. Mechanism for self-immolation via the formation of quinone.<sup>18</sup>**

### (iii) Depolymerization via cyclization reactions:

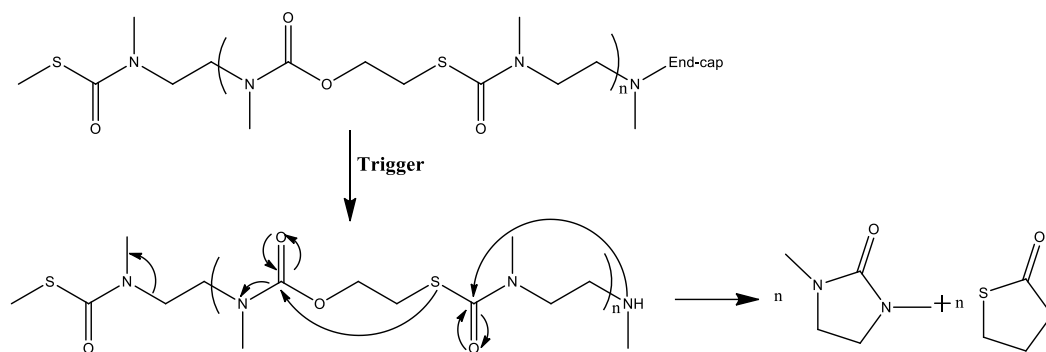
Following reports suggesting that the quinone methide intermediates involved in the 1, 6-elimination reactions might in fact be toxic, the DeWit group set out to develop a SIP with a backbone that did not contain any hydrobenzyl or aminobenzyl alcohols.<sup>19, 20</sup> This venture led to the first example of a SIP that degraded entirely via cyclization reactions.<sup>19</sup>

The development of polymers capable of degrading via cyclization mechanisms required careful design. Of particular concern, was preventing the cyclization of the active monomer (Scheme 2.4).<sup>19</sup> Previous work by the DeWit group had shown the use of activated dimers, particularly that of heterodimers, to be an effective strategy to overcome this issue. The approach calls for the activated leaving group to be distant from the nucleophilic moiety, such that the resultant ring size renders cyclization less favourable.<sup>21</sup> Following this approach, a SIP based on 2-mercaptoethanol and *N,N'*-dimethylethylenediamine with alternating carbamate and thiocarbamate linkages was presented (Scheme 2.5).<sup>19</sup> Upon removal of its end-cap, the polymer undergoes a cascade of alternating cyclization reactions, resulting in the release of *N,N'*-dimethylimidazolidinone and 1,3-oxathiolan-2-one.<sup>19</sup> Overall, this class of polymer offers relatively good control over the degradation process as the polymer backbone is very stable under physiological conditions.<sup>19</sup> It also avoids the production of the potentially toxic quinone methide species.<sup>19</sup> The rate of degradation however, was found to be very poor due to the slow cyclization kinetics of the *N,N'*-dimethylethylenediamine based monomer, and took several days to run to completion.<sup>8, 19</sup>



**Scheme 2.4. Undesired cyclization of the activated 2-mercaptoethanol based monomer that prevents polymerization from occurring.<sup>19</sup>**

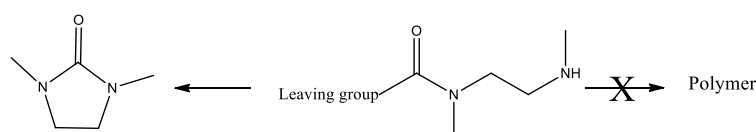
## Chapter 2

Scheme 2.5. Mechanism of self-immolation via cyclization.<sup>19</sup>

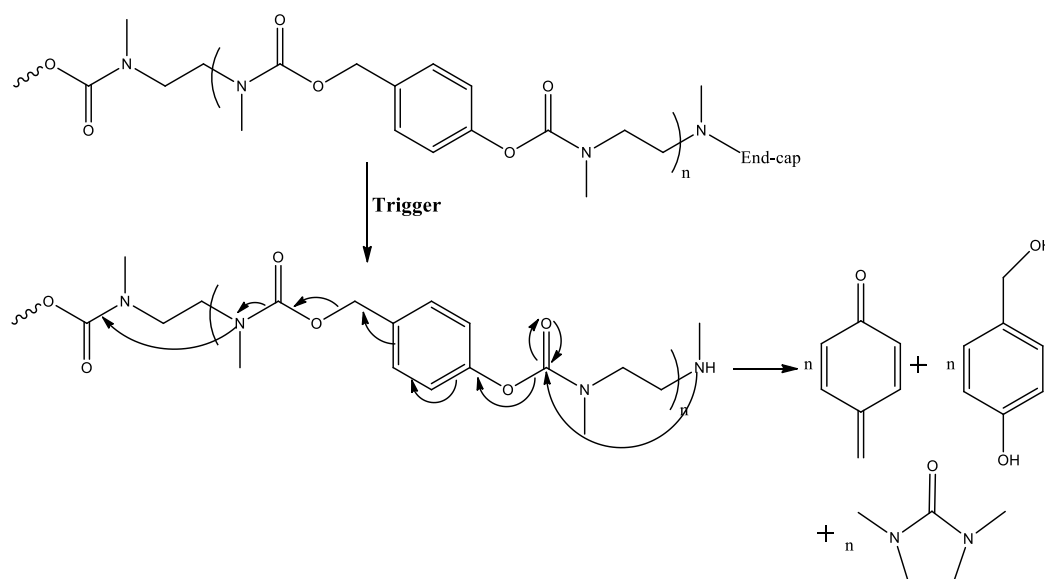
## (iv) Depolymerization via a combination of cyclization and 1,6-elimination reactions:

The first example of an SIPs that degrades by alternating 1,6-elimination and cyclization reactions was reported in 2009.<sup>21</sup> The idea was inspired by the promising results reported by the Haba group, after they incorporated alternating 1,6-elimination and cyclization spacers into a dendritic system.<sup>21, 22</sup> *N,N'*-dimethylethylenediamine has been incorporated into a number of previously reported cascade degradable polymers, where protecting groups can be carefully manipulated during the step-wise synthesis of the dendrimer.<sup>21</sup> However, as previously mentioned, linear polymers based on this monomer presents a challenge, as the activation of the monomer can result in intramolecular rather than intermolecular polymerization to occur (Scheme 2.6).<sup>19, 20, 21</sup>

To overcome this issue, DeWit and co-workers proposed that *N,N'*-dimethylethylenediamine units should be alternated with 4-hydroxybenzyl alcohol units, linked by carbamates as shown in Scheme 2.7.<sup>21</sup> By doing so, the activated site for the polymerization would be moved distal to the diamine, thereby slowing down intramolecular cyclization and effectively allowing the polymerization of the activated heterodimer. Upon removal of the end-cap, cyclization of the diamine would occur, releasing the *N,N'*-dimethylimidazolidinone and exposing the phenol. The phenol would then undergo 1,6-elimination reactions to release 4-hydroxybenzyl alcohol and carbon dioxide and to reveal another amine terminus, from which these cascade reactions could continue until depolymerization was complete.<sup>21</sup>

Scheme 2.6. Undesired cyclization of the activated monomer.<sup>21</sup>

## Chapter 2



**Scheme 2.7. Mechanism of self-immolation via a combination of cyclization and 1,6-elimination.<sup>21</sup>**

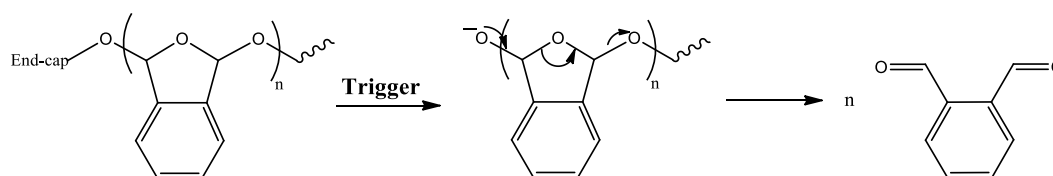
### (v) Depolymerization via acetal chemistry: aldehydes

When end-capped, polyaldehydes such as PPA is stable at room temperature and even at elevated temperatures.<sup>24, 27</sup> However, upon removal of the end-cap, a highly unstable hemiacetal is revealed.<sup>27</sup> The subsequent reversion of the free aldehyde eliminates the next hemiacetal, thereby propagating a cascade of reactions that ultimately leads to complete depolymerization (Scheme 2.8).<sup>27</sup> In solution, depolymerization of PPA occurs within seconds, and in the solid state it takes only a few minutes.<sup>27</sup> This is an astonishingly fast rate of depolymerization when compared to the other classes of SIPs and has opened up a wide range of potential applications for PPA.<sup>24, 26</sup>

Whilst rapid rates of depolymerization are considered to be an advantage, the application of PPA is hindered by a number of synthetic issues.<sup>24</sup> These issues include long reaction times, limited solubility of the monomer in most common solvents and delicate experimental conditions.<sup>24-26</sup> Whilst the issue of long reaction times have been overcome by using non-organometallic catalysts such as phosphazene base catalysts instead of organometallic catalysts, a method that does not call for delicate experimental conditions is yet to be developed.



## Chapter 2



**Scheme 2.8. Mechanism of self-immolation for poly(*o*-phthaldialdehydes).**

## 2.3 Methods of synthesis

Extensive research has been devoted to the development of SIPs in order to open the door to a wider range of potential applications. However, as was the case with the preparation of dendritic analogues, designing a SIP that can be prepared by simple, fast, reproducible and environmentally-friendly methods remains an issue.<sup>73</sup>

### 2.3.1 Poly(benzyl carbamate):

Prior to the development of SIPs, oligomers comprising of linearly arranged SI units were prepared by stepwise synthesis.<sup>9</sup> Over time these methods have been improved upon and adapted for the polymerization of SIPs. Poly(benzyl carbamate) is one such an example as its development was inspired by work done on the preparation of oligomeric polyurethanes.<sup>19</sup> These oligomers were originally prepared by an iterative deprotection-extend type of strategy. The method required the activation of a benzyl alcohol chain-end via the incorporation of a nitrophenyl carbonate and the subsequent coupling with aminobenzyl alcohol in order to extend the chain by one repeat unit.<sup>19, 9</sup>

This method however, required long reaction times and the chromatographic separation of each of the step-wise products. In an attempt to overcome these drawbacks, the Shabat group developed a more direct one-pot synthesis dibutyltindilaurate-catalyzed method.<sup>9</sup> The same method has since been used for the polymerization of masked isocyanates with positive results.<sup>9</sup>

### 2.3.2 Poly(benzyl ether):

Depolymerizable poly(benzyl ether) are generally prepared by the anionic polymerization of a stabilized quinone methide monomer such as 2,6-dimethyl-7-phenyl-1,4-benzoquinone methide.<sup>18</sup> Stabilization of the repeating unit by the incorporation of a pendant phenyl group for example, is important as the quinone methide functionality is enthalpically less favourable than the benzene based repeat unit.<sup>18</sup> Extended conjugation of the pendant phenyl group in the

## Chapter 2

---

monomer helps to balance this difference in stability. In addition, the design of the polymer generally includes dimethyl substituents to provide an enthalpic driving force for depolymerization.<sup>18</sup>

### 2.3.3 Cyclization elimination SIPs:

Gillies *et al.* achieved the condensation polymerization of carbamate and thiocarbamate based SIPs that are capable of depolymerizing via only cyclization and via a combination of cyclization and 1,6-elimination reactions respectively. For the synthesis of these SIPs, monomers that feature an electrophilic *p*-nitrophenyl carbonate end-group and a Boc-protected amine at opposite ends are utilized.

To prevent coupling during and after deprotection, the amine group is maintained as an ammonium salt. Polymerization occurs upon the addition of DMAP and trimethylamine.<sup>19, 21</sup>

### 2.3.4 Polyaldehydes:

Thus far, PPA has been the most intensively studied self-immolative polyaldehyde. PPA is typically prepared by the anionic polymerization of 1,2-benzenedicarboxyaldehyde.<sup>24, 27, 73</sup> Once capped, PPA is stable up to 150 °C.<sup>24, 64</sup> However, before quenching the polymerization reaction, the polymer chain-end is terminated by an unstable hemiacetal.<sup>24, 27, 64</sup> PPA terminated with this acetal group has a  $T_c$  of -40 °C.<sup>24, 27, 64</sup> As a result of the poor thermal stability of the uncapped polymer, the polymerization reaction of PA must be carried out at sub-zero temperatures. Recent years have shown the replacement of the traditionally used organometallic catalysts for the anionic polymerization of PA with non-organometallic catalysts such as phosphazene base catalysts. The application of these metal free catalysts have been shown to eliminate the need for long reaction times that was associated with the use of metal catalysts.<sup>24, 73</sup> However, the use of phosphazene base catalysts has not eliminated the need for delicate experimental conditions as their air and moisture sensitivity calls for the use of a glovebox.<sup>24, 27, 73</sup>

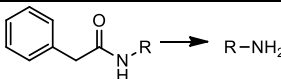
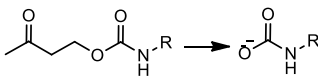
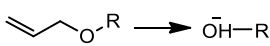
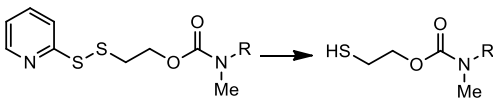
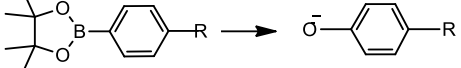
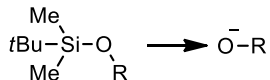
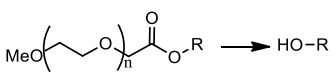
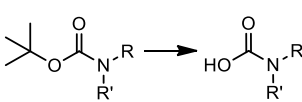
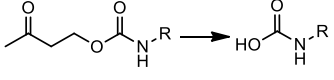
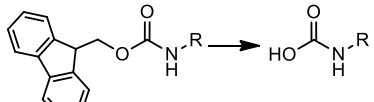
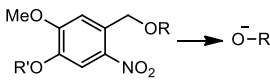
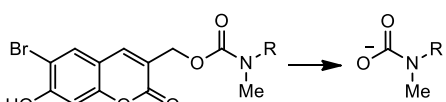
Compared to the other methods that are currently available for the preparation of SIPs, non-organometallic catalyst based anionic polymerizations appears to be the most attractive and promising way of preparing controlled SIPs. The method allows for the preparation of SIPs in a much shorter time compared to the other methods. Moreover, the method allows for the preparation of SIPs with tailored molecular weights and produces no toxic side products.

## **2.4 Potential triggers**

What is especially exciting about SIPs, is that they can be designed to selectively respond to a specific stimulus. By carefully choosing the end-cap, one can design a variety of SIPs from the same polymer backbone that differ only in the stimulus that they respond to. A number of triggers have already been reported and are summarized in Table 2.1, grouped according to the type of stimulus required for their activation. These groups or classes consist of enzyme, redox, nucleophile, acid/base and photo mediated cleavage. In most cases, cleavage of the end-cap reveals a carbamate or carbonate which then undergoes decarboxylation to reveal an amine or alcohol group, respectively (entries 2, 8-10 and 12). In some cases however, exposure to a stimulus directly converts the trigger into an electron-donating moiety without any intermediate steps (entries 1, 3-7). The histories as well as the current and potential applications of each of the classes of trigger/ stimulus combinations are discussed further below.<sup>9</sup>

## Chapter 2

Table 2.1. Triggers that induce depolymerization of self-immolative polymers.<sup>9</sup>

Entry	Trigger Class	Structure before and after response to stimulus	Stimulus
1	E <sup>a</sup>		Penicillin G amidase
2	E <sup>a</sup>		Antibody 38C2
3	R <sup>b</sup>		Pd, Pd/NaBH <sub>4</sub>
4	R <sup>b</sup>		Dithiothreitol
5	R <sup>b</sup>		H <sub>2</sub> O <sub>2</sub>
6	N <sup>c</sup>		Fluoride
7	N <sup>c</sup>		H <sub>2</sub> O
8	A <sup>d</sup>		H <sup>+</sup>
9	A <sup>d</sup>		Piperidine, morpholine
10	A <sup>d</sup>		Piperidine
11	P <sup>e</sup>		UV radiation
12	P <sup>e</sup>		NIR radiation

<sup>a</sup> Enzyme-mediated cleavage of end-cap.<sup>b</sup> Redox-mediated cleavage of end-cap.<sup>c</sup> Nucleophile-mediated cleavage of end-cap.<sup>d</sup> Acid/Base-mediated cleavage of end-cap.<sup>e</sup> Photo-mediated cleavage of end-cap.

## Chapter 2

### 2.4.1 Enzyme-mediated cleavage:

Enzymatic substrates were the first triggers reported to be capable of multiple elimination events.<sup>28</sup> They are mainly used in biological systems and intensive research has led to the successful application of enzymatic substrates, which are both native and foreign to the human physiology.<sup>11, 12, 28-32</sup> The majority of the research done on enzymatic substrates as triggers for SIPs have been led by the Shabat group and focus mainly on linear SIPs.<sup>12</sup> It follows, therefore, that the application of more complex biological systems may require the design of equally complex SIPs.<sup>9</sup> Nonetheless, the vast amounts of knowledge available on the kinetics involved in enzyme-mediated cleavage promotes the use of this type of trigger in applications that require fine tuning of the initiation kinetics of specific triggering events.<sup>9</sup>

### 2.4.2 Redox-mediated cleavage

The ease with which redox mediated triggers are incorporated, facilitated their introduction into SIPs.<sup>9</sup> Examples of redox-mediated triggers include transition metal-mediated reductions, reduction of disulphide linkages and the oxidation of boronates with peroxides.<sup>4, 19, 33-35</sup>

Redox-type triggers were originally designed for dendritic and oligomeric systems and it was Phillips who began to adapt their structure to allow for their utilization in linear polymers as well.<sup>27</sup> This was first achieved by including an allyl carbonate in the structure of the aryl allyl ether trigger so that it could be installed at the chain-end of a PPA based SIP (Figure 2.1).<sup>27</sup> Exposure to a palladium source resulted in the removal of the allyl fragment and subsequent decarboxylation to reveal an unstable hemiacetal followed by the immediate depolymerization of the uncapped polymer.<sup>37</sup>

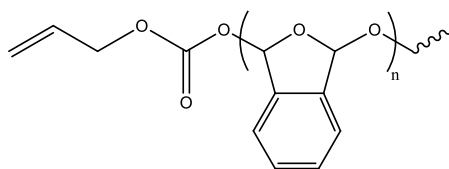


**Figure 2.1. Preparation of PPA that depolymerizes upon exposure to palladium.<sup>27</sup>**

Disulfide linkages are another example of redox-mediated triggers that have been developed for SIPs.<sup>34</sup> They have become especially attractive for biological applications since they can be activated under reducing intracellular environments.<sup>34</sup> The use of phenylborates has introduced the possibility of triggering depolymerization under oxidative conditions.<sup>4</sup>

## Chapter 2

---

Conversion of the boronate moiety in the presence of hydrogen peroxide into an electron-releasing phenol leads to the initiation of the self-immolation of the polymer, resulting in the formation of multiple azaquinone units.<sup>4</sup>

### 2.4.3 Nucleophile-mediated cleavage:

The use of a nucleophilic attack to liberate electron-releasing functionalities have been researched to a much lesser extent in comparison to the other types of triggering agents.<sup>21, 27, 36</sup> However, it is an option that should be considered in cases where components of the SIP are unstable in aqueous conditions.<sup>27</sup> The need for water, however, can be eliminated by using tetrabutylammonium fluoride for the cleavage of the silyl ether instead.<sup>27</sup>

### 2.4.4 Acid/Base-mediated cleavage:

The use of traditional acid and base sensitive end-caps has become an increasingly popular option.<sup>21, 37-39</sup> The reagents required for their incorporation and activation are inexpensive and readily available, and pH modulation is a simple procedure of triggering.<sup>9</sup> What is more, they have been shown to be ideal candidates for use in advanced materials that are capable of on-demand depolymerization.<sup>9</sup> The Boc and Fmoc protecting groups in particular, have established themselves as the standards for comparison for all other developing end-caps.<sup>9</sup> Their reactivities make them ideally suited for SIP applications, as both are capable of diminishing the electron-donating ability of the amine and amino acid groups that they protect.<sup>9</sup>

### 2.4.5 Photo-mediated cleavage:

The photo-mediated cleavage of triggers such as nitrobenzyl carbamates and bromocoumarins (entries 11 and 12, Table 2.1), requires only the correct wavelength and intensity of light.<sup>37, 40</sup> No additional chemicals are required. Their application is mostly focused on drug delivery as it introduces the potential for spatiotemporal control of release profiles in a manner that is non-invasive. A relatively new proposal, involves the application of one such a trigger for the spatiotemporal control, relating to both space and time, of release profiles in a manner that is non-invasive.<sup>41</sup>

Of the various triggers that have been reported thus far, those that induce photo-mediated cleavage of the SIP appear to hold the most advantages. No harsh chemicals or tedious experimental procedures are required. In addition, no undesired by-products are formed since no additional chemicals are added to induce depolymerization.

## **2.5 Potential applications**

SI materials have been developed over time to allow for higher levels of control and amplification.<sup>8</sup> Thus far, the design and synthesis of a number of different polymer backbones and architectures have led to the application of SIPs in signal amplification, photoresists, and drug delivery.<sup>16</sup>

### **2.5.1 Signal amplification:**

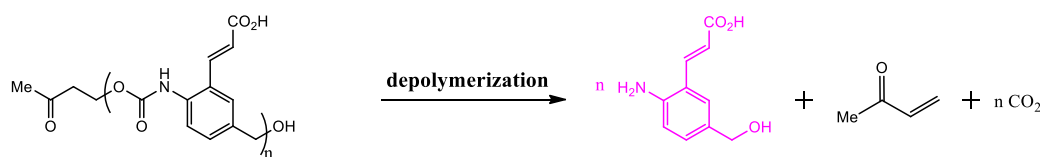
In the early stages of development, most SIDs contained output molecules that were either fluorescent or UV-visible to allow for easy detection following the depolymerization of the SID.<sup>42</sup> Even though these early stage models were designed to act only as proof of concept, they served as inspiration for the design of SIPs that could serve as sensors.<sup>42</sup> These SIPs were designed to, upon removal of the end-cap, depolymerize into monomeric units that could be observed via UV-vis or photoluminescence.<sup>11, 12</sup>

The majority of the applications for self-immolative materials today, rely on their ability to respond to a specific stimulus both selectively and with an amplified response.<sup>27</sup> In principle, the extent of the amplification increases linearly with the degree of polymerization.<sup>27</sup> It stands to reason therefore that a polymer with a 1000 repeat units would provide a 1000× signal amplification when the end-cap responds to a single unit of an analyte. This example clearly illustrates why the use of SIPs in sensory applications now exceeds that of SIDs, as linear polymers have a much higher degree of polymerization and therefore a much greater amplification capability.

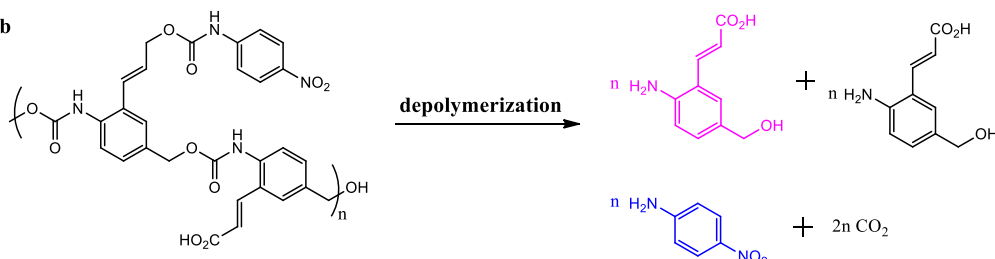
Today these sensors have found applications in environmental analysis (detection of metals, contaminants and pathogens) and in clinical diagnostics (detection of disease related biomarkers, bacteria, virus and proteins).<sup>42</sup> Poly(benzyl carbamate) is one example of a SIP commonly used in sensory applications.<sup>11, 12</sup> Its analyte-induced depolymerization generates fluorescent monomeric units as shown in Scheme 2.9a.<sup>12</sup> Another interesting example is that of a comb polymer (Shown in Scheme 2.9b) that contains two types of repeat units: one that depolymerizes into fluorescent monomeric units and another that releases a coloured output molecule in a subsequent post-depolymerization reaction.<sup>11</sup>

## Chapter 2

a



b



**Scheme 2.9. (a) The application of poly(benzyl carbamate) in sensory applications and (b) the application of comb polymers in sensory applications.<sup>11, 12</sup>**

These two examples illustrate that with creative design, the repeating units of a SIP can serve a secondary function beyond that of simply forming a part of the polymer backbone.

### 2.5.2 Photoresists

Patterning of resists and the transfer of patterns onto various underlying substrates is a well-known and versatile method for device production and has become the driving technology for micro- and nanofabrication.<sup>58-60, 63</sup> There are four basic components of a photoresist: the polymer, solvent, photosensitizers and other additives.<sup>59</sup> The role of the polymer is to either cross-link or photosolubilize upon exposure to UV-light.<sup>59</sup> The solvent is required to make the photoresist a liquid so that it may be spun onto a substrate by spin-coating.<sup>59</sup> The photosensitizers are used to either control or induce polymer reactions, resulting in the photosolubilization or cross-linking of the polymer.<sup>59</sup> Finally, additives are used to enhance the properties of the material.<sup>59</sup> Photoresists can be classified into either positive or negative photoresists.<sup>59, 62</sup> In negative photoresists, exposure to UV-light causes the polymer to cross-link, resulting in the polymer being insoluble in the photoresist developer solution.<sup>59, 62</sup> In the case of positive photoresist materials, exposure to UV-light changes the chemical structure of the polymer so that it becomes more soluble in the photoresist developer solution.<sup>59, 62</sup> In 1980 Ito prepared a positive self-developing photoresist through the acid-catalyzed depolymerization of PPA.<sup>58</sup> Since then a number of research groups have further developed the



## Chapter 2

---

PPA containing photoresist and it has become the resist of choice in microelectromechanical system applications.<sup>27, 58, 61, 63</sup>

### 2.5.3 Drug delivery:

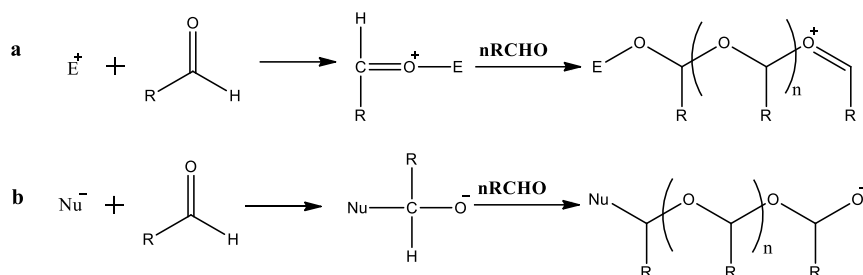
Drug delivery systems have alleviated many of the problems associated with the drugs themselves such as poor solubility, bio-distribution and pharmacokinetics as well as severe side effects.<sup>43, 44</sup> In an attempt to design systems that can both protect and preserve the drug, drug delivery systems have been endowed with stimuli-responsiveness.<sup>43, 52, 53</sup> SIPs that have been designed to contain therapeutic drugs at the tail or along the backbone of the polymer backbone offers the unique opportunity to create drug delivery systems that can both protect and preserve the therapeutic drug.<sup>42</sup> After navigating along the blood stream, the drug carrier system with pre-designed stimuli responsiveness will accumulate or enter the target area, after which it will disintegrate following exposure to an external or environmental stimulus, thereby releasing the therapeutic drugs as products of the depolymerization process.<sup>51</sup> To improve the control of these drug carriers they have been endowed with pH-, redox, light-, magnet-, thermal-, gas- and ultrasonic-responsiveness, depending on the application for which they are intended.<sup>54-57</sup>

## 2.6 Polyaldehydes as SIPs:

Approximately fifty years ago, different research groups began to study the polymerization reaction of acetaldehyde and other higher aldehydes in an attempt to better understand their underlying mechanisms and thermodynamics. Since then, a number of aldehyde monomers have been successfully polymerized along with the discovery of some interesting generic properties.<sup>63</sup>

Aldehydes, like olefins, have a double bond that is susceptible to polymerization. Unlike olefins however, the carbonyl bond of aldehydes is highly polarized because of the difference in the electronegativity of the carbon-oxygen bond.<sup>63-65</sup> As a result, aldehydes are susceptible to ionic polymerization and not radical polymerization.<sup>65</sup> Ionic polymerization of aldehydes takes place via cationic or anionic mechanisms.<sup>63-65</sup> Cationic polymerization (Scheme 2.10a) occurs by the addition of an electrophile to the carbonyl oxygen, whilst anionic polymerization (Scheme 2.10b) entails the addition of a suitable anion to the carbonyl carbon to produce an alkoxide.<sup>64</sup> The structure of the polymer obtained from either forms of ionic polymerization is that of a polyacetal, a polymer chain that consists of alternating carbon and oxygen atoms.<sup>63, 64</sup>

## Chapter 2



**Scheme 2.10. (a) The cationic and (b) the anionic polymerization of aldehydes.**

Polyaldehydes have received much attention for their ability to form highly ordered structures with macromolecular asymmetry.<sup>63, 65</sup> These polymers can differ in tacticity, depending on the monomer structure, identity of the initiator, the size and bulkiness of the R group and polymerization conditions.<sup>63, 65</sup> Cationic polymerization of sterically unhindered aldehydes results in atactic polyaldehydes that are amorphous.<sup>68</sup> Anionic polymerization of most aldehydes on the other hand, leads to high fractions of isotactic polymers with crystalline structures.<sup>69, 70</sup> In addition, large and bulky R groups favour the formation of isotactic polymers.<sup>63</sup>

Arguably the most distinguished property of polyaldehydes is that the ceiling temperatures ( $T_c$ ) for most aldehyde polymerizations are very low, ranging between room temperature and sub-zero temperatures.<sup>65</sup> The  $T_c$  of a polymer can be defined as the temperature above which a polymer becomes thermodynamically unstable.<sup>63</sup> As a result, no polymer will form above this temperature.<sup>63</sup>

The possibility of the polymerization of liquid monomers occurring at a given temperature ( $T$ ) can be discussed in terms of the Gibbs free energy ( $G$ ) which in turn is determined by the enthalpy ( $H$ ) and entropy ( $S$ ) of a given system or reaction (Equation 2.1).<sup>63, 65, 71</sup>

$$\Delta G = \Delta H - (T\Delta S) \quad (\text{Eq 2.1})$$

For the polymerization reaction to be thermodynamically favoured, the Gibbs free energy of polymerization must be lower than that of the monomer. However, in some cases the Gibbs free energy of the liquid monomer at room temperature is lower than that of the polymer and so polymerization becomes unfavourable.<sup>71</sup> This problem can be solved by taking Equation 2.2, applicable for both monomer and polymer, into consideration:

$$\left(\frac{\partial G}{\partial T}\right) = -S \quad (\text{Eq 2.2})$$

## Chapter 2

---

Equation 2.2 shows that the Gibbs free energy will increase with a decreasing temperature for both the monomer and the polymer. Since the entropy for liquid monomers is generally considered to be greater than that of their polymers, it may be possible to find a temperature for which  $G_{\text{monomer}} > G_{\text{polymer}}$ . This limiting temperature is what is commonly referred to as the  $T_c$ .<sup>71</sup>

In the case of polyaldehydes, the entropy of polymerization is comparable to that of olefins.<sup>63</sup> However, their enthalpy of polymerization is much higher, resulting in a more positive Gibbs free energy of polymerization.<sup>65</sup> This translates into poor thermal stability and low ceiling temperatures.<sup>63</sup> On the other hand, their  $T_c$  corresponds into fast, quantitative and controllable degradation, making polyaldehydes ideal for applications that require SIPs capable of rapid depolymerization.<sup>63</sup>

Above their ceiling temperature, depolymerization of polyaldehydes starts at the hemiacetal chain-ends and continues by an unzipping reaction that follows the same mechanisms as chain growth.<sup>24, 71, 72</sup> To prevent depolymerization from taking place and to allow for the application of polyaldehydes above room temperature, the labile hemiacetal chain-ends are capped with functional groups, commonly referred to as end-caps, that can be chosen to be trigger moieties.<sup>24, 65, 72</sup> As previously discussed, a wide range of end-caps have been reported, differing only in the stimulus required to cleave them and induce depolymerization.<sup>63</sup>

It is important to note that polyaldehydes are capable of degrading by mechanisms other than the unzipping reaction caused by removal of the end-cap. The polyaldehyde backbone consists of acetal groups, making these polymers susceptible to acid-catalyzed cleavage.<sup>66, 75, 79</sup> Under acidic conditions, polyaldehydes can therefore be cleaved at any position along the polymer backbone by the heterolytic rupture of an acetal group.<sup>75, 79</sup> The two hemiacetal groups formed by this rupture can then act as the starting point for the complete depolymerization of the polymer via the unzipping reaction.<sup>75, 79</sup> Ultrasound-induced cavitation has also been shown capable of causing chain scission in the polyaldehyde backbone, resulting in rapid and complete depolymerization.<sup>9</sup>

### 2.7 Polyaldehyde homopolymers:

Apart from poly(oxymethylene), very few polyaldehydes have found industrial applications.<sup>64</sup> This is mainly due to their association with low thermal and chemical stability.<sup>64</sup> However, advancements in research and technology have allowed for a number of applications that are

## Chapter 2

---

based on the low  $T_c$  of polyaldehydes.<sup>64</sup> With applications in triggered release, nanolithography and various biomedical devices, polyaldehydes may well become the material of choice when designing stimuli-responsive materials.<sup>63,64, 65</sup>

To date, PPA has attracted the most attention because of its unique ability to respond to both chemical and physical stimuli.<sup>63, 73, 74</sup> The most commonly used example of a chemical stimulus is pH and of a physical stimulus is temperature. Chemical stimuli generally refers to changes in pH and physical stimuli to changes in temperature.<sup>14</sup> Other positive attributes include its ease of synthesis and well defined polymerization, compared to other SIPs that are prepared by iterative/stepwise methods.<sup>63, 73, 74</sup> PPA's most desirable attribute however, is its unique capability of fast and controlled depolymerization upon the removal of its end-cap.<sup>63, 72, 73, 74</sup> Other SI systems suffer from slow rates of depolymerization, making PPA an especially attractive material for applications that require fast rates of degradation.<sup>8, 17, 19, 27, 75</sup>

Various routes for the preparation of PPA have been reported over the years. The polymerization of aldehydes via coordinative processes using catalysts such as chelated organoaluminium catalyst was amongst the first methods reported to produce crystalline polyaldehydes in high yields.<sup>80</sup> With the evolution of technology, ionic processes using organometallic catalysts such as butyl lithium and triethylaluminium became more popular.<sup>67</sup> However, various issues related to the use of organometallic catalysts such as long reaction times and the presence of residual metal ions in the product has been identified.<sup>72</sup> De Winter *et al.* overcame this issue when they proposed the use of non-organometallic catalysts, specifically metal-free phosphazene bases catalysts, for the anionic polymerization of *o*-phthaldialdehyde. Three different phosphazene base catalysts were investigated, differing only in their size and basicity. From this study they were able to conclude that the basicity of the catalysts had a definite effect on the control of the polymerization, with the least reactive phosphazene base catalysts allowing for the best control. In addition, they were able to prepare a well-defined PEO-*b*-PPA copolymers using the same method and catalyst.<sup>72</sup>

Apart from PPA, the only other polyaldehyde that have found some commercial application is poly(glyoxylate) (PMGx). Its main product of depolymerization is glyoxylic acid which is completely biodegradable. It does however, also produce methanol which hampers any in-vivo applications. A promising alternative is to use the ethyl ester derivative, poly(ethyl glyoxylate) (PEGx), prepared via the anionic polymerization of ethyl glyoxylate.<sup>63, 76</sup>

## Chapter 2

---

Up to date, there have been very few studies focusing on polyaldehydes and their self-immolative nature other than those that have already been discussed in this literature review. In 1964, Vogl reported on the mechanism of polymerization of higher aldehydes in general.<sup>69</sup> He also discussed the influence of the solvent, temperature, initiator and monomer on the polymerization reaction with particular emphasis on the effect of each on the stereoregularity of the resulting polymer.<sup>69</sup> Then in 1997, Mohammed *et al.* set out to investigate the effect of these factors on *n*-butyraldehyde in particular.<sup>78</sup> They investigated the polymerization of the aldehyde with cationic and anionic initiators, in various solvents and at varying temperatures.<sup>78</sup> Vogl and Mohammed's studies concluded that the ideal temperature for the ionic polymerization of aldehydes falls within the range of -50 and -95 °C, depending on the identity of the monomer.<sup>67</sup> Both showed alkali metal oxides to be the best anionic initiators for higher aldehydes because of their high solubility, although other initiators such as alkali metals and Grignard reagents were shown to work effectively as well.<sup>67, 77</sup> Their observations with regard to the effect of the solvent were also in agreement. Polar solvents such as THF were shown to promote unidentified side reactions, whereas non-polar solvents such as *n*-pentane limited the occurrence of these side reactions.<sup>67, 7</sup>

Apart from these two studies, very little attention has been given to PBA from both a synthetic and application point of view.<sup>63, 73, 74</sup> This is surprising, seeing that it has a  $T_c$  that is similar to that of PPA.<sup>72, 67</sup> In addition, *n*-butyraldehyde is inexpensive and highly volatile.

This work aims to establish a facile method for the preparation of well-defined PPA by non-organometallic catalyst based anionic polymerization using different initiating groups. This method is then applied to the preparation of polystyrene-*b*-poly(phthaldialdehyde) copolymers. Furthermore, the metal free non-organometallic catalyst based anionic polymerization of butyraldehyde (BA) is introduced.

### References:

- (1) Holowka, E. P.; Pochan, D. J.; Deming, T. J. *J. Am. Chem. Soc.* **2005**, 127, 12423–12428.
- (2) Betancourt, E.; Rivera, M. *J. Am. Chem. Soc.* **2009**, 131, 16666–16668.
- (3) Thornton, P. D.; Ulijn, R. V.; McConnell, G.; Ulijn, R. V. *Chem. Commun.* **2005**, 47, 5913–5915.

**Chapter 2**

---

- (4) Andersen, E. S.; Dong, M.; Nielsen, M. M.; Jahn, K.; Subramani, R.; Mamdouh, W.; Golas, M. M.; Sander, B.; Stark, H.; Oliveira, C. L. P.; Pedersen, J. S.; Birkedal, V.; Besenbacher, F.; Gothelf, K. V.; Kjems, J. *Nature* **2009**, 459, 73–76.
- (5) Braunecker, W. A.; Matyjaszewski, K. J. *Mol. Catal. A Chem.* **2006**, 254, 155–164.
- (6) Matyjaszewski, K.; Davis, K.T.P., *Handbook of Radical Polymerization*, Wiley/Interscience, Hoboken, **2002**.
- (7) Matyjaszewski, K. *J. Am. Chem. Soc.* **2003**, 125, 854. 1–9.
- (8) Chen, E. K. Y.; McBride, R. A.; Gillies, E. R. *Macromolecules* **2012**, 45, 7364–7374.
- (9) Peterson, G. I.; Larsen, M. B.; Boydston, A. J. *Macromolecules* **2012**, 45, 7317–7328.
- (10) Dilauro, A. M.; Zhang, H.; Baker, M. S.; Wong, F.; Sen, A.; Phillips, S. T. *Macromolecules* **2013**, 46, 7257–7265.
- (11) Weinstain, R.; Sagi, A.; Karton, N.; Shabat, D. *Chem. Eur. J.* **2008**, 14, 6857–6861.
- (12) Sagi, A.; Weinstain, R.; Karton, N.; Shabat, D. *J. Am. Chem. Soc.* **2008**, 130, 5434–5435.
- (13) De Groot, F. M. H.; Albrecht, C.; Koekkoek, R.; Beusker, P. H.; Scheeren, H. W. *Angew. Chemie Int. Ed.* **2003**, 42, 4490–4494.
- (14) Esser-Kahn, A. P.; Odom, S. A.; Sottos, N. R.; White, S. R.; Moore, J. S. *Macromolecules* **2011**, 44, 5539–5553.
- (15) Amir, R. J.; Pessah, N.; Shamis, M.; Shabat, D. *Angew. Chemie Int. Ed.* **2003**, 42, 4494–4499.
- (16) McBride, R. A.; Gillies, E. R. *Macromolecules* **2013**, 46, 5157–5166.
- (17) Robbins, J. S.; Schmid, K. M.; Phillips, S. T. *J. Org. Chem.* **2013**, 78, 3159–3169.
- (18) Olah, M. G.; Robbins, J. S.; Baker, M. S.; Phillips, S. T. *Macromolecules* **2013**, 46, 5924–5928.
- (19) Dewit, M. A.; Beaton, A.; Gillies, E. R. *J. Polym. Sci. Part A Polym. Chem.* **2010**, 48, 3977–3985.
- (20) Guyton, K. Z.; Thompson, J. A.; Kensler, T. W. *Chem. Res. Toxicol.* **1993**, 6, 731–738.
- (21) DeWit, M. A.; Gillies, E. R. *J. Am. Chem. Soc.* **2009**, 131, 18327–18334.
- (22) Haba, K.; Popkov, M.; Shamis, M.; Lerner, R.A.; Barbas III, C.F.; Shabat, D. *Angew. Chemie Int. Ed.* **2005**, 44, 726–730.
- (23) Saari, W. S.; Schwering, J. E.; Lyle, P. A.; Smith, S. J.; Engelhardt, E. L. *J. Med. Chem.* **1990**, 33, 2590–2595.
- (24) Dilauro, A. M.; Robbins, J. S.; Phillips, S. T. *Macromolecules* **2013**, 46, 2963–2968.

**Chapter 2**

---

- (25) Lopez Hernandez, H.; Kang, S. K.; Lee, O. P.; Hwang, S. W.; Kaitz, J. A.; Inci, B.; Park, C. W.; Chung, S.; Sottos, N. R.; Moore, J. S.; Rogers, J. A.; White, S. R. *Adv. Mater.* **2014**, 26, 7637–7642.
- (26) Kaitz, J. A.; Diesendruck, C. E.; Moore, J. S. *J. Am. Chem. Soc.* **2013**, 135, 12755–12761.
- (27) Seo, W.; Phillips, S. T. *J. Am. Chem. Soc.* **2010**, 132, 9234–9235.
- (28) De Groot, F.M.H.; Loos, W.J.; Kockkock, R.; van Berkom, L.W.A.; Busscher, G.F.; Seelen, A.E.; Albrecht, C.; de Bruijn, P.; Scheeren, H.W. *J. Org. Chem.* **2001**, 66, 8815–8830.
- (29) Grinda, M.; Clarhaut, J.; Renoux, B.; Tranoy-Opalinski, I.; Papot, S. *Medchem. Comm.* **2012**, 3, 68–70.
- (30) Amir, R. J.; Popkov, M.; Lerner, R. A.; Barbas, C. F.; Shabat, D. *Angew. Chemie Int. Ed.* **2005**, 44, 4378–4381.
- (31) Erez, R.; Shabat, D. *Org. Biomol. Chem.* **2008**, 6, 2669–2672.
- (32) Meyer, Y.; Richard, J. A.; Delest, B.; Noack, P.; Renard, P. Y.; Romieu, A. *Org. Biomol. Chem.* **2010**, 8, 1777–1780.
- (33) Weinstain, R.; Baran, P. S.; Shabat, D. *Bioconjug. Chem.* **2009**, 20, 1783–1791.
- (34) Zhang, L.; Liu, W.; Lin, L.; Chen, D.; Stenzel, M. H. *Biomacromolecules* **2008**, 9, 3321–3331.
- (35) Redy, O.; Kisin-Finfer, E.; Sella, E.; Shabat, D. *Org. Biomol. Chem.* **2012**, 10, 710–715.
- (36) Zhang, H.; Yeung, K.; Robbins, J. S.; Pavlick, R. A.; Wu, M.; Liu, R.; Sen, A.; Phillips, S. T. *Angew. Chemie Int. Ed.* **2012**, 51, 2400–2404.
- (37) Amir, R. J.; Pessah, N.; Shamis, M.; Shabat, D. *Angew. Chemie Int. Ed.* **2003**, 42, 4494–4499.
- (38) Esser-Kahn, A. P.; Sottos, N. R.; White, S. R.; Moore, J. S. *J. Am. Chem. Soc.* **2010**, 132, 10266–10268.
- (39) Perry, R.; Amir, R. J.; Shabat, D. *New J. Chem.* **2007**, 31, 1307–1312.
- (40) De Gracia Lux, C.; McFearin, C. L.; Joshi-Barr, S.; Sankaranarayanan, J.; Fomina, N.; Almutairi, A. *ACS Macro Lett.* **2012**, 1, 922–926.
- (41) Tibbitt, M. W.; Han, B. W.; Kloxin, A. M.; Anseth, K. S. *J. Biomed. Mater. Res. Part A.* **2012**, 100, 1647–1654.
- (42) Wang, R. E.; Costanza, F.; Niu, Y.; Wu, H.; Hu, Y.; Hang, W.; Sun, Y.; Cai, J. *J. Control. Release.* **2012**, 159, 154–163.



**Chapter 2**

---

- (43) Huo, M.; Yuan, J.; Tao, L.; Wei, Y. *Polym. Chem.* **2014**, 5, 1519–1528.
- (44) Allen, T. M.; Cullis, P. R. *Science* **2004**, 303, 1818–1822.
- (45) Warnecke, A.; Kratz, F. *J. Org. Chem.* **2008**, 73, 1546–1552.
- (46) Ortiz, A.; Shanahan, C. S.; Sisk, D. T.; Perera, S. C.; Rao, P.; McGrath, D. V. *J. Org. Chem.* **2010**, 75, 6154–6162.
- (47) Kevitch, R. M.; Shanahan, C. S.; McGrath, D. V. *New J. Chem.* **2012**, 36, 492–505
- (48) Sella, E.; Shabat, D. *J. Am. Chem. Soc.* **2009**, 131, 9934–9936.
- (49) Polaske, N. W.; Szalai, M. L.; Shanahan, C. S.; McGrath, D. V. *Org. Lett.* **2010**, 12, 4944–4947
- (50) Sella, E.; Shabat, D. *Chem. Commun.* **2008**, 44, 5701–5703
- (51) Sun, Q.; Radosz, M.; Shen, Y. J. *Control. Release* **2012**, 164, 156–169.
- (52) Sukhorukov, G. B.; Möhwald, H. *Trends Biotechnol.* **2007**, 25, 93–98.
- (53) Angelova, N.; Hunkeler, D. *Trends Biotechnol.* **1999**, 17, 409–421.
- (54) Pillai, O.; Panchagnula, R. *Curr. Opin. Chem. Biol.* **2001**, 5, 447–451.
- (55) Kim, D.; Termsarasab, U.; Cho, H.; Yoon, I.; Lee, J.; Moon, H.T.; Kim, D.; *Int. J. Nanomedicine* **2014**, 9, 5711–5727.
- (56) Madsen, S. K.; Mooney, D. *J. Pharm. Sci. Technol. Today.* **2000**, 3, 381–384.
- (57) Galaev, I.Y.; Mattiasson, B. *Trends Biotechnol.* **1991**, 17, 335–340.
- (58) Hiroshi, I. *J. Polym. Sci. Part A Polym. Chem.* **2003**, 41, 3863–3870.
- (59) Shirai, M.; Tsunooka, M. *Prog. Polym. Sci.* 1996, 21, 1–45.
- (60) Lin, Q. Properties of Photoresist Polymers. In *Physical Properties of Polymer Handbook*. **2006**, 941–955.
- (61) Tsuda, M.; Hata, M.; Nishida, R.; Oikawa, S. *J. Polym. Sci. Part A Polym. Chem.* **1997**, 35, 77–89.
- (62) Krongauz, V.V.; Trifunac, A.D. *Processes in Photoreactive Polymers*, 2nd ed.; Springer Science & Business Media, 2013.
- (63) Coulembier, O.; Knoll, A.; Pires, D.; Gotsmann, B.; Duerig, U.; Frommer, J.; Miller, R. D.; Dubois, P.; Hedrick, J. L. *Macromolecules* **2010**, 43, 572–574.
- (64) Köstler, S. *Polym. Int.* **2012**, 61, 1221–1227.
- (65) Vogl, O. *J. Polym. Sci. Part A Polym. Chem.* **2000**, 38, 2293–2299.
- (66) Delzenne, G.; Smuts, G. *Makromol. Chem.* **1957**, 23, 16–30.
- (67) Vogl, O. *J. Polym. Sci. A Polym. Chem.* **1964**, 2, 4607–4620.
- (68) Vogl, O.; Bryant, W.M.D.; *J. Polym. Sci. A Polym. Chem.* **1964**, 2, 4633–4645.
- (69) Vogl, O. *J. Polym. Sci. A Polym. Chem.* **1964**, 2, 4591–4606



**Chapter 2**

---

- (70) Vogl O (du Pont de Nemour). Crystalline Aldehyde Polymers, Belgian Patent 580553. 1959.
- (71) Heikens, D.; Geelen, H. *Polymer* **1962**, 3, 591–594.
- (72) Graessley, W. W.; Nagasubramanian, K.; Advani, R.; Huetter, D. F. *J Polym. Sci A Polym Phys.* **1968**, 6, 1021–1033
- (73) De Winter, J.; Dove, A. P.; Knoll, A.; Gerbaux, P.; Dubois, P.; Coulembier, O. *Polym. Chem.* **2014**, 5, 706–711.
- (74) Kaitz, J. A.; Diesendruck, C. E.; Moore, J. S. *J. Am. Chem. Soc.* **2013**, 135, 12755–12761.
- (75) Kaitz, J. a.; Possanza, C. M.; Song, Y.; Diesendruck, C. E.; Spiering, A. J. H.; Meijer, E. W.; Moore, J. S. *Polym. Chem.* **2014**, 5, 3788–3794.
- (76) Yeung, K.; Kim, H.; Mohapatra, H.; Phillips, S. T. *J. Am. Chem. Soc.* **2015**, 137, 5324–5327.
- (77) Brachais, C. H.; Huguet, J.; Bunel, C.; Brachais, L. *Polym. Degrad. Stab.* **1999**, 64, 243–249.
- (78) Mohammed, F.; Moreau, M.; Vairon, J.P. Thermodynamic Study of the Ionic Polymerization of *n*-Butyraldehyde. In *Cationic Polymerization*. **1997**, 50–62.
- (79) Carl, P. L.; Chakravarty, P. K.; Katzenellenbogen, J. A. *J. Med. Chem.* **1981**, 24, 479–480.
- (80) Vandenberg, E. J. Process for the polymerization of aldehydes using a chelated organoaluminium catalyst. 3208975, September 28, 1965.

## Chapter 3

### 3.1 Introduction

In the early 1960s, Vogl presented a series of detailed studies on the synthesis of polyaldehydes, by anionic and cationic mechanisms, that investigated the influence of reaction parameters such as solvent polarity, temperature and catalyst type.<sup>1</sup> Vogl's studies showed that higher polyaldehydes could be obtained when the polymerization reactions were conducted in solvents with low dielectric constants, at very low temperatures and in the presence of organometallic catalysts.<sup>1</sup>

Whilst these findings were used as strict guidelines for the polymerization of aldehydes in the decades that followed, recent years have shown a shift from the use of organometallic catalysts to non-organometallic catalysts instead.<sup>2-5</sup> This shift follows the realization of the disadvantages associated with the use of organometallic catalysts such as slow polymerization rates, poor solubility in most common solvents and the presence of residual metal contaminants in the resultant material.<sup>2, 3, 4</sup>

Nitrogen-phosphorous hybrid organobases such as phosphazene bases have been studied intensively as they have shown great promise as a non-organometallic alternative.<sup>2</sup> Phosphazene bases are strong, uncharged Brønsted bases which contain at least one phosphorous atom bonded to four nitrogen functions of three amine and one imine substituent.<sup>2</sup> According to Schwesinger's nomenclature these bases are designated according to the number of P=N units as shown below in Figure 3.1.<sup>2</sup> Among these bases the most commonly used are *N'*-*tert*-butyl-*N,N,N',N',N'',N'''*- hexamethylphosphorimidictriamide ( $P_1$ -*t*-Bu), 1-*tert*-butyl-2,2,4,4,4-pentakis(dimethylamino)-2  $\Delta$  <sup>5</sup>,4  $\Delta$  <sup>5</sup>-catenadi(phosphazene) ( $P_2$ -*t*-Bu) and 3-*t*-butylimino-1,1,1,5,5,5-hexakis(dimethylamino)-3-[tris(dimethylamino)phosphoranylidene]amino}-1  $\Delta$  <sup>5</sup>,3  $\Delta$  <sup>5</sup>,5  $\Delta$  <sup>5</sup>-1,4-triphosphazadiene ( $P_4$ -*t*-Bu).<sup>2, 3</sup> Phosphazene bases have become popular alternatives to organometallic catalysts as they offer a number of interesting features such as remarkably high basicity, high solubility in organic solvents of different polarities and good thermal stability.<sup>2</sup>



## Chapter 3

catalysts. Whilst not as thoroughly researched in the anionic polymerization of aldehydes as organometallic and phosphazene base catalysts, DBU and TBD (Figure 3.2) are similar in reactivity to some phosphazene base catalysts and could provide a much simpler method for the preparation of polyaldehydes.<sup>8</sup>

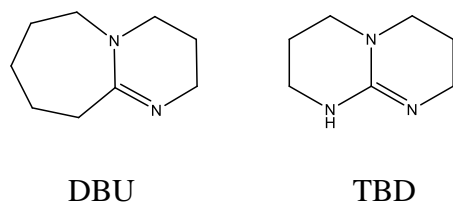


**Figure 3.2. Amine base catalysts DBU and TBD.**

This chapter will focus on optimizing the method for the non-organometallic catalyst based anionic polymerization of *o*-phthaldialdehyde (PA). The versatility of the polymerization system will be demonstrated by preparing PPA using different initiating groups and quenching agents. Finally, the microstructure and thermal properties of PPA prepared under the optimized conditions determined in this work will also be investigated.

### 3.2 Experimental

### 3.2.1 Materials

Acetic anhydride (99 %), *n*-butyraldehyde (99 %), 1, 8-diazabicyclo [5.4.0] undec-7-ene (DBU) (98 %), *o*-phthaldialdehyde (97 %), 1, 5, 7-triazabicyclo [4.4.0] dec-5-ene (TBD) (98 %), *tert*-butylimino-tris(dimethylamino)phosphorane, calcium hydride anhydrous (99.5 %), *N'*-*tert*-butyl-*N,N,N',N',N'',N''*-hexamethylphosphorimidictriamide (P<sub>1</sub>-*t*-Bu) (97 %), 1-*tert*-butyl-2,2,4,4,4-pentakis(dimethylamino)-2  $\Lambda^5$ ,4  $\Lambda^5$ -catenadi(phosphazene) (P<sub>2</sub>-*t*-Bu), 2 M in THF, 3-*t*-butylimino-1,1,1,5,5,5-hexakis(dimethylamino)-3-[tris(dimethylamino)phosphoranylidene]amino}-1  $\Lambda^5$ ,3  $\Lambda^5$ ,5  $\Lambda^5$ -1,4-triphosphazadiene, (P<sub>4</sub>-*t*-Bu), 0.85 M in hexane (all Sigma-Aldrich) were used as received. Benzyl alcohol was purified by distillation from calcium hydride and stored over molecular sieves. Dichloromethane (DCM) was purified by first stirring over calcium hydride for 24 h and then refluxing for 2 h, before distillation, and stored over molecular sieves. Diethyl ether (DEE) was purified by drying over anhydrous magnesium sulphate for 24 h and distilling, and stored over molecular sieves. Methanol was used as received. Pentane was distilled from calcium hydride and stored over molecular sieves. Tetrahydrofuran (THF) was dried by stirring over calcium hydride for

## Chapter 3

---

24 h, refluxed over sodium and benzophenone for 4 h before distillation, and stored over molecular sieves. Toluene was dried by stirring over calcium hydride for 24 h, refluxing for 2 h, followed by distillation, and stored over molecular sieves.

### 3.2.2 Methods

#### 3.2.2.1 NMR

One dimensional  $^1\text{H}$  NMR and  $^{13}\text{C}$  NMR spectra were acquired with a Varian VXR-Unity (400 MHz). Samples were prepared in deuterated solvents obtained from Sigma Aldrich. All chemical shifts are reported as parts per million (ppm) with tetramethylsilane as reference.

#### 3.2.2.2 SEC

A Waters 1515 isocratic HPLC pump and a Waters 717 plus auto-sampler by Breeze Version 3.30 SPA software was used. A Waters in-line degasser and a Waters 2414 differential refractometer were operated at 30 °C whilst in series with a Waters 2487 dual wavelength absorbance UV/Vis detector set to 254 nm and 365 nm. THF was used as the eluent (HPLC grade, stabilized with 0.125 % BHT) with a flow rate of 1 mL/min. An injection volume of 100  $\mu\text{L}$  was used to introduce the sample into Two PLgel (Polymer Laboratories) 5  $\mu\text{m}$  Mixed-C (300 $\times$ 7.5 mm) columns and a pre-column (PLgel 5  $\mu\text{m}$  Guard, 50 $\times$ 7.5 mm) which were kept at 30 °C. PS standards ranging from 580 g/mol to  $2\times 10^6$  g/mol were used as calibration standards in a 5 mg/mL concentration.

#### 3.2.2.3 TGA

TGA was performed on a Perkin Elmer TGA 7 instrument. Samples were heated from 20 °C to 300 °C at 20 °C/min under nitrogen atmosphere.

### 3.2.3 Polymer Synthesis

#### 3.2.3.1 General polymerization procedure

The theoretical molecular weight ( $M_n^{\text{Theoretical}}$ ) was calculated using Equation 3.1

$$M_n^{\text{Theoretical}} = \frac{[\text{monomer}]_0}{[\text{initiator}]_0} \times Mr_{\text{monomer}} \times \text{Conversion} + Mr_{\text{initiator}} \quad (\text{Eq 3.1})$$

The anionic polymerization of PA were conducted using benzyl alcohol as initiator and a phosphazene base as catalyst. All polymerizations were run at -75 °C, in THF for ten minutes before quenching by the addition of acetic anhydride, unless specified otherwise.

## Chapter 3

---

### 3.2.3.1.1 Anionic polymerization: Phosphazene base catalysts

For a  $M_n^{\text{Target}}$  of 10 000 g/mol, a catalyst to initiator ratio of 1:1 and a monomer concentration of 0.5 M, the following procedure was typical: in a glovebox, under an argon atmosphere, the monomer (0.20 g, 1.5 mmol), THF (1.5 mL) and a stirrer bar was added to the reaction flask. Benzyl alcohol (2.0  $\mu\text{L}$ , 0.020 mmol) and THF (0.5 mL) was then added to a second flask. To a third flask, the catalyst (0.020 mmol) and THF (0.5 mL) was added. Finally, the quenching agent (0.70 mL, 7.5 mmol) and THF (0.5 mL) was added to a fourth flask. All four flasks were then sealed with a rubber septum and secured with a cable tie before removing them from the glovebox. All four flasks were then placed in a liquid nitrogen/ethyl acetate bath (prepared to  $-78\text{ }^\circ\text{C}$ ) and allowed to cool to the desired temperature. The initiator solution was added to the solution first via a degassed syringe, followed by the addition of the catalyst via a degassed syringe two minutes later. After 10 min the quenching agent was added via a degassed syringe. After thirty minutes, the polymer was precipitated into cold methanol, isolated via centrifugation and dried at room temperature. Following analysis, all samples were stored under methanol at room temperature to avoid depolymerization from taking place.

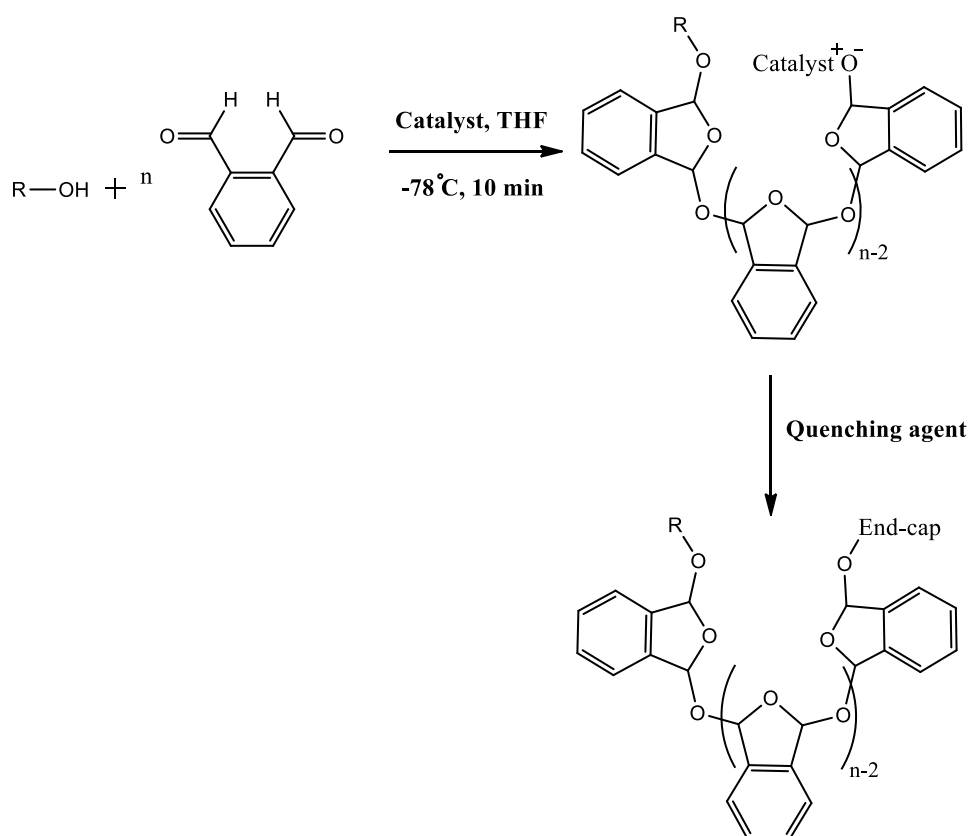
### 3.2.3.1.2 Anionic polymerization: Amine base catalysts

For a  $M_n^{\text{Target}}$  of 10 000 g/mol, a catalyst to initiator ratio of 1:1 and a monomer concentration of 0.5 M, the following procedure was typical: outside of a glovebox, the monomer (0.20g, 1.5 mmol) and THF (1.5 mL) was added to the reaction flask containing a stirrer bar. Benzyl alcohol (2.0  $\mu\text{L}$ , 0.020 mmol), the catalyst (0.020 mmol) and THF (1 mL) was then added to a second flask. The quenching agent (0.70 mL, 7.5 mmol) and THF (0.5 mL) was added to a third flask. All three flasks were sealed with a rubber septum and secured with a cable tie. All three flasks were then placed in a liquid nitrogen/ethyl acetate bath (set to  $-78\text{ }^\circ\text{C}$ ) and allowed to cool down to the desired temperature. After degassing both flasks with argon, the initiator/catalyst solution was added to first the reaction flask via a degassed syringe. After the polymerization reaction was complete the quenching agent was added to the first flask via a degassed syringe. After thirty minutes, the polymer was precipitated into cold methanol, isolated via centrifugation and dried at room temperature. Following analysis, all samples were stored under methanol at room temperature to avoid degradation from occurring.

### 3.3 Results and Discussion

#### 3.3.1 Systematic study of the influence of experimental parameters:

This study aimed to simplify the method by which to synthesize PPA via non-organometallic catalyst based anionic polymerization (Scheme 3.2). This entailed looking at various experimental parameters e.g. the catalyst type, catalyst to initiator ratio, monomer concentration, reaction time and solvent polarity.



Scheme 3.2. The anionic polymerization of *o*-phthalaldehyde.

##### 3.3.1.1 Effect of the catalyst type:

The effect the catalyst type and also the catalyst to initiator ratio (catalyst:initiator) have been investigated for the phosphazene base catalyzed anionic polymerization of EO.<sup>5</sup> In 1996, Möller and co-workers successfully polymerized EO with  $P_4-t\text{-Bu}$  for the first time. Even though this method allowed for a simple one-pot-synthesis of PEO, the polymers were characterized by broad dispersities ( $D$ ), attributed to chain transfer reactions.<sup>5</sup> Then, Zhao *et al.* reported the use of the less reactive  $P_2-t\text{-Bu}$  in the preparation of well-defined PEO without the appearance of any chain transfer reactions.<sup>6</sup>  $P_1-t\text{-Bu}$  has been reported as being unable to

### Chapter 3

---

catalyze the polymerization of certain monomers due to insufficient basicity.<sup>7</sup> In cases where this catalyst is successful, the results are often better than those obtained with the more reactive phosphazene base catalysts.<sup>7</sup> Optimum catalyst:initiator have been shown to depend on the catalysts activity/basicity.<sup>3</sup> For the more active catalysts a ratio of 1:1 is sufficient to obtain well-defined polymers.<sup>3,9</sup> For the less reactive catalysts, an excess of the catalyst is required.<sup>3,9</sup> However, studies by Zhao *et al.* have shown that this ratio should be lowered depending on the activity of the catalyst.<sup>6,8</sup> For the more active P<sub>4</sub>-*t*-Bu, it has been reported that a catalyst:initiator as low as 0.01:1 aids in suppressing the appearance of side reactions.<sup>9</sup>

Table 3.1 shows the results obtained for the phosphazene base catalyzed anionic polymerization of PA. Similar to the results obtained by DeWinter *et al.*, the results in Table 3.1 strongly suggest that the more reactive P<sub>4</sub>-*t*-Bu (pK<sub>a</sub> 42.7) does not allow for good control over the anionic polymerization of PA.<sup>3,6,8,10</sup> A decrease in the amount of catalyst relative to that of the initiator led to improved control and an increase in the molecular weight, with equimolar amounts of the initiator and catalyst producing the best results. Improved results in terms of control and molecular weight were obtained for the less reactive P<sub>2</sub>-*t*-Bu (pK<sub>a</sub> 33.5) catalyst.<sup>10</sup> A similar relationship between the catalyst:initiator, dispersity and molecular weight was observed.

Results for the polymerization of PA using the least reactive P<sub>1</sub>-*t*-Bu (pK<sub>a</sub> 28.3) catalyst, shows that the reactions proceeded with good control.<sup>10</sup> It stands to reason therefore that the diminished polymerization activity of P<sub>1</sub>-*t*-Bu allows for it to be used in excess whilst still maintaining control over the reaction. An equimolar amount of the catalyst and initiator resulted in no polymer being formed. This can be ascribed to insufficient basicity of the system and could also explain the improvement in polydispersity with increasing amount of catalyst relative to that of the initiator.<sup>7</sup> As the catalyst:initiator increases, so does the basicity of the system, enabling the catalyst to act more efficiently.



## Chapter 3

**Table 3.1. Results for the anionic polymerization of PA with P<sub>1</sub>-*t*-Bu, P<sub>2</sub>-*t*-Bu and P<sub>4</sub>-*t*-Bu phosphazene base catalysts with different catalyst:initiator.**

Catalyst	[Cat]:[Init]	$M_n^{\text{Theoretical}}$ (g/mol)	$M_n^{\text{SEC}}$ (g/mol)	$\bar{D}$	Yield (%)
P <sub>1</sub> - <i>t</i> -Bu	1:1	No polymer			
	2:1	4 200	2 500	1.3	42
	4:1	4 400	2 300	1.2	44
	6:1	4 300	2 200	1.1	43
P <sub>2</sub> - <i>t</i> -Bu	1:1	4 100	3 500	1.5	41
	2:1	4 400	3 200	1.6	44
	4:1	4 200	2 700	2.0	42
P <sub>4</sub> - <i>t</i> -Bu	1:1	4 300	3 700	1.8	43
	2:1	4 000	2 300	2.5	40
	4:1	4 200	2 000	3.0	42

All reactions were run in THF, with a [monomer] of 0.5 M for 10 min before quenching with acetic anhydride.  
 $M_n^{\text{Target}} = 10\,000$  g/mol

Figure 3.3 shows an overlay of the SEC traces for PPA prepared in the presence of P<sub>4</sub>-*t*-Bu with different catalyst:initiator. The trace representing the polymerization run with equimolar amounts of catalyst and initiator shows a highly symmetrical peak. In contrast to this, the traces representing polymerizations run with an excess amount of catalyst relative to that of the initiator shows the appearance of a prominent shoulder peak on the lower elution time/high molecular weight side of the spectrum. These results are in good agreement with those obtained by DeWinter *et al.*, who reasoned that the appearance of these peaks along with the broad dispersities obtained suggests the appearance of possible reshuffling reactions typical of anionic polymerizations.<sup>3</sup>

## Chapter 3

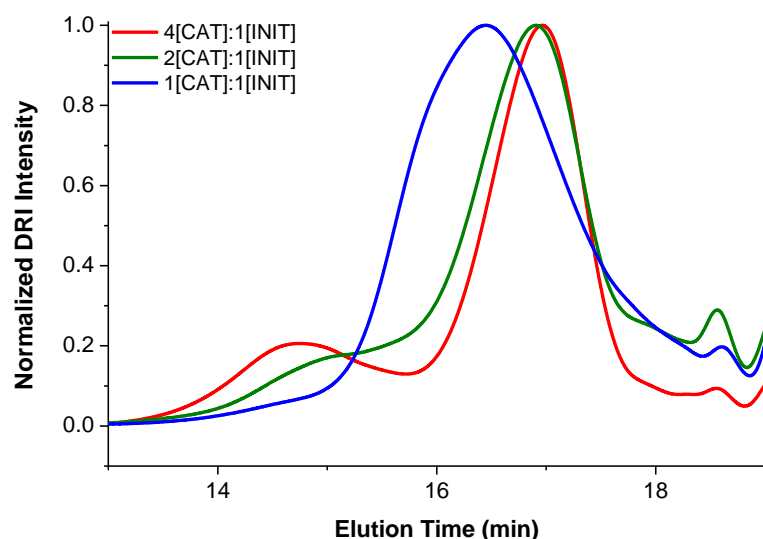


Figure 3.3. An overlay of the SEC traces of PPA prepared with  $P_4$ -*t*-Bu with different catalyst:initiator.

Figure 3.4 shows an overlay of the SEC traces for PPA prepared using  $P_1$ -*t*-Bu with different catalyst:initiator. As expected no shoulder peaks are present, suggesting the absence of any side reactions. From these results, one can conclude that  $P_1$ -*t*-Bu, when used in excess, is the most suitable of the three commercially available phosphazene base catalysts for the anionic polymerization of PA.

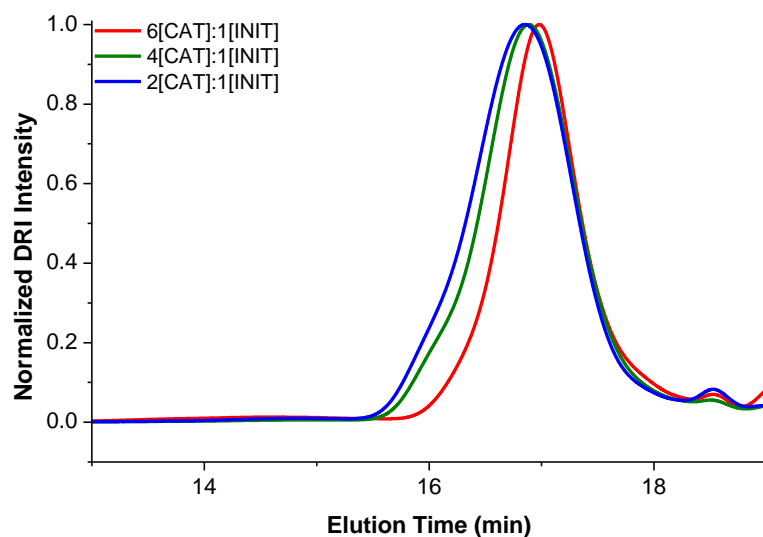


Figure 3.4. An overlay of the SEC traces of PPA prepared with  $P_1$ -*t*-Bu with different catalyst:initiator.

Whilst phosphazene base catalysts have shown great promise as non-organometallic alternatives to organometallic catalysts, they are highly sensitive to air and oxygen and must therefore be handled in a glovebox. They are also very expensive. Amine base catalysts such as TBD and DBU on the other hand require less delicate experimental conditions and are much more affordable. Table 3.2 is a summary of the results obtained for the amine base catalyzed

### Chapter 3

---

anionic polymerization of PA. Of the two amine base catalysts, the more reactive TBD was unable to catalyze the reaction. DBU on the other hand, led to the successful polymerization of PA with similar control and improved conversions when compared to P<sub>1</sub>-*t*-Bu. This was a surprising result as one would not expect the less reactive DBU to be able to catalyze the polymerization reaction if the more reactive TBD was unable to do so. This was however the case regardless of the catalyst:initiator and solvent, as the TBD catalyzed polymerization of PA was attempted in both DCM and THF.

A possible reason for the lack of activity when using TBD is that it is poorly solvated in both THF and DCM. Its poor solubility can be promoted even further by the need for low very temperatures when polymerizing PA. Horn *et al.* compared the ability of TBD and DBU to catalyze transesterification reactions using both computational and experimental approaches.<sup>11</sup> Their calculations predicted that TBD would be a more active catalyst, however, their experimental results showed that DBU was in fact more effective in catalyzing the transesterification reactions.<sup>11</sup> They concluded that their calculations were not as accurate due to the fact that they ignored solvation effects.<sup>11</sup> In an unrelated study, Xue *et al.* compared the use of DBU and TBD as catalysts in the transesterification of soybean oil and ethanol.<sup>12</sup> They found that DBU was an effective homogeneous catalyst as it was able to dissolve the alcohol, whilst TBD was not.<sup>12</sup> The results of these studies indicates that DBU reacts more readily with an alcohol than TBD. This can possibly explain the success of DBU as a catalyst in the anionic polymerization of PA compared to TBD, since the initiator used in this work is a primary alcohol.

## Chapter 3

**Table 3.2. Results for the TBD and DBU catalyzed anionic polymerization of PA with different catalyst:initiator.**

Catalyst	[Cat]:[Init]	Solvent	$M_n^{\text{Theoretical}}$ (g/mol)	$M_n^{\text{SEC}}$ (g/mol)	$\bar{D}$	Yield (%)
TBD	1:1	THF		No polymer		
		DCM				
	2:1	THF		No polymer		
		DCM				
	4:1	THF		No polymer		
		DCM				
	6:1	THF		No polymer		
		DCM				
DBU	1:1	THF		No polymer		
	2:1	THF	6 200	5 500	1.3	60
	4:1	THF	6 000	5 200	1.2	62
	6:1	THF	5 900	5 000	1.2	60

All reactions were with a [monomer] of 0.5 M for 10 min before quenching with acetic anhydride.

$M_n^{\text{Target}} = 10\,000$  g/mol

In the case of DBU, catalyst:initiator did not have an influence on the monomer conversion, however,  $\bar{D}$  values slightly decreased with increasing catalyst:initiator. Noticeably higher  $M_n^{\text{Theoretical}}$  and  $M_n^{\text{SEC}}$  were obtained for the DBU catalyzed polymerization reactions compared to that which was obtained with the  $P_1$ -*t*-Bu catalyzed polymerization reactions.

Figure 3.5 shows an overlay of the SEC traces of PPA prepared in the presence of DBU with different catalyst:initiator. High symmetry peaks without the appearance of any shoulder peaks can be seen for all catalyst:initiator. The absence of any shoulder peaks in the SEC traces suggests that the DBU catalyzed anionic polymerization of PA proceeds without the appearance of any side reactions.

## Chapter 3

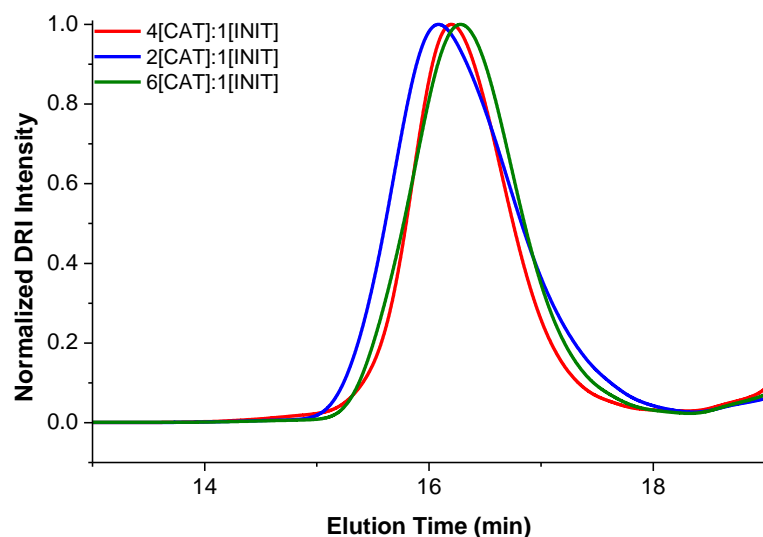


**Figure 3.5. SEC traces for DBU catalyzed anionic polymerization of PA with different catalyst:initiator.**

The absence of any side reactions, higher gravimetric yields and improved correlations between the  $M_n^{\text{Theoretical}}$  and  $M_n^{\text{SEC}}$  suggests that DBU is a more efficient catalyst than  $P_1-t\text{-Bu}$ . Further justification for this conclusion, is the fact that DBU is much less expensive than the phosphazene base catalyst and does not require delicate experimental conditions such as the need to work in a glovebox. The ability of DBU to act as a more efficient catalyst when compared to  $P_1-t\text{-Bu}$ , even though it is a weaker base, is believed to lie in its stability as a compound when compared to the highly sensitive phosphazene base.

The results shown in Table 3.2 indicates that DBU could be used optimally in a catalyst:initiator of 4:1. Figure 3.6 shows the assigned  $^1\text{H}$  NMR spectrum of PPA prepared under these conditions.

## Chapter 3

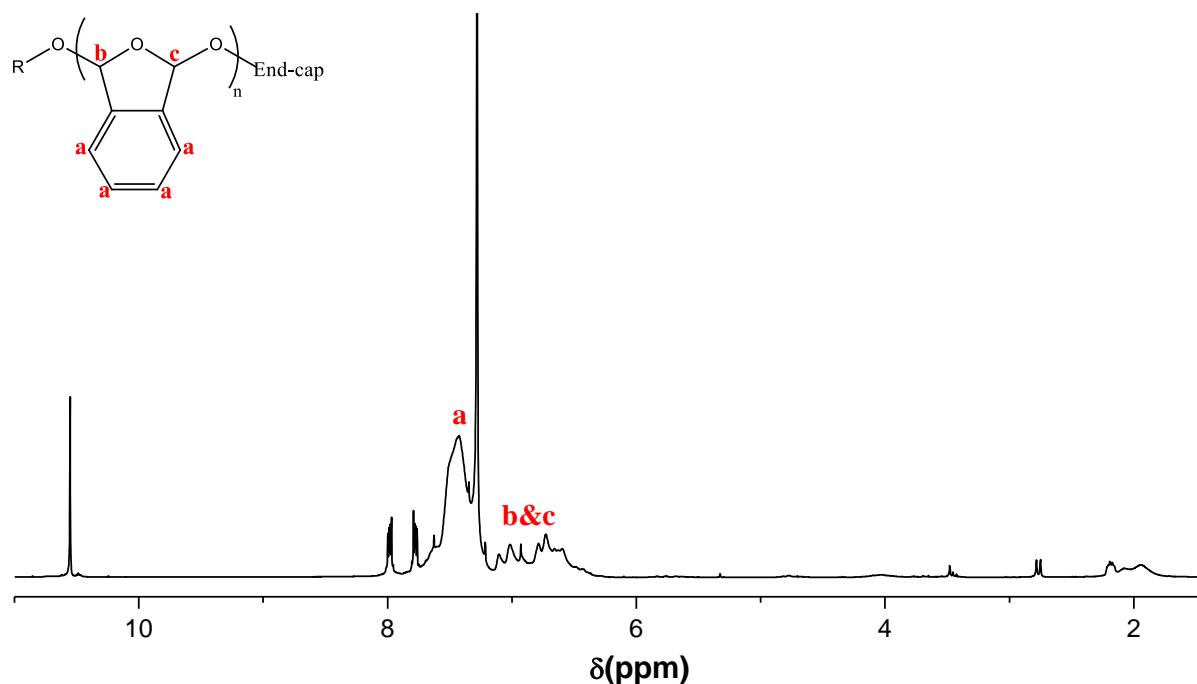


Figure 3.6.  $^1\text{H}$  NMR spectrum ( $\text{CDCl}_3$ ) of PPA prepared with DBU as catalyst, a with catalyst:initiator of 4:1, monomer concentration of 0.5 M, THF as solvent and reaction time of ten minutes.

### 3.3.1.2 Monomer concentration

Table 3.3 summarizes the effects of monomer concentration on the anionic polymerization of PA, comparing  $\text{P}_1$ -*t*-Bu and DBU catalyzed polymerizations. Yields were found to be higher for polymerizations catalyzed by DBU, whilst lower  $\bar{D}$  were obtained in the case of  $\text{P}_1$ -*t*-Bu catalyzed polymerizations that were run with a catalyst:initiator of 1:1. A more interesting observation however, is that the agreements between the  $M_n^{\text{Theoretical}}$  and  $M_n^{\text{SEC}}$  were better for polymerizations catalyzed by DBU at higher monomer concentrations (1.0 M).

Table 3.3. Results for the anionic polymerization of PA with different monomer concentrations.

Catalyst	[Monomer] (M)	$M_n^{\text{Theoretical}}$ (g/mol)	$M_n^{\text{SEC}}$ (g/mol)	$\bar{D}$	Yield (%)
$\text{P}_1$ - <i>t</i> -Bu <sup>a</sup>	0.5	4 000	2 100	1.1	40
	1	4 300	3 500	1.3	43
DBU <sup>b</sup>	0.5	6 000	5 400	1.3	60
	1	9 200	9 000	1.4	92

All reactions were run in THF for 10 minutes before quenching with acetic anhydride.

$M_n^{\text{Target}} = 10\,000$  g/mol

<sup>a</sup> catalyst:initiator of 6:1

<sup>b</sup> catalyst:initiator of 4:1

### Chapter 3

Figure 3.7 and 3.8 shows an overlay of the SEC traces for polymerizations catalyzed by  $P_1$ -*t*-Bu and DBU, respectively, at different monomer concentrations. Both figures show a shift to a lower elution time, signifying an increase in molecular weight, upon increasing the monomer concentration from 0.5 M to 1.0 M.

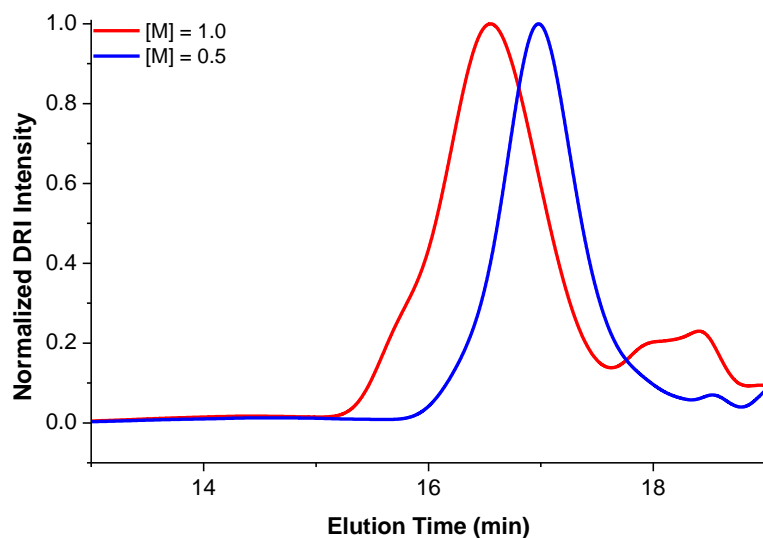


Figure 3.7. An overlay of the SEC traces for the  $P_1$ -*t*-Bu catalyzed anionic polymerization of PA with different monomer concentrations.

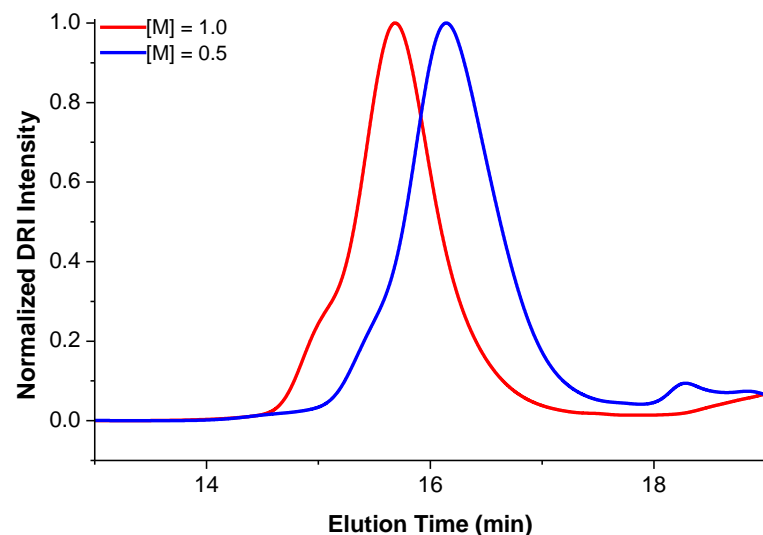


Figure 3.8. An overlay of the SEC traces for the DBU catalyzed anionic polymerization of PA with different monomer concentrations.

## Chapter 3

### 3.3.1.3 Reaction time:

Kinetic studies for both the  $P_1$ -*t*-Bu and DBU catalyzed polymerization of PA were carried out to determine the effect of reaction time on polymerization control and as such, determine the ideal reaction time.

Table 3.4 is a summary of the results obtained for the two kinetic studies. It is apparent that the polymerization of PA occurs very fast as maximum conversions were obtained after only 10 minutes. This is consistent with Vogl's findings in his 1964 study, in which he concluded that the organometallic anionic polymerization of aldehydes reaches a polymerization-depolymerization equilibrium within ten minutes.<sup>1</sup> At this equilibrium, the system is more susceptible to side reactions such as reshuffling reactions, resulting in loss of control, as can be seen by the gradual increase in the  $\bar{D}$  values with increasing reaction time.

**Table 3.4. Results for the kinetic study of both the  $P_1$ -*t*-Bu and DBU catalyzed polymerization of PA.**

Catalyst	Time (min)	$M_n^{\text{Theoretical}}$ (g/mol)	$M_n^{\text{SEC}}$ (g/mol)	$\bar{D}$	Yield (%)
$P_1$ - <i>t</i> -Bu <sup>a</sup>	10	4 300	2 400	1.1	43
	20	4 200	2 500	1.2	42
	30	4 000	2 300	1.5	40
DBU <sup>b</sup>	10	6 100	5 500	1.3	61
	20	6 200	5 200	1.4	62
	30	6 200	5 600	1.6	62

All reactions were run in THF with a [monomer] of 0.5 M with acetic anhydride as quenching agent.

$M_n^{\text{Target}} = 10\,000$  g/mol

<sup>a</sup> catalyst:initiator of 6:1

<sup>b</sup> catalyst:initiator of 4 :1

### 3.3.1.4 Solvent

The solubility of the PA was tested in a range of common solvents that vary in polarity. These solvents included: THF, DCM, DEE, toluene and pentane. However, PA was found to be soluble only in THF and DCM. As a result, an in-depth study investigating the effect of a range of solvents on the anionic polymerization of PA was not possible. The results for the polymerization of PA in THF and DCM is shown in Table 3.5.



### Chapter 3

**Table 3.5. Results for the anionic polymerization of PA in THF and DCM.**

Solvent	$M_n^{\text{Theoretical}}$ (g/mol)	$M_n^{\text{SEC}}$ (g/mol)	$\bar{D}$	Yield (%)
THF	6 100	5 500	1.3	61
DCM	4 800	4 300	1.8	48

All reactions were run in the presence of DBU with a catalyst:initiator of 4:1 and a [monomer] of 0.5 M for 10 minutes before quenching with acetic anhydride.

$M_n^{\text{Target}} = 10\,000$  g/mol

The study showed that DCM could be used as an alternative solvent to THF as it led to the successful polymerization of PA. However, the polymerization reaction that was run in DCM resulted in a lower  $M_n^{\text{Theoretical}}$  and  $M_n^{\text{SEC}}$  when compared to the reaction that was run in THF, suggesting that THF is the preferred solvent of the two. The favourable polymerization of PA in THF can be attributed to the poor solubility of the monomer in DCM, which is promoted even further by the sub-zero reaction temperatures.

#### 3.3.1.5 Molecular weight

The optimum conditions for the non-organometallic anionic polymerization of PA, determined in this work, was applied to the preparation of a series of PPA polymers with different targeted molecular weights. Table 3.6 is a summary of the results obtained from the study.

**Table 3.6. Summary of the results obtained for the preparation of PPA with different  $M_n^{\text{Target}}$ .**

$M_n^{\text{Target}}$ (g/mol)	$M_n^{\text{Theoretical}}$ (g/mol)	$M_n^{\text{SEC}}$ (g/mol)	$\bar{D}$	Yield (%)
2 500	2 400	2 100	1.3	96
5 000	4 800	4 600	1.1	96
7 500	6 800	6 200	1.2	90
10 000	8 800	7 600	1.2	88

All reactions were run in the presence of DBU with a catalyst:initiator of 4:1, in THF with a [monomer] of 1.0 M for 10 minutes before quenching with acetic anhydride.

Figure 3.9 shows an overlay of the SEC traces of the polymers prepared for the molecular weight study. The results shows that the molecular weight of PPA can be tailored by adjusting the monomer to initiator ratios when using DBU as catalyst. Figure 3.10 shows a comparison between the  $M_n^{\text{Theoretical}}$  and  $M_n^{\text{SEC}}$ . The figure shows that a linear relationship can be drawn

## Chapter 3

between the two. This study therefore confirms that the optimized DBU catalyzed system allows for the preparation of well-defined PPA with narrow  $\bar{D}$  and a good agreement between the  $M_n^{\text{Theoretical}}$  and  $M_n^{\text{SEC}}$ .

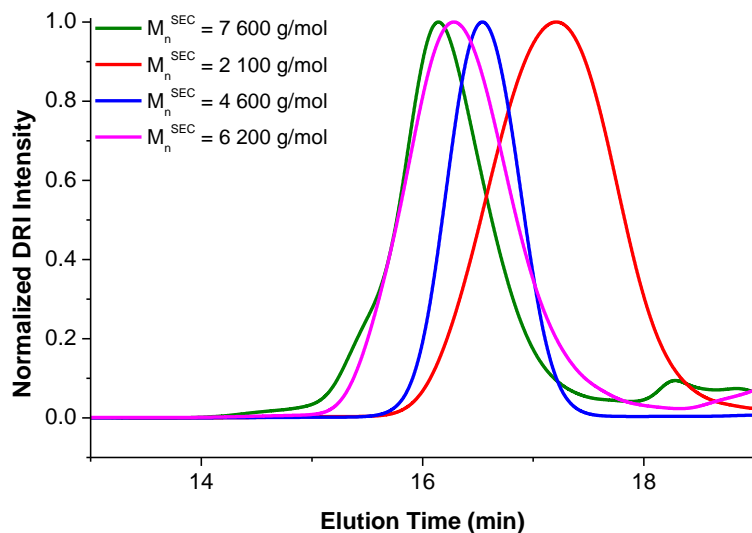


Figure 3.9. An overlay of the SEC traces for PPA polymers prepared with different  $M_n^{\text{Target}}$ .

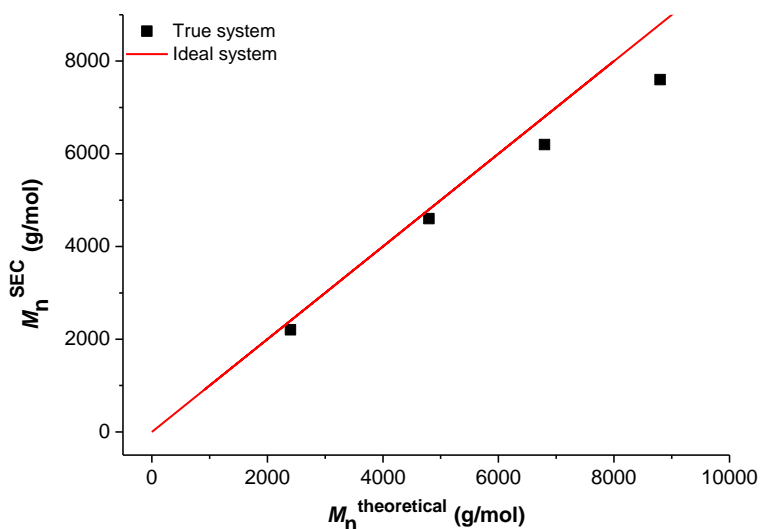
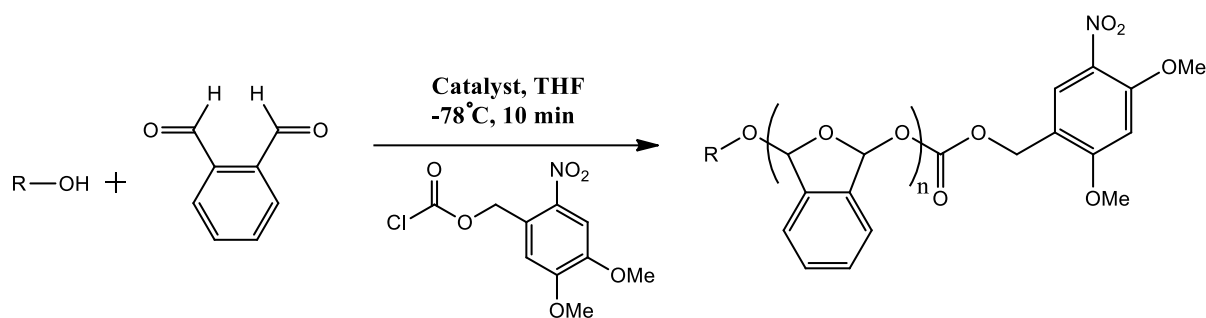


Figure 3.10. Graph showing the relationship between the  $M_n^{\text{Theoretical}}$  and  $M_n^{\text{SEC}}$ . The solid red line acts as a representation of an ideal system with a 100% conversion.

### 3.3.2 UV-labile end-caps:

4,5-Dimethoxy-2-nitrobenzyl carbonochloridate, a commercially available UV-labile end-cap, was used to demonstrate that the DBU catalyzed system is amendable to end-functionalization with end-groups that are desirable for applications that require UV-type triggers for self-immolation.<sup>5</sup> Scheme 3.3 shows the preparation of PPA with the UV-labile end-cap.

## Chapter 3



**Scheme 3.3.** Preparation of PPA with 4,5-dimethoxy-2-nitrobenzyl carbonochloridate as quenching agent.

Table 3.7 shows the results for the DBU catalyzed anionic polymerization of PA using 4,5-dimethoxy-2-nitrobenzyl carbonochloridate as quenching agent. Analysis of these polymers by SEC indicates that they were successfully capped with the UV-labile end-cap. It was observed that the yields reported for these reactions were very poor compared to those where acetic anhydride was used as quenching agent. This is believed to be due to the poor solubility of the quenching agent in THF. DCM was considered as an alternative. However, the compound was found to be completely insoluble in the solvent.

**Table 3.7.** Results for the anionic polymerization of PA with 4,5-dimethoxy-2-nitrobenzyl carbonochloridate as quenching agent.

Entry	$M_n^{\text{Target}}$ (g/mol)	$M_n^{\text{Theoretical}}$ (g/mol)	$M_n^{\text{SEC}}$ (g/mol)	$\bar{D}$	Yield (%)
1	5 000	2 700	2 400	1.4	54
2	5 000	2 500	2 200	1.3	50

All reactions were run in the presence of DBU with a catalyst:initiator of 4:1, in THF and a [monomer] of 1.0 M for 10 minutes before quenching with 4,5-dimethoxy-2-nitrobenzyl carbonochloridate.

To confirm that the PPA polymers had indeed been capped by the UV-labile end-cap, the UV end-capped PPA was analyzed by SEC, with the UV-detector of the SEC instrument set to a wavelength that would allow for the selective detection of a specific chain-end.<sup>22</sup> The wavelength at which 4,5-dimethoxy-2-nitrobenzyl carbonochloridate shows absorbance was first confirmed by UV spectroscopy. Figure 3.11 shows an overlay of the UV spectra for the UV-labile end-cap only (green), PPA believed to be capped with the UV-labile end-cap (red) and PPA prepared with acetic anhydride as quenching agent (blue). The UV spectrum for 4,5-dimethoxy-2-nitrobenzyl carbonochloridate shows two peaks at 297 nm and 345 nm. The peak at 297 nm represents the absorption of the carbonyl group whilst the peak at 345 nm represents that of the aromatic ring.<sup>15</sup> The UV spectrum of PPA capped with the UV-labile end-cap overlays almost perfectly with the spectrum of 4,5-dimethoxy-2-nitrobenzyl

### Chapter 3

carbonochloridate. The UV spectrum of PPA prepared with acetic anhydride as quenching agent shows only the peak representing the absorption of the aromatic ring at 297 nm.<sup>15</sup> Based on these results it was concluded that PPA capped with the UV-labile end-cap would be detected at a wavelength of 345 nm.

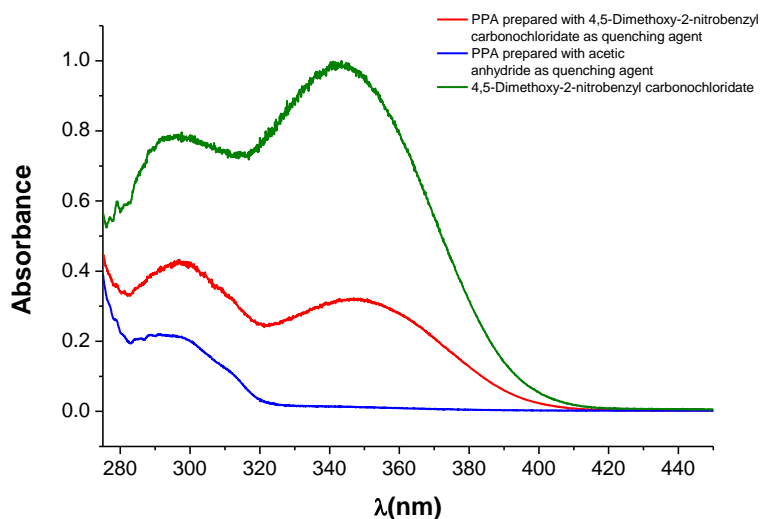


**Figure 3.11.** An overlay of the UV-vis spectra for 4,5-dimethoxy-2-nitrobenzyl carbonochloridate (green), PPA prepared with 4,5-dimethoxy-2-nitrobenzyl carbonochloridate as quenching agent (red) and PPA prepared with acetic anhydride as quenching agent (blue).

Figure 3.12 shows an overlay of the SEC traces of the UV (red) and DRI (blue) signals for run 2 (Table 3.7) with the UV detector set to 345 nm. The overlay of the two traces is evidence that the PPA chain-ends had indeed been capped by the UV-labile end-cap.

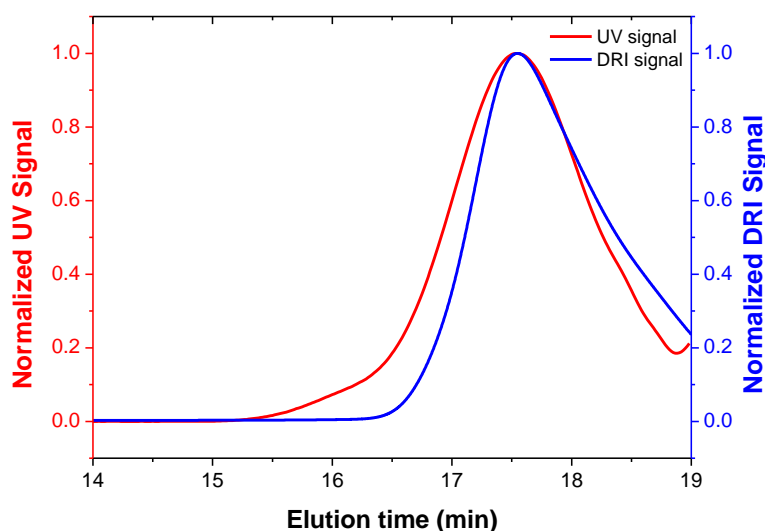


**Figure 3.12.** An overlay of the SEC trace comparing the UV (red) and the DRI (blue) signals of PPA prepared with 4,5-dimethoxy-2-nitrobenzyl carbonochloridate as quenching agent.

### Chapter 3

#### 3.3.3 Carboxylic acids as initiators for the anionic polymerization of PA

Previous reports on the non-organometallic anionic polymerization of PA have all made use of a primary alcohol as the initiator.<sup>2, 3, 4, 8, 14</sup> Whilst this is not surprising when taking the sensitivity of the SIP into consideration, it does limit its potential application. In an effort to broaden the scope of method development, the DBU catalyzed anionic polymerization of PA was attempted with a carboxylic acid as the initiator. Table 3.8 shows the results obtained for the polymerization of PA using either benzoic, linoleic or pyrenebutyric acid as the initiator. The results show that the reactions had all proceeded with good control and a good agreement between the  $M_n^{\text{Theoretical}}$  and  $M_n^{\text{SEC}}$ . Figure 3.13 shows an overlay of the SEC traces for entry 1, 3 and 5 (Table 3.8). The high symmetry of the peaks confirms that the polymers were all prepared with narrow molecular weight distributions. Figure 3.14 shows the  $^1\text{H}$  NMR spectrum of PPA prepared using linoleic acid as initiator (entry 3, Table 3.8). The signals representing the initiating group would be expected to appear in the region of 1.9-2.2 ppm and 5.7-6.5 ppm. However, none of these signals were visible on the  $^1\text{H}$  NMR spectrum of the polymer. This was also the case for PPA prepared using pyrenebutyric acid as the initiator. These results indicate that the polymerization reactions had been initiated by something other than the carboxylic acids. One possible explanation might be that the DBU catalyst is capable of initiating the polymerization of PA by itself. However, this would take further investigation to prove.

**Table 3.8. Results for the DBU catalyzed anionic polymerization of PA from different initiating groups.**

Entry	Initiator	$M_n^{\text{Target}}$ (g/mol)	$M_n^{\text{Theoretical}}$ (g/mol)	$M_n^{\text{SEC}}$ (g/mol)	$M_n^{\text{NMR}}$ (g/mol)	$\bar{D}$	Yield (%)
1	Benzoic acid	5 000	3 000	2 600	-	1.3	60
2	Benzoic acid	5 000	3 100	2 700	-	1.3	62
3	Linoleic acid	5 000	3 500	3 200	3 100	1.1	70
4	Linoleic acid	5 000	3 400	2 600	2 300	1.3	67
5	Pyrenebutyric acid	5 000	3 000	2 300	2 400	1.2	60
6	Pyrenebutyric acid	5 000	3 600	3 300	3 400	1.2	71

All reactions were run in the presence of DBU with a catalyst:initiator of 4:1 and a [monomer] of 1.0 M for 10 minutes before quenching with acetic anhydride.

## Chapter 3

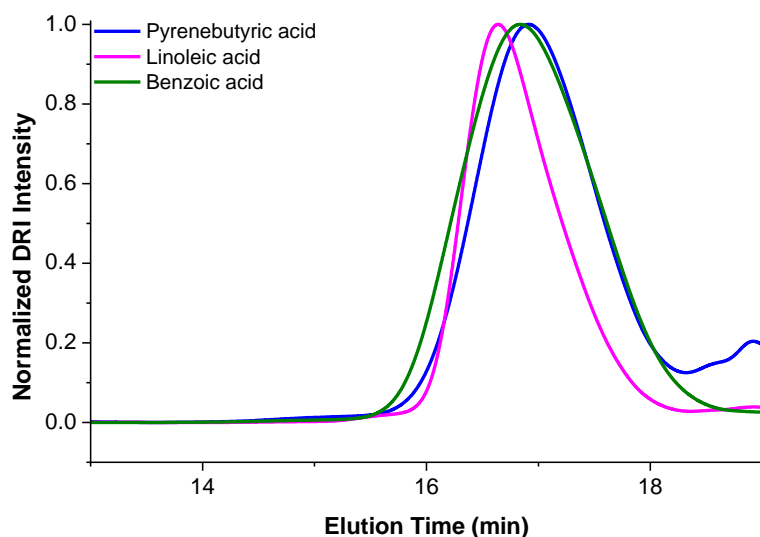


Figure 3.13. An overlay of the SEC traces for the anionic polymerization of PA with a carboxylic acid as initiator (entry 1, 3 and 5, Table 3.8).

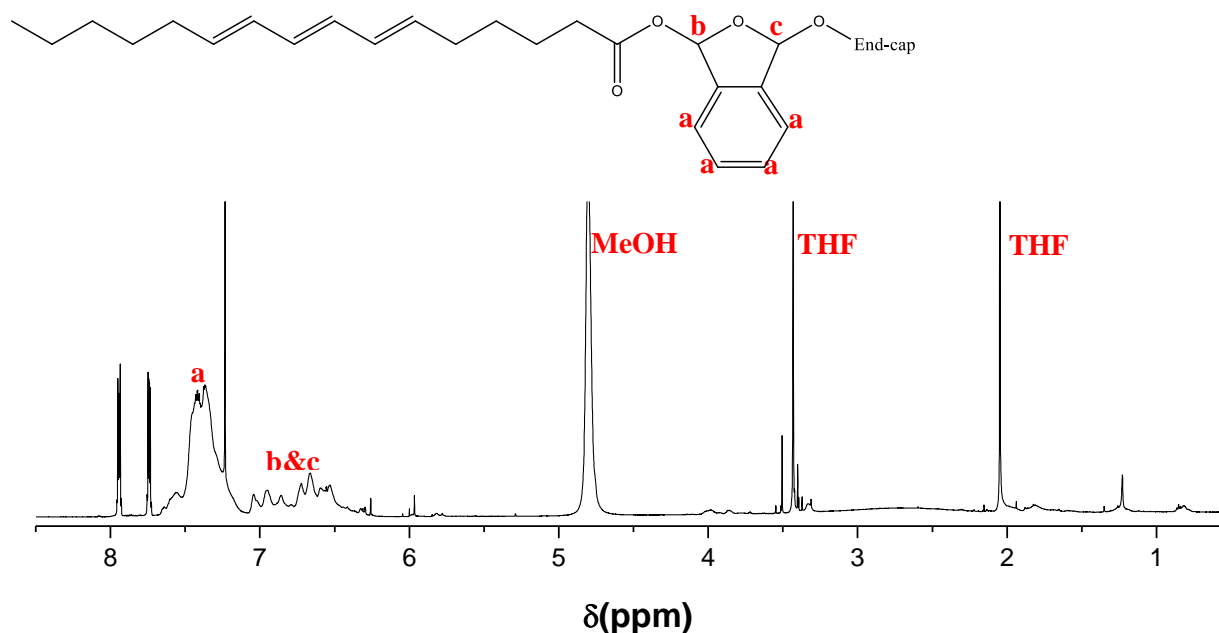


Figure 3.14. <sup>1</sup>H NMR spectrum (CDCl<sub>3</sub>) of PPA prepared with linoleic acid as initiator (entry 3, Table 3.8).

### 3.3.4 Investigation of polymer microstructure:

In 1969, Aso and Tagami prepared PPA by organometallic catalyst-based anionic polymerization.<sup>17</sup> They then determined the stereochemical structure (*cis* or *trans*) of the polymer by <sup>1</sup>H NMR spectroscopy. Their results indicated that the anionic polymerization process favoured the formation of the *cis*-stereoisomer (~ 60 mol %).

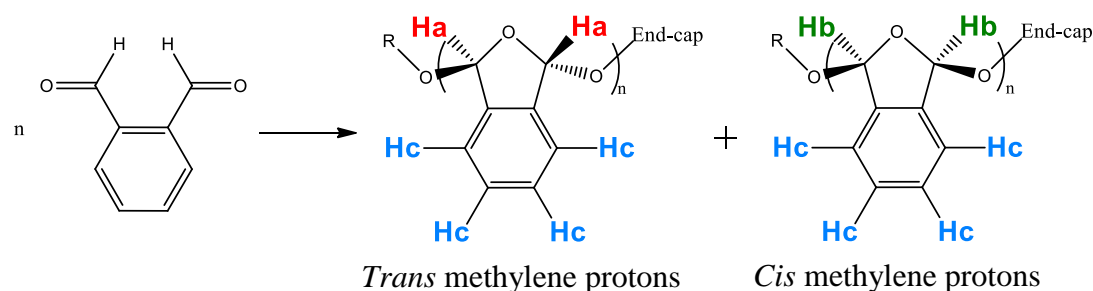
### Chapter 3

Since then, other research groups have reported similar results for the phosphazene base catalyzed anionic polymerization of PA.<sup>13</sup>

Scheme 3.4 shows the two possible stereoisomers of PPA. Figure 3.15 shows the <sup>1</sup>H NMR spectrum of the polymer prepared under the optimum conditions determined in this work. Consistent with the <sup>1</sup>H NMR spectroscopy results in previous reports, two signals appear at 6.90 ppm and 6.59 ppm.<sup>13, 17</sup> Aso and Tagami stated that these signals corresponded to the *trans* (H<sub>a</sub>) and *cis* (H<sub>b</sub>) methylene protons of PPA, respectively. This statement was made based on the fact that the distance between peaks H<sub>a</sub> and H<sub>b</sub> for PPA were very similar to the distance between the methine peaks of two isomers of model compounds, 1,3-dimethoxyphthalan and 1,3-diethoxyphthalan.<sup>17</sup> The *trans* content of the polymer could therefore be determined from Equation 3.2.<sup>17</sup>

$$\% \text{ trans stereoisomer} = \frac{H_a}{(H_a + H_b)} \times 100 \quad (\text{Eq 3.2})$$

By applying Equation 3.2 to the integration values of Figure 3.15 it was determined that PPA, prepared under the optimum conditions determined in this work, consisted of a 40 % *trans* and 60 % *cis* mixture of the two stereoisomers. The same method was applied to determine the stereochemical structure of PPA prepared using P<sub>1</sub>-*t*-Bu with a catalyst: initiator of 6:1. It was determined that the polymer prepared under these conditions consisted of a 36 % *trans* and 64 % *cis* mixture of the two stereoisomers. The similarity in the stereochemical structure of PPA prepared by the two non-organometallic catalysts and that which has been reported in literature, confirms the preferred formation of the *cis*-stereoisomer for the anionic polymerization of PA.<sup>13, 17</sup>



**Scheme 3.4.** A mixture of the *trans* and *cis* stereoisomers of PPA, following the anionic polymerization of PA.

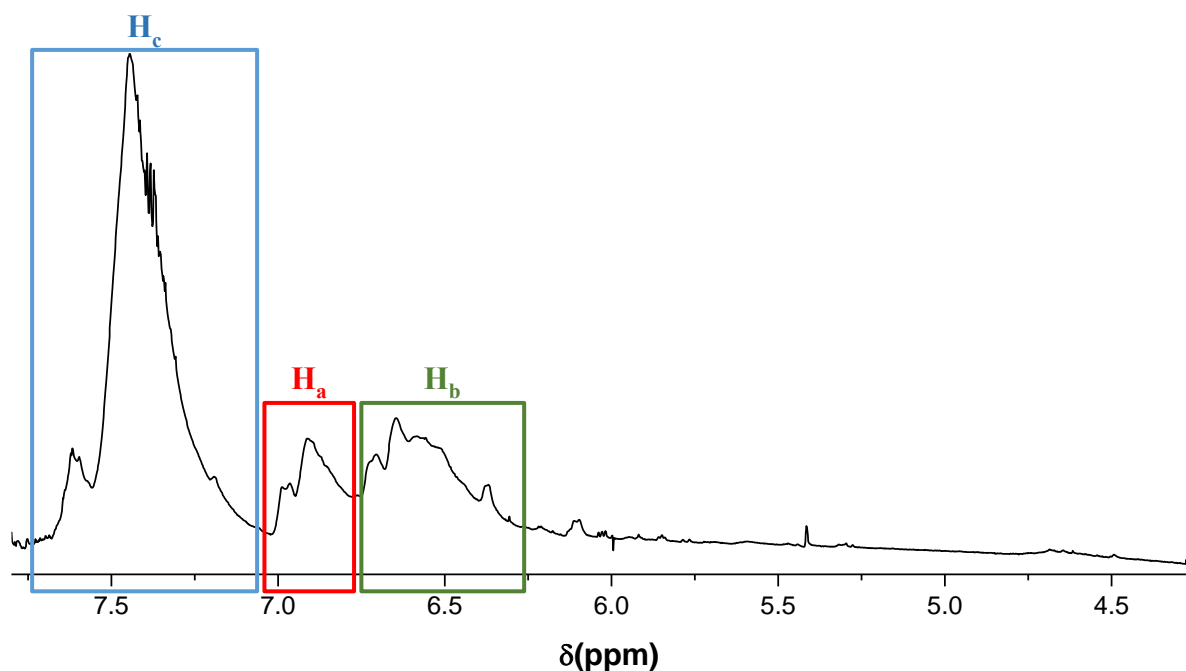


**Figure 3.15.** <sup>1</sup>H NMR spectrum (CDCl<sub>3</sub>) of PPA prepared with DBU as catalyst, a with catalyst:initiator of 4:1, monomer concentration of 1.0 M, THF as solvent and reaction time of ten minutes.

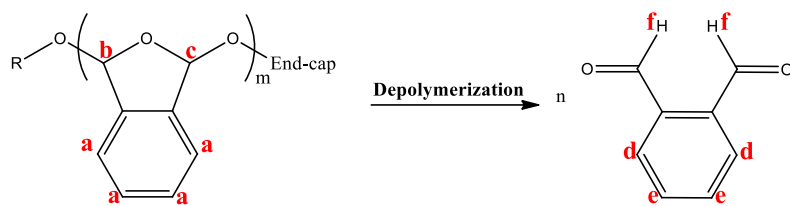
### 3.3.5 Investigation of the self-immolative nature of PPA.

To demonstrate the degradability/self-immolative nature of the PPA prepared under the optimum conditions determined in this work, <sup>1</sup>H NMR spectra of the same sample left undisturbed in a deuterated solvent, was taken over a two month period.

Scheme 3.5 shows the depolymerization of PPA into its monomeric units. Figure 3.16 shows an overlay of these <sup>1</sup>H NMR spectra. Figure 3.16a shows the spectrum of the sample taken shortly after the polymer had been prepared. The spectrum is dominated by the polymer chain's signals, with monomer signals being barely observable. The spectrum taken one month later indicates that some degradation had occurred as signals representing both the monomer and polymer are clearly visible (Figure 3.16b). Finally, Figure 3.16c shows that complete degradation had occurred after two months as only signals representing the monomer is observed. The complete degradation of PPA over time, even when left undisturbed in a deuterated solvent, testifies to the ready degradability of the polymer. The result of this study is in good agreement with what has been reported in literature on the inherent instability of PPA.<sup>3,4</sup>



## Chapter 3



Scheme 3.5. The depolymerization of PPA into its monomeric units.

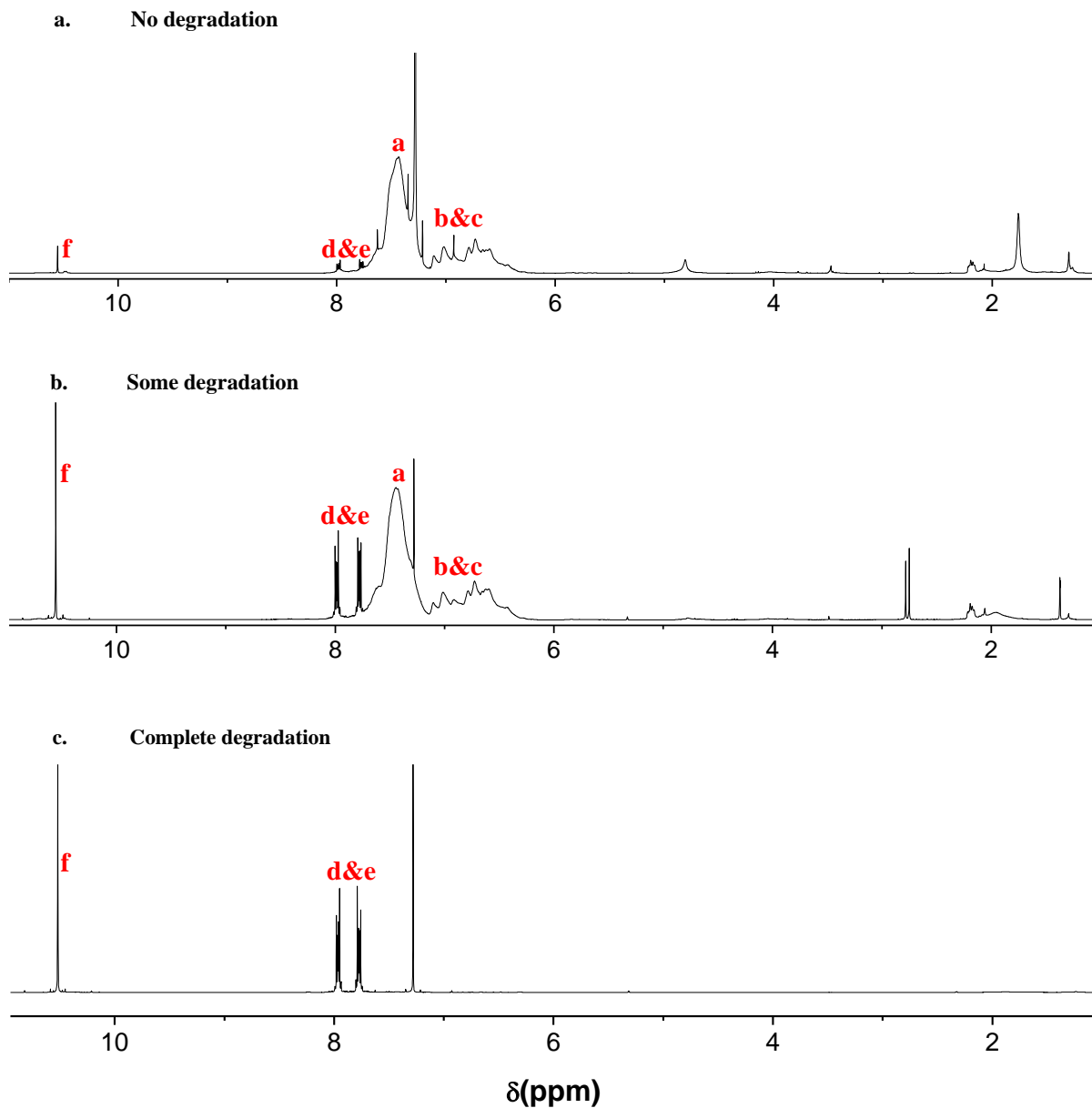
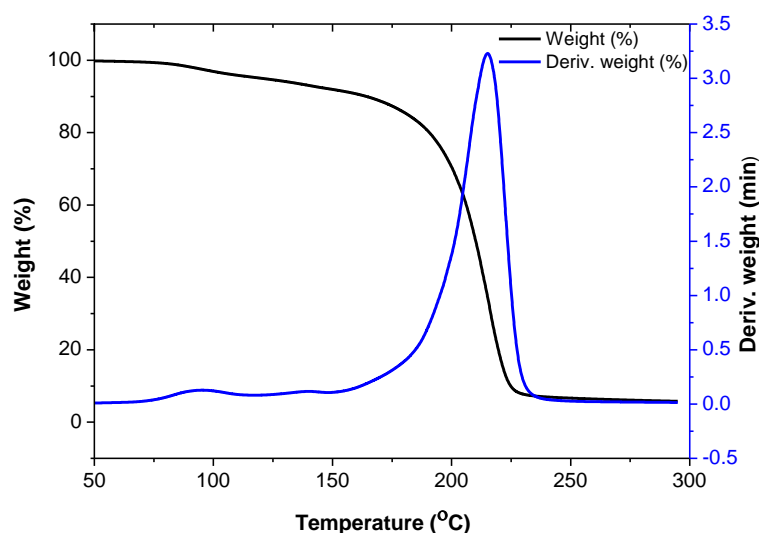


Figure 3.16. An overlay of the  $^1\text{H}$  NMR spectra ( $\text{CDCl}_3$ ) of PPA, prepared under the optimum conditions determined in this work, taken over a two month period: (a) no degradation, (b) some degradation after one month, (c) complete degradation after two months.

## Chapter 3

### 3.3.6 Thermal analysis:

The thermal stability of PPA, prepared under the optimum conditions determined in this work, was investigated by TGA. Figure 3.17 presents the TGA results for PPA. The derivative of the thermogravimetric curve shows one well-defined weight loss step within the temperature range of 156-230 °C, as well as an insignificant weight loss step at 100 °C. The 7 % weight loss at 100 °C can be attributed to the evaporation of water. The major weight loss of 93 % between 156-230 °C is the result of the degradation of PPA. This result is in good agreement with what has been reported in literature.<sup>18, 19, 21</sup> The single well-defined weight loss step confirms the preparation of well-defined PPA and also demonstrates the ready degradability of the polymer system.



**Figure 3.17.** TGA thermogram of PPA prepared with DBU as catalyst, a with catalyst:initiator of 4:1, monomer concentration of 1.0 M, THF as solvent and reaction time of ten minutes.

## 3.4 Conclusions

A facile method for the non-organometallic catalyst based anionic polymerization of PA was introduced. The method is an improvement on those that have been reported thus far as it eliminates the need for a glovebox and expensive reagents, whilst still allowing for the preparation of well-defined PPA. It was also shown that the DBU catalyzed system allowed for the use of different quenching agents, thereby broadening its scope of potential applications.

The method was successfully optimized by carrying out a systematic study investigating the effect of several experimental parameters on the polymerization reaction. These parameters included the effect of the catalyst type, catalyst to initiator ratio, monomer concentration,

### Chapter 3

---

reaction time and solvent polarity. The effect of three different phosphazene base catalysts, P<sub>1</sub>-*t*-Bu, P<sub>2</sub>-*t*-Bu and P<sub>4</sub>-*t*-Bu, and two amine base catalysts, TBD and DBU, were investigated. Of the three phosphazene base catalysts, the least reactive P<sub>1</sub>-*t*-Bu allowed for the best control. The more reactive P<sub>2</sub>-*t*-Bu and P<sub>4</sub>-*t*-Bu was found to promote the appearance of side reactions, resulting in broad *D*. Of the two amine base catalysts investigated, only DBU was able to catalyze the polymerization of PA. Upon comparing the results obtained for reactions catalyzed by P<sub>1</sub>-*t*-Bu to that of the reactions that were catalyzed by DBU, it was concluded that the ideal catalytic system consisted of DBU as catalyst with a catalyst to initiator ratio of 4:1, as it allowed for good control, and better agreement between the  $M_n^{\text{Theoretical}}$  and  $M_n^{\text{SEC}}$ . For the DBU catalyzed system, increasing the monomer concentration from 0.5 M to 1.0 M was found to greatly improve the agreement between the  $M_n^{\text{Theoretical}}$  and  $M_n^{\text{SEC}}$ . THF was identified as the most favourable solvent and the anionic polymerization of PA was found to reach its maximum conversion under ten minutes. The preparation of a series of PPA polymers with different  $M_n^{\text{Target}}$ , confirmed that the optimized method allowed for the preparation of PPA with narrow *D* and a good agreement between the  $M_n^{\text{Theoretical}}$  and  $M_n^{\text{SEC}}$ .

The microstructure, self-immolative nature and thermal properties of PPA, prepared under the optimum conditions determined in this work, was also investigated. Analysis of the polymer by <sup>1</sup>H NMR showed that polymer consisted of a 60 % *cis* and 40 % *trans* mixture of the two stereoisomers, consistent with what has been reported for the organometallic and non-organometallic anionic polymerization of PA. <sup>1</sup>H NMR spectra taken of the same sample over two months showed the complete degradation of the polymer within this period, showing that the polymer had maintained its self-immolative nature. TGA showed a single well-defined weight loss step of 93 %, in the temperature range of 156-230 °C, attributed to the degradation of the main polymer product.

### References

- (1) Vogl, O. *J. Polym. Sci.* **1964**, 2, 4607–4620.
- (2) Boileau, S.; Illy, N. *Prog. Polym. Sci.* **2011**, 36, 1132–1151.
- (3) De Winter, J.; Dove, A. P.; Knoll, A.; Gerbaux, P.; Dubois, P.; Coulembier, O. *Polym. Chem* **2014**, 5, 706–711.
- (4) Dilauro, A. M.; Robbins, J. S.; Phillips, S. T. *Macromolecule* **2013**, 46, 2963–2968.
- (5) Eßwein, B.; Steidl, N. M.; Möller, M. *Macromol. Rapid Commun.* **1996**, 143–148.

**Chapter 3**

---

- (6) Zhao, J.; Pahovnik, D.; Gnanou, Y.; Hadjichristidis, N. *Polym. Chem.* **2014**, *5*, 3750–3753.
- (7) Misaka, H.; Tamura, E.; Makiguchi, K.; Kamoshida, K.; Sakai, R.; Satoh, T.; Kakuchi, T. *J. Polym. Sci. Part A Polym. Chem.* **2012**, *50*, 1941–1952.
- (8) Zhao, J.; Hadjichristidis, N.; Gnanou, Y. **2014**, 1. Zhao, J.; Pahovnik, D.; Gnanou, Y.; Hadjichristidis, N. *Macromolecules* **2014**, *47*, 3814–3822.
- (9) Schwesinger, R.; Schlemper, H.; Hasenfratz, C.; Willaredt, J.; Dambacher, T.; Breuer, T.; Ottaway, C.; Fletschinger, M.; Boele, J.; Fritz, H.; Putzas, D.; Rotter, H. W.; Bordwell, F. G.; Satish, A. V.; Ji, G.; Peters, E.-M.; Peters, K.; von Schnering, H. G.; Walz, L. *Liebigs Ann.* **1996**, *7*, 1055–1081.
- (10) Ishikawa, T. *Superbases for Organic Synthesis: Guanidines, Amidines, Phosphazenes and Related Organocatalysts*; **2009**, 1–362.
- (11) Horn, H. W.; Jones, G. O.; Wei, D. S.; Fukushima, K.; Lecuyer, J. M.; Coady, D. J.; Hedrick, J. L.; Rice, J. E. *J. Phys. Chem. A* **2012**, *116*, 12389–12398.
- (12) Xue, D.; Mu, Y.; Mao, Y.; Yang, T.; Xiu, Z. *Green Chem.* **2014**, *16*, 3218–3223.
- (13) Coulembier, O.; Knoll, A.; Pires, D.; Gotsmann, B.; Duerig, U.; Frommer, J.; Miller, R. D.; Dubois, P.; Hedrick, J. L. *Macromolecules* **2010**, *43*, 572–574.
- (14) Peterson, G. I.; Boydston, A. J. *Macromol Rapid Commun* **2014**, *35*, 1611–1614.
- (15) Klán, P.; Šolomek, T.; Bochet, C. G.; Blanc, A.; Givens, R.; Rubina, M.; Popik, V.; Kostikov, A.; Wirz, J. *Chem. Rev.* **2013**, *113*, 119–191.
- (16) Köstler, S. *Polym. Int.* **2012**, *61*, 1221–1227.
- (17) Aso, C.; Tagami, S. *Macromolecules* **1969**, *3*, 414–419.
- (18) Kaitz, J.A. Doctoral Dissertation, University of Illinois. **2015**.
- (19) Kaitz, J. A.; Moore, S. *J. Am. Chem Soc.* **2014**, 5059–5513.
- (20) Kubisa, P.; Neeld, K.; Starr, J.; Vogl, O. *Polymer (Guildf)*. **1980**, *21*, 1433–1447.
- (21) Pessoni, L.; De Winter, J.; Surin, M.; Hergué, N.; Delbosc, N.; Lazzaroni, R.; Dubois, P.; Gerbaux, P.; Coulembier, O. *Macromolecules* **2016**, *49*, 3001–3008.
- (22) Reader, P. W.; Pfukwa, R.; Jokonya, S.; Arnott, G. E.; Klumperman, B. *Polym. Chem.* **2016**, *7*, 6450–6456.
- (23) Vogt, A. P.; De Winter, J.; Krolla-Sidenstein, P.; Geckle, U.; Coulembier, O.; Barner-Kowollik, C. *J. Mater. Chem. B* **2014**, *2*, 3578–3591.
- (24) Coulembier, O.; Knoll, A.; Pires, D.; Gotsmann, B.; Duerig, U.; Frommer, J.; Miller, R. D.; Dubois, P.; Hedrick, J. L. *Macromolecules* **2010**, *43*, 572–574.

## **Chapter 4**

### **4.1 Introduction**

Block copolymers (BCPs) constitute a class of complex, soft materials that are composed of macromolecules with long, covalently bonded segments of two or more repeat units<sup>1, 2</sup>. These fascinating hybrid materials are capable of combining the physical attributes of their parent structures for improved properties that better suit the desired application.<sup>1</sup> Block copolymer (BCP) self-assembly and its ability to yield ordered structures in a wide range of morphologies has attracted considerable attention for many decades.<sup>7</sup> The thermodynamics that govern the self-assembly behaviour of diblock copolymers have been researched to such an extent that we can now predict their phase behaviour beforehand, provided that the materials are of an appropriate molecular weight, incompatibility and composition.<sup>2</sup> We now know that when the tails of two incompatible polymers are covalently bonded via self-assembly, one of many microphase separated morphologies can be observed.<sup>2</sup> These morphologies include, among others: lamellar, cylindrical, discontinuous gyroid and hexagonally packed.<sup>2</sup> The formation of these different morphologies is driven by the thermodynamic incompatibility of the two or more polymer segments that make up a BCP, as it enables the system to minimize contact between the immiscible segments.<sup>6, 7</sup> The size of the regions are determined by the energy cost of internal interfaces that separate the segments, and their geometry by the relative entropy cost of stretching these regions.<sup>7</sup>

Over the past five decades, BCPs have traditionally been employed as thermoplastic elastomers, adhesives and property-enhancing additives.<sup>1</sup> However, interest in the application of BCPs as precursors to highly ordered nanoporous structures generated by the removal of one of the components of the self-assembled material has increased considerably over the last few years.<sup>2</sup> These nanoporous materials exhibit tunable pore size, narrow molecular weight distributions and allows for selective functionalization.<sup>1, 2, 6, 7</sup> These properties have allowed for size-dependant applications such as nanolithography, drug delivery and separation membranes.<sup>1</sup>

Nanoporous materials are prepared from block copolymers by a degradation process known as etching (Shown in Scheme 4.1). There are currently many etching techniques that allow for the selective removal of one of the components of a BCP. Commonly used techniques include

## Chapter 4

fuming nitric acid etching or the use of liquid etchants such as chromic acid, a solution of chromium trioxide and sulphuric acid or a sulphuric–phosphoric acid mixture.<sup>1, 8</sup> Other techniques include gas, plasma and irradiation etching.<sup>8</sup> All of these current techniques mentioned are tedious and requires harsh experimental conditions.<sup>1</sup>

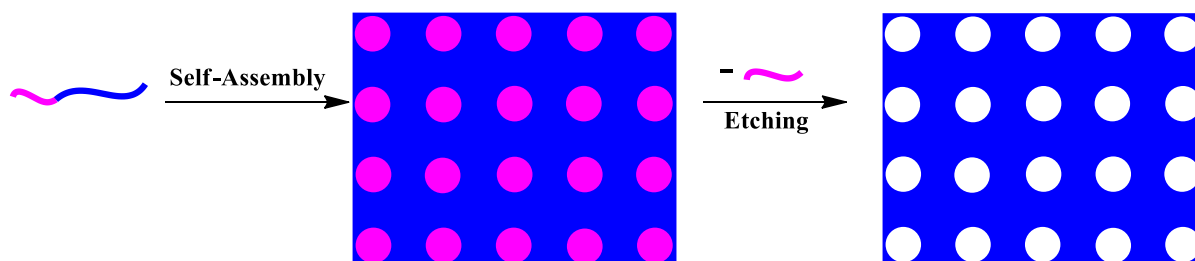
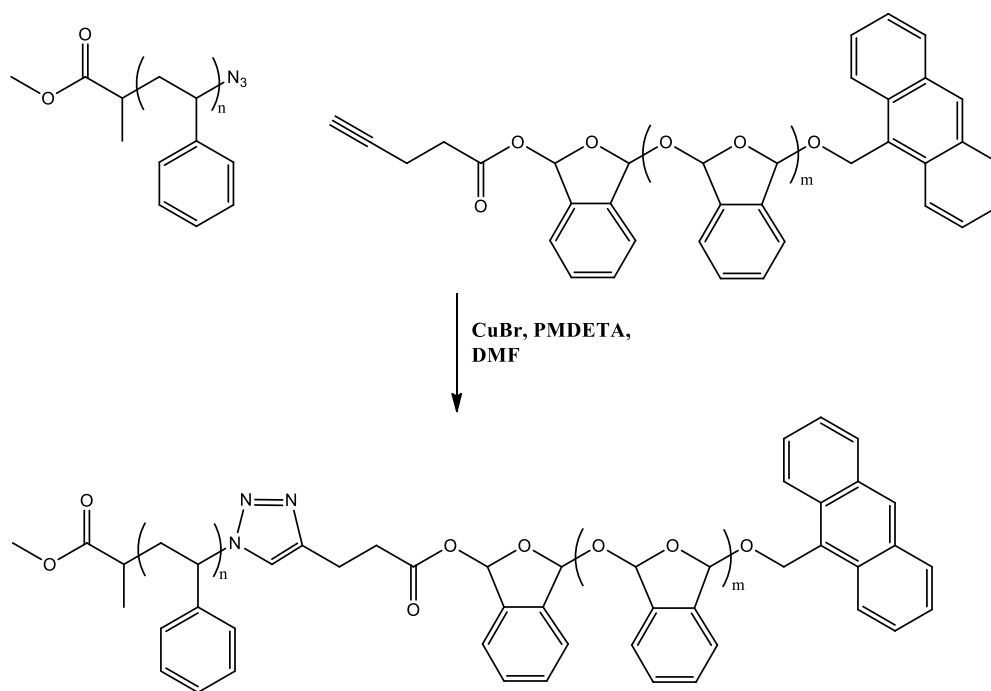


**Figure 4.1.** Schematic representation of a cylinder-forming block copolymer thin film and the corresponding nanoporous thin film obtained via selective etching of the minority domains.

Vogt and coworkers reported the preparation of BCPs consisting of PPA as a degradable segment and polystyrene (PS) as the matrix forming segment.<sup>9</sup> In their report, they showed that they could remove the degradable segment simply by exposing the BCP to acid, thereby inducing the depolymerization of PPA without affecting the PS segment. Whilst this method for the etching of a BCP is highly effective, it calls for harsh chemicals to be used. In addition, the method by which they prepared these BCPs required multiple synthesis and purification steps (Scheme 4.1).<sup>9</sup> Vogt and coworkers prepared PS-*b*-PPA BCPs by first synthesizing alkyne-terminated PPA and azide terminated PS. The PPA and PS segments were then coupled using a copper-catalyzed azide-alkyne cycloaddition reaction that required the purification of the product before it could be analyzed and altered.

## Chapter 4



**Scheme 4.1. Synthesis route for the preparation of PS-*b*-PPA, reported by Vogt and coworkers.<sup>9</sup>**

Following the results reported in Chapter 3, that showed the preparation of well-defined PPA by a facile and inexpensive method, we propose the preparation of PS-*b*-PPA by a much simpler method than that which has been reported thus far.<sup>9-11</sup> This chapter shows the preparation of PS macroinitiators via ARGET ATRP and RAFT-mediated polymerization. The optimized method for the preparation of PPA, determined in this work, is then applied to the preparation of PS-*b*-PPA copolymers

## 4.2 Experimental

### 4.2.1 Materials

Tris(2-aminoethyl) amine (tren) (96 %), formic acid (95 %), formaldehyde solution (36.5 %), diethyl ether (99 %), styrene (99 %), tin (II) 2-ethylhexanoate (Sn(EH)<sub>2</sub>) (92.5-100 %), 2-hydroxyethyl 2-bromoisobutyrate (HEBIB) (95 %), tributyltin hydride (97 %), benzene (99 %), *o*-phthaldialdehyde (97 %), 1, 8-diazabicyclo [5.4.0] undec-7-ene (DBU ) (98 %), (all Sigma-Aldrich) were used as received. Cu(I)Br was purified by stirring it in glacial acetic acid for minimum of 24 h, during which the glacial acetic acid was repeatedly replaced until it no longer changed colour. The powder was then washed with degassed ethanol and dried under vacuum. Tetrahydrofuran (THF) was purified and stored as described in Chapter 3.

## Chapter 4

---

### 4.2.2 Methods

Refer to Section 3.2.2

### 4.2.3 Preparation of the macroinitiator: Polystyrene

#### 4.2.3.1 Preparation of polystyrene by ARGET ATRP

##### 4.2.3.1.1 Synthesis of the ligand: tris [2-(dimethylamino) ethyl] amine (Me<sub>6</sub>TREN)

The method for the synthesis of Me<sub>6</sub>TREN was reported by Fu and coworkers.<sup>4</sup> A mixture of tren (1.8 g, 12 mmol), water (1.5 mL), formic acid (10 mL of an 85 % aqueous solution) and formaldehyde (9 mL of an 30 % aqueous solution) was added to a 100 mL round bottom flask and heated to 120 °C until no CO<sub>2</sub> was produced. All volatile fractions were then removed under vacuum. To the isolated solid residue, was added 100 mL of a 10 % wt NaOH aqueous solution. An oily layer formed, which was extracted with diethyl ether. The ether extract was then dried over KOH for 12 h before removing the solvent under vacuum to produce a colourless oil (80 %). The structure was confirmed by <sup>1</sup>H-NMR spectroscopy. (CDCl<sub>3</sub>) ppm: 2.2 (18H, CH<sub>3</sub>), 2.3 (6H, CH<sub>2</sub>), 2.5-2.6 (6H, CH<sub>2</sub>).<sup>4</sup>

##### 4.2.3.1.2 General polymerization procedure

For the ARGET ATRP of styrene: Cu(I)Br was used as the copper catalyst, Me<sub>6</sub>TREN as ligand and HEBIB as initiator.

For a  $M_n^{\text{Target}}$  of 10 000 g/mol, the following procedure was typical: the following procedure was typical: To a dry pear shaped flask was added half of the total amount of the styrene monomer (2.2 mg, 22 mmol) to be used for the reaction, Sn(EH)<sub>2</sub> (3.9 µL, 0.012 mmol) and a magnetic stirrer bar, the flask was then sealed with a rubber septum and degassed. The other half of the styrene monomer was added to vial A. The Cu(I)Br salt (3.3 mg, 0.023 mmol) and a magnetic stirrer bar was added to a vial B. The ligand (12 µL, 0.046 mmol) and a magnetic stirrer bar was added to vial C. Finally, the initiator (54 µL, 0.46 mmol) was added to a vial D. All four vials were then sealed with rubber septums and degassed with argon. Half of the amount of degassed styrene (1.1 mg, 0.11 mmol) from vial A was added to the vial containing the ligand (vial C) via a degassed syringe. The remaining degassed styrene (1.1 mg, 0.11 mmol) was added to the vial containing the initiator (vial D), also via a degassed syringe. Vials B, C and D were then degassed for several minutes more. The contents of vial C were then added to



## Chapter 4

---

vial B via a degassed syringe and allowed to stir until the mixture turned a bright green, thereby confirming that the complex had indeed been formed. The contents of vial B was then added to the pear shaped flask via a degassed syringe. The flask was lowered into the oil bath, heated to 90 °C, and allowed to reach the desired temperature before adding the contents of vial D via a degassed syringe. The polymerization was allowed to run for 24 h before it was stopped by removing the flask from the oil bath and exposing it to air. The polymer was dissolved in THF and precipitated from cold methanol. Precipitation from methanol was repeated twice. The polymer was isolated via filtration and dried under vacuum. Theoretical molecular weights were calculated using Equation 3.1.

### 4.2.3.1.3 Debromination of ARGET ATRP-made polystyrene

The debromination of the ARGET ATRP-made PS was carried out according to a method reported by Oswald and coworkers.<sup>5</sup> PS (0.20 mmol) and a magnetic stirrer bar was placed in a round bottom flask and sealed with a rubber septum after which the flask was degassed with argon. In a separate flask, benzene (7 mL) was degassed for twenty minutes before it was added to the PS via a degassed syringe. The flask was then lowered into an oil bath, heated to 85 °C, and allowed to stir. Tributyltin hydride (0.16 mL, 0.60 mmol) was added to a small vial which was then sealed and also degassed. After several minutes, the tributyltin hydride was added to the round bottom flask via a degassed syringe. The reaction was allowed to run for an hour before removing the round bottom flask from the oil bath and its contents to air. The reaction mixture was then dissolved in chloroform (5 mL) before it was precipitated into cold methanol. The product was isolated and dried under vacuum. For purification, the polymer was dissolved in THF and dialysed for 24 h. The purified product was then precipitated into methanol, isolated and dried under vacuum (98 % yield). The replacement of the bromine with a proton was confirmed by <sup>1</sup>H NMR spectroscopy.

### 4.2.3.2 Preparation of polystyrene by RAFT-mediated polymerization

#### 4.2.3.2.1 Synthesis of 2-(((butylthio)carbonothioyl)thio)-2-methylpropanoic acid

The synthesis of 2-(((butylthio)carbonothioyl)thio)-2-methylpropanoic acid was carried out according to a method reported by Jia.<sup>14</sup> Potassium phosphate tribasic (16 g, 75 mmol) was dissolved in acetone (130 mL) in a 500 mL round bottom flask. The reaction mixture was allowed to stir for 5 h before adding 1-butanethiol (8 mL, 74 mmol). After 1 hour of stirring, carbon disulfide (9.1 mL, 151 mmol) was added in a drop wise manner. The round bottom flask

## Chapter 4

---

was then immersed in an ice bath and allowed to stir for 2 h before adding 2-bromo-2-methylpropionic acid (11 g, 70 mmol). The round bottom flask was then removed from the ice bath and the reaction allowed to run overnight at room temperature. The following day the filtrate was isolated by filtration and its volume reduced to a third by rotary evaporation. A cold 10 % HCl solution (100 mL) was added before allowing the reaction mixture to stir overnight at room temperature. The solution was then extracted with *n*-hexane (2 × 50 mL) after which the organic phase was dried over anhydrous MgSO<sub>4</sub>, filtered and the solvent removed by rotary evaporation. The residual bright yellow solid was purified by column chromatography (ethyl acetate /pentane: ¼ on silica). The purified product was dried under vacuum, producing a yield of 72%. The structure was confirmed by <sup>1</sup>H-NMR spectroscopy. (CDCl<sub>3</sub>) ppm: 0.90 (3H, CH<sub>3</sub>), 1.4 (2H, CH<sub>2</sub>), 1.6 (6H, CH<sub>3</sub>), 1.9 (2H, CH<sub>2</sub>), 3.2 (2H, CH<sub>2</sub>)

### 4.2.3.2.2 General polymerization procedure

For a  $M_n^{\text{Target}}$  of 20 000 g/mol, the following procedure was typical: styrene (2 g, 16 mmol), 2-(((butylthio)carbonothioyl)thio)-2-methylpropanoic acid (0.24 g, 0.97 mmol), AIBN (16 mg, 0.097 mmol) and THF (2 mL) was added to a pear shaped flask. The contents of the flask was then purged with argon for 15 min before lowering the flask into an oil bath, set to 65 °C. The polymerization was allowed to run overnight before stopping the reaction by exposing the contents of the flask to air. The polymer was then precipitated from cold methanol and dried under vacuum. Theoretical molecular weights were calculated using Equation 3.1.

## 4.3 Preparation of polystyrene-*b*-polyphthaldialdehyde

Synthesis of the PS-*b*-PPA was conducted via anionic polymerization with PS as macro initiator, DBU as catalyst and acetic anhydride as quenching agent (unless specified otherwise). A catalyst:initiator of 4:1 was used (unless specified otherwise).

### 4.3.1 General polymerization procedure

The synthesis of the PS-*b*-PPA was conducted via anionic polymerization with PS as macro initiator, DBU as catalyst and acetic anhydride as quenching agent (unless specified otherwise).

For a  $M_n^{\text{Target}}$  of 20 000 g/mol with a PS macroinitiator of 10 000 g/mol, the following procedure was typical: The monomer (0.2 g, 1.5 mmol) and THF (1.0 mL) was added to the reaction flask containing a stirrer bar. In a separate flask, the macroinitiator (0.2 g, 0.020 mmol)

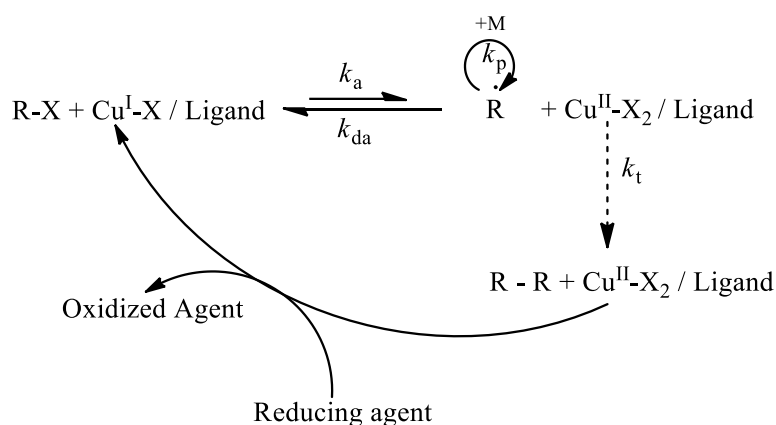
## Chapter 4

and the catalyst (23  $\mu\text{L}$ , 0.16 mmol) was dissolved in THF (1.5 mL). The quenching agent, acetic anhydride (0.70 mL, 7.5 mmol), and THF (0.5 mL) were added to a third flask. All three flasks were sealed with a rubber septum. The reaction flask and the flask containing the initiator/catalyst solution was placed in a liquid nitrogen/ethyl acetate bath (set to  $-75\text{ }^{\circ}\text{C}$ ) and degassed with argon for five minutes before adding the initiator/catalyst solution to the reaction flask via a degassed syringe. The flask containing the quenching agent was then placed in the liquid nitrogen/ethyl acetate bath and degassed. After the reaction time had passed, the quenching agent was added to the reaction flask via a degassed syringe. After thirty minutes, the polymer was precipitated into cold methanol, isolated via centrifugation and dried at room temperature. Following analysis, all samples were stored under methanol at room temperature.

### 4.4 Results and discussion

#### 4.4.1. Synthesis of polystyrene by ARGET ATRP

ATRP has become a popular method for the preparation of well-defined polymers as it is robust, can be used for a wide range of monomers, with a variety of solvents and tolerates a wide range of functional groups.<sup>3, 12</sup> ATRP relies on an equilibrium between a low concentration of active propagating chains and a high concentration of dormant chains as shown in Scheme 4.2.



**Scheme 4.2. The ARGET ATRP mechanism.<sup>3</sup>**

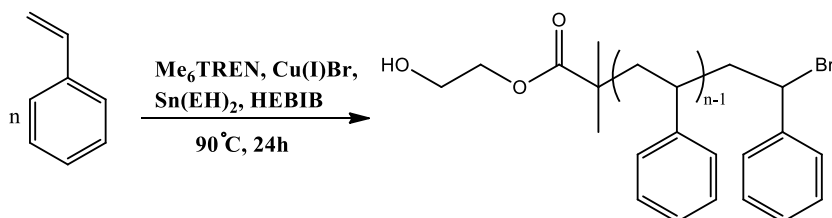
The propagating chains are generated through a reversible redox process that is catalyzed by a transition metal complex,  $\text{Cu}^{\text{I}}\text{-X}$  ligand. However, studies have shown that living polymer chains capped by a halogen for polymers prepared by ATRP is less than a hundred percent. This may be due to termination reactions and the presence of side reactions between growing

## Chapter 4

radicals and the copper catalyst. Following these revelations, Matyjaszewski and coworkers improved the ATRP process by selecting a highly active copper catalyst which can be used in minute amounts in the presence of an excess amount of a reducing agent.<sup>3</sup> This system is called ARGET ATRP. In the case of ARGET ATRP, the reducing agent reacts with the copper (II) deactivator that is generated in termination reactions, thereby returning the oxidized species to its active copper (I) state which is required for activation. By reducing the Cu(II) deactivator, any side reactions that would have been catalyzed by its presence is prevented. ARGET ATRP is therefore not only more environmentally friendly but also reduces catalyst-induced side reactions, resulting in well-defined polymers with improved chain-end functionality (*f*) when compared to normal ATRP.<sup>3</sup>

ARGET ATRP requires the homolytic cleavage of a carbon-halogen bond in the initiator for chain growth to begin (Scheme 4.2). The initiator can be a small molecule, or it can be tethered to a macromolecule or a surface of any topology. Studies have shown chlorine and bromine to be the preferred choice of halogens.<sup>12, 13</sup> What makes this method especially relevant for this work however, is that it can tolerate many functional groups in the initiator molecule including hydroxyl, amino and cyano groups.<sup>12</sup> This method therefore allows one to combine different chemistries to prepare sophisticated BCPs.<sup>12</sup>

Another important aspect of ARGET ATRP is the choice of ligand. The primary role of the ligand is to solubilize the copper salt and tune the catalytic activity of the complex to ensure a well-controlled polymerization.<sup>12</sup> Me<sub>6</sub>TREN was chosen as the ligand for this work as it has been shown that the highly active catalytic system of Me<sub>6</sub>TREN/CuBr is less likely to oxidize polystyryl radicals and participate in  $\beta$ -H-elimination reactions that would produce unsaturated chains ends.<sup>3</sup> A general scheme of the ARGET ATRP of styrene is shown in Scheme 4.3.



**Scheme 4.3. The ARGET ATRP of styrene.**

## Chapter 4

### 4.4.1.1 Control over molecular weight distribution and end-group functionality.

Table 4.1 is a summary of the results obtained for the ARGET ATRP of styrene. The results show that the polymerization reactions proceeded with excellent control as evidenced by the good agreement between the  $M_n^{\text{Theoretical}}$ ,  $M_n^{\text{SEC}}$  and  $M_n^{\text{NMR}}$  values and the low  $D$ . The  $M_n^{\text{NMR}}$  was not determined for entry 5 as this method of determining the molecular weight is unreliable for polymers with a molecular weight above 20 000 g/mol.

**Table 4.1. Results for the ARGET ATRP of styrene.**

Entry	$M_n^{\text{Target}}$ (g/mol)	$M_n^{\text{Theoretical}}$ (g/mol)	$M_n^{\text{SEC}}$ (g/mol)	$M_n^{\text{NMR}}$ (g/mol)	$D$	$f(\%)^a$	Yield (%)
1	10 000	6 000	6 200	5 500	1.2	85	60
2	10 000	8 700	9 900	9 000	1.1	87	87
3	10 000	5 800	4 300	4 000	1.1	88	58
4	20 000	18 500	19 500	19 000	1.1	87	85
5	40 000	36 000	39 000	-	1.1	80	90

<sup>a</sup> Percentage chain-end functionality

<sup>1</sup>H NMR spectroscopy was used to determine the percentage  $f$  of the various polymers and to investigate the presence of termination reactions during the ARGET ATRP of styrene. Figure 4.2 shows the <sup>1</sup>H NMR spectrum for the hydroxyl end-functional PS (entry 2, Table 4.1).

## Chapter 4

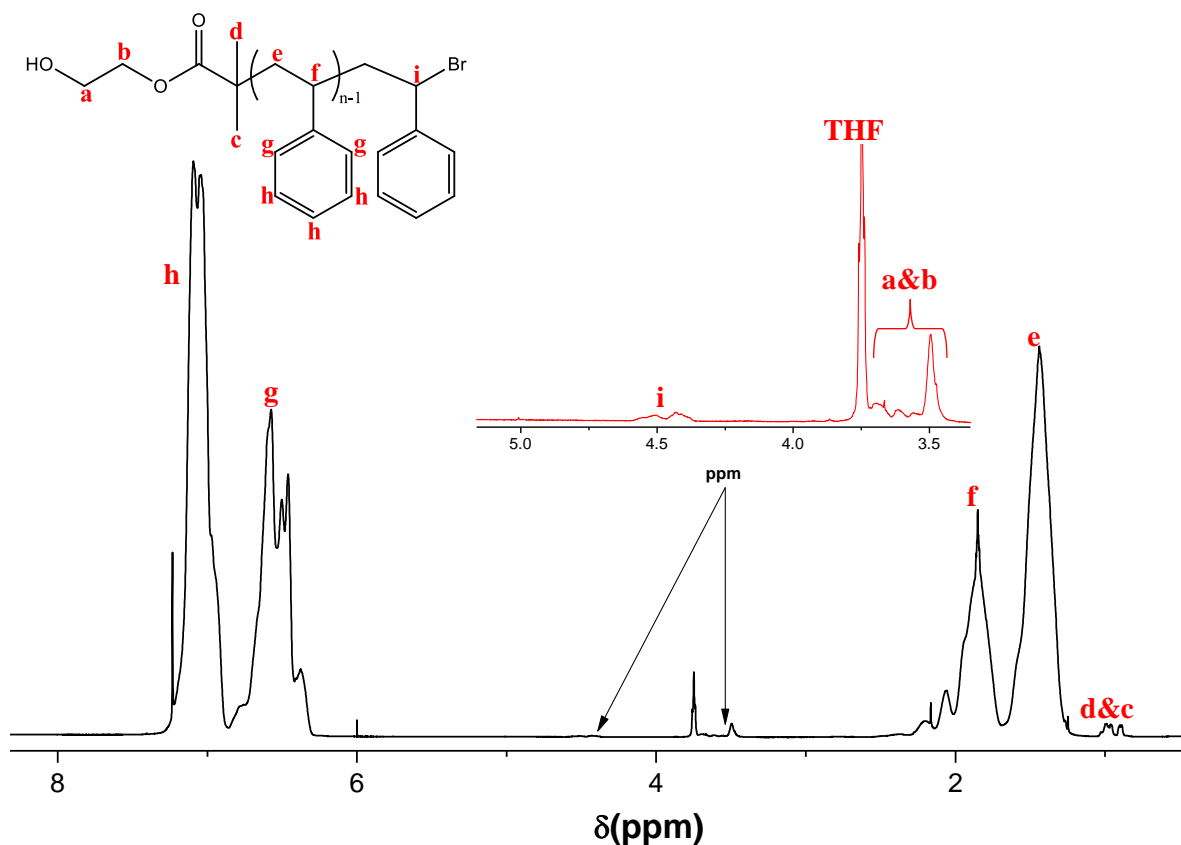


Figure 4.2. The  $^1\text{H}$  NMR spectrum ( $\text{CDCl}_3$ ) of polystyrene (entry 2, Table 4.1) prepared via ARGET ATRP.

Matyjaszewski and coworkers reported that the percentage  $f$  of PS prepared via ARGET ATRP could be determined by comparing the integration areas of the signals  $\text{H}_a$  and  $\text{H}_b$  to that of  $\text{H}_i$  (Equation 4.1).<sup>3</sup> The percentage  $f$  based on Equation 4.2 for each polymerization that was conducted, is shown in Table 4.1.

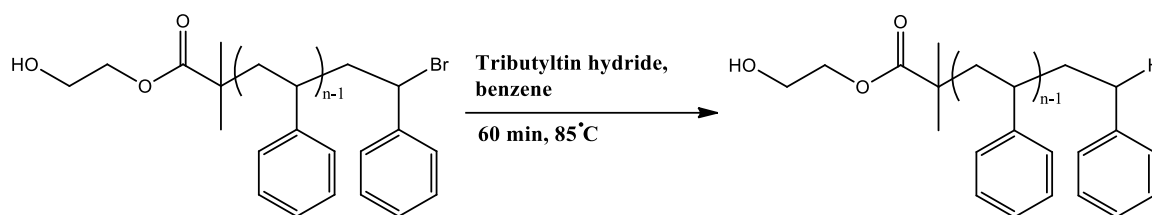
$$\% f = 100 \left[ \frac{H_i}{\frac{H_a + H_b}{4}} \right] \quad (\text{Eq 4.1})$$

The relatively high percentage  $f$ , ranging between 80-90 %, suggests that deleterious elimination reactions were significantly suppressed, resulting in excellent chain end-functionalization. The absence of any signals in the region of 6.1-6.3 ppm confirms the absence of any elimination reactions as signals in this region would normally be attributed to double bond terminated PS.<sup>3</sup>

## Chapter 4

## 4.4.1.2 Debromination of ARGET ATRP-made polystyrene

To prevent the possible replacement of the bromine end-group via nucleophilic substitution during the chain extension reaction of PS with the PA monomer, it was decided to replace the bromine end-group with a proton. This was done following an approach reported by Oswald *et al.* for the debromination of polymers prepared via ATRP (Scheme 4.4).<sup>5</sup> Figure 4.3 shows an overlay of the  $^1\text{H}$  NMR spectra of the polymer before (entry 2 Table 4.1) and after it was reacted with tributyltin hydride.



Scheme 4.4. The debromination of PS prepared via ARGET ATRP.

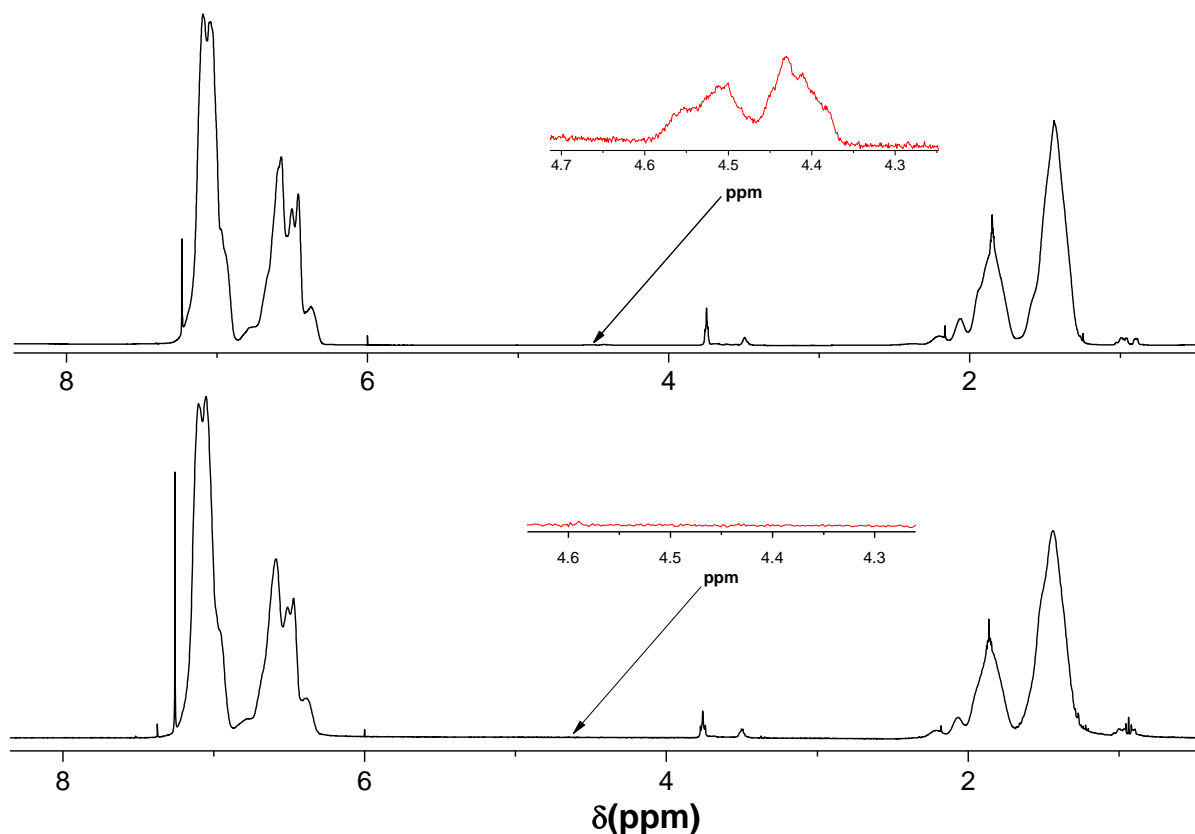


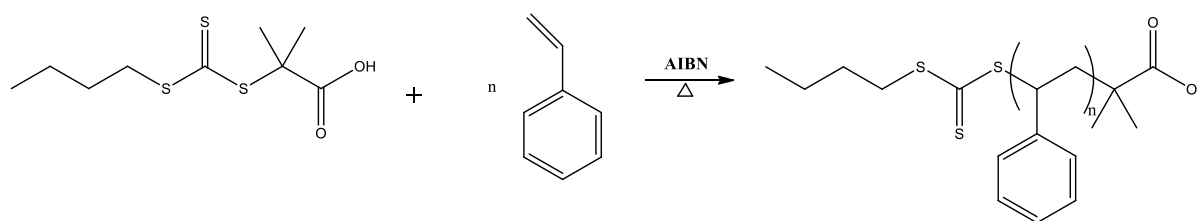
Figure 4.3. An overlay of the  $^1\text{H}$  NMR spectra ( $\text{CDCl}_3$ ) of polystyrene (entry 2 Table 4.1) (a) before and (b) after debromination.

## Chapter 4

As shown in Figure 4.2, the signals appearing in the region of 4.4-4.5 ppm can be assigned to the proton attached to the carbon adjacent to the bromine. These signals are clearly visible in Figure 4.3a. After reacting the polymer with tributyltin hydride, these two signals disappear (Figure 4.3b), thus confirming that debromination of the polymer had indeed been successful.

### 4.4.2. Synthesis of polystyrene by RAFT- mediated polymerization

Reversible-addition fragmentation chain transfer (RAFT) polymerization has been shown to be an extremely versatile process.<sup>15-17</sup> It is compatible with a wide range of functionalities in monomers, solvents and initiators and can be applied to the preparation of well-defined polymers or copolymers.<sup>15-17</sup> RAFT polymerization utilizes chain transfer agents (RAFT agents) to control the molecular weight and end-group functionality, with the overall process resulting in the insertion of the monomer units into the C-S bond of the RAFT agent.<sup>15, 15</sup> A typical RAFT agent is made up of what is referred to as the Z (thiocarbonyl) and R (leaving group).<sup>15-17</sup> To obtain optimum control in a RAFT polymerization, it is critical to choose an appropriate RAFT agent for the monomer to be polymerized and the reaction conditions.<sup>15</sup> Trithiocarbonates and dithioesters, which have a carbon or sulfur adjacent to the trithiocarbonyl group, have been shown to be among the most reactive RAFT agents.<sup>15</sup> In this work, the RAFT-mediated polymerization of styrene by 2-(((butylthio)carbonothioyl)thio)-2-methylpropanoic acid (Scheme 4.5) will be described.



**Scheme 4.5.** RAFT-mediated polymerization of styrene, with 2-(((butylthio)carbonothioyl)thio)-2-methylpropanoic acid as RAFT agent.

#### 4.4.1.1 Control over molecular weight distribution and end-group functionality.

Table 4.2 shows the results for the RAFT-mediated polymerization of PS. The reaction proceeded with good control and a good agreement between the  $M_n^{\text{Theoretical}}$ ,  $M_n^{\text{SEC}}$  and  $M_n^{\text{NMR}}$ . Figure 4.4 shows the  $^1\text{H}$  NMR spectrum of PS prepared using 2-(((butylthio)carbonothioyl)thio)-2-methylpropanoic acid as RAFT agent. The percentage  $f$  was determined by applying Equation 4.2 to the integration values of  $\text{H}_a$  to that of  $\text{H}_e$  and  $\text{H}_f$ . Although the



## Chapter 4

percentage  $f$  was not as good as that which was obtained with ARGET ATRP, the method still allowed for the preparation of well-defined PS.

**Table 4.2. Results for the RAFT-mediated polymerization of PA with 2-(((butylthio)carbonothioyl)thio)-2-methylpropanoic acid as RAFT agent.**

$M_n^{\text{Target}}$ (g/mol)	$M_n^{\text{Theoretical}}$ (g/mol)	$M_n^{\text{SEC}}$ (g/mol)	$M_n^{\text{NMR}}$ (g/mol)	$D$	$f(\%)^a$	Yield (%)
20 000	18 000	19 000	18 500	1.2	75	80

<sup>a</sup> Percentage chain-end functionality

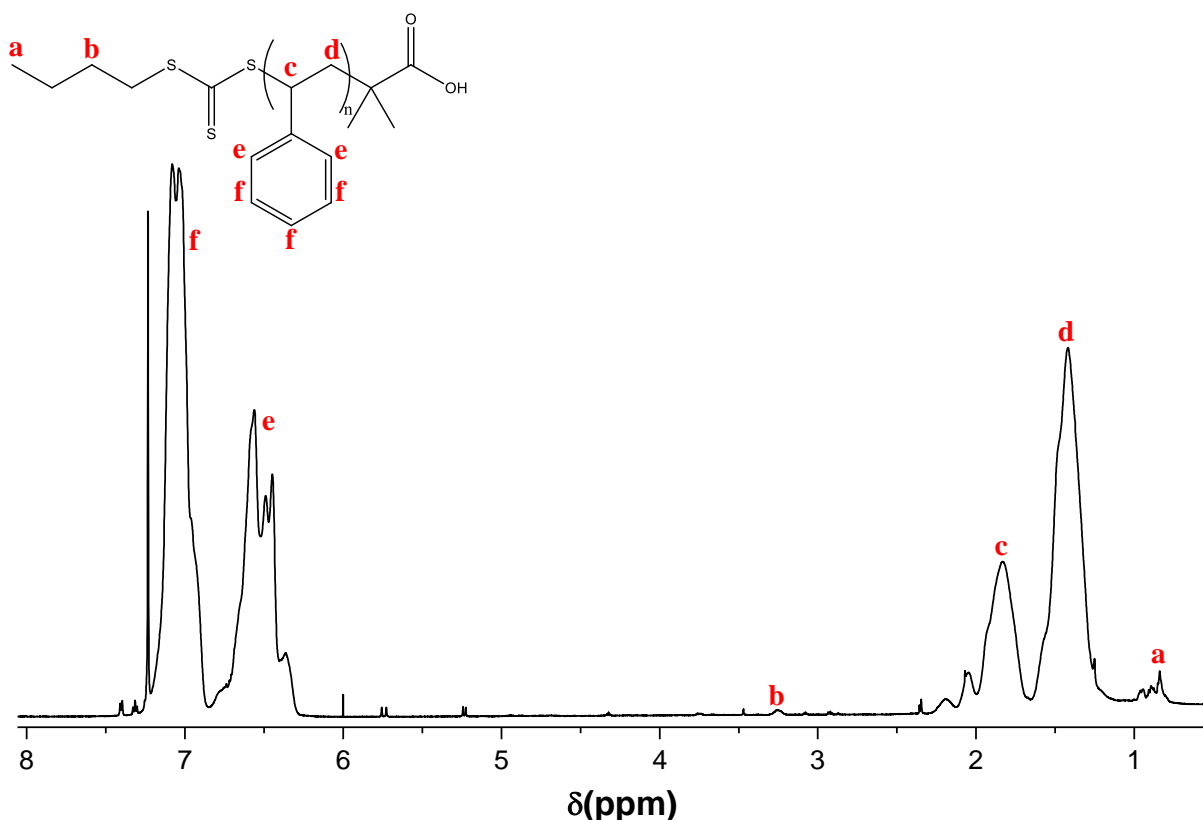


**Figure 4.4. The  $^1\text{H}$  NMR spectrum ( $\text{CDCl}_3$ ) of polystyrene prepared by RAFT-mediated polymerization.**

### 4.4.3. Synthesis of PS-*b*-PPA

Chain extension of the various PS macroinitiators with the PA monomer was performed using the optimized conditions defined for the preparation of the PPA homopolymer, described in Chapter 3. The bromine end-functional and proton end-functional PS prepared by ARGET ATRP as well as the carboxylic acid end-functional PS prepared by RAFT-mediated polymerization were used as macroinitiators. In addition, either acetic anhydride or the UV-labile 4,5-dimethoxy-2-nitrobenzyl carbonochloridate were used as quenching agents. Scheme 4.6 shows the preparation of the various BCPs. Table 4.3 is a summary of the results obtained

## Chapter 4

for the block copolymerization reactions. Two different mole ratios,  $1n_{PS}:1n_{PPA}$  and  $2n_{PS}:1n_{PPA}$ , were targeted. The SEC results show that the chain extension of the two hydroxyl end-functional PS macroinitiators with the PA monomer proceeded with excellent control, with a good agreement between the  $M_n^{\text{Theoretical}}$  and  $M_n^{\text{SEC}}$ , and  $\bar{D}$  values below 1.2. The BCPs prepared using the carboxylic acid end-functional PS as macroinitiator degraded during analysis. However, the gravimetric yield, observations during the copolymerization reactions as well as the  $^1\text{H}$  NMR data for the BCPs indicated that chain-extension had indeed occurred.

**Table 4.3. Results for the preparation of different PS-*b*-PPA copolymers.**

Entry	$n_{PS}:n_{PPA}$	$M_n^{\text{Theoretical}}$ (g/mol)	$M_n^{\text{SEC}}$ (g/mol)	$\bar{D}$	Yield (%)
1 <sup>a, c</sup>	2:1	14 400	14 200	1.1	96
2 <sup>a, c</sup>	2:1	14 600	15 000	1.2	97
3 <sup>b, c</sup>	2:1	14 000	13 900	1.1	93
4 <sup>b, c</sup>	2:1	14 300	14 100	1.2	95
5 <sup>b, d</sup>	2:1	14 800	14 000	1.1	92
6 <sup>e, c</sup>	2:1	28 000	-	-	96
7 <sup>a, c</sup>	1:1	19 700	19 500	1.1	97
8 <sup>b, c</sup>	1:1	19 600	19 900	1.2	96
9 <sup>b, d</sup>	1:1	19 000	18 700	1.2	90
10 <sup>e, c</sup>	1:1	39 800	-	-	97

<sup>a</sup> Macroinitiator = PS prepared by ARGET ATRP with a bromine chain-end functionality

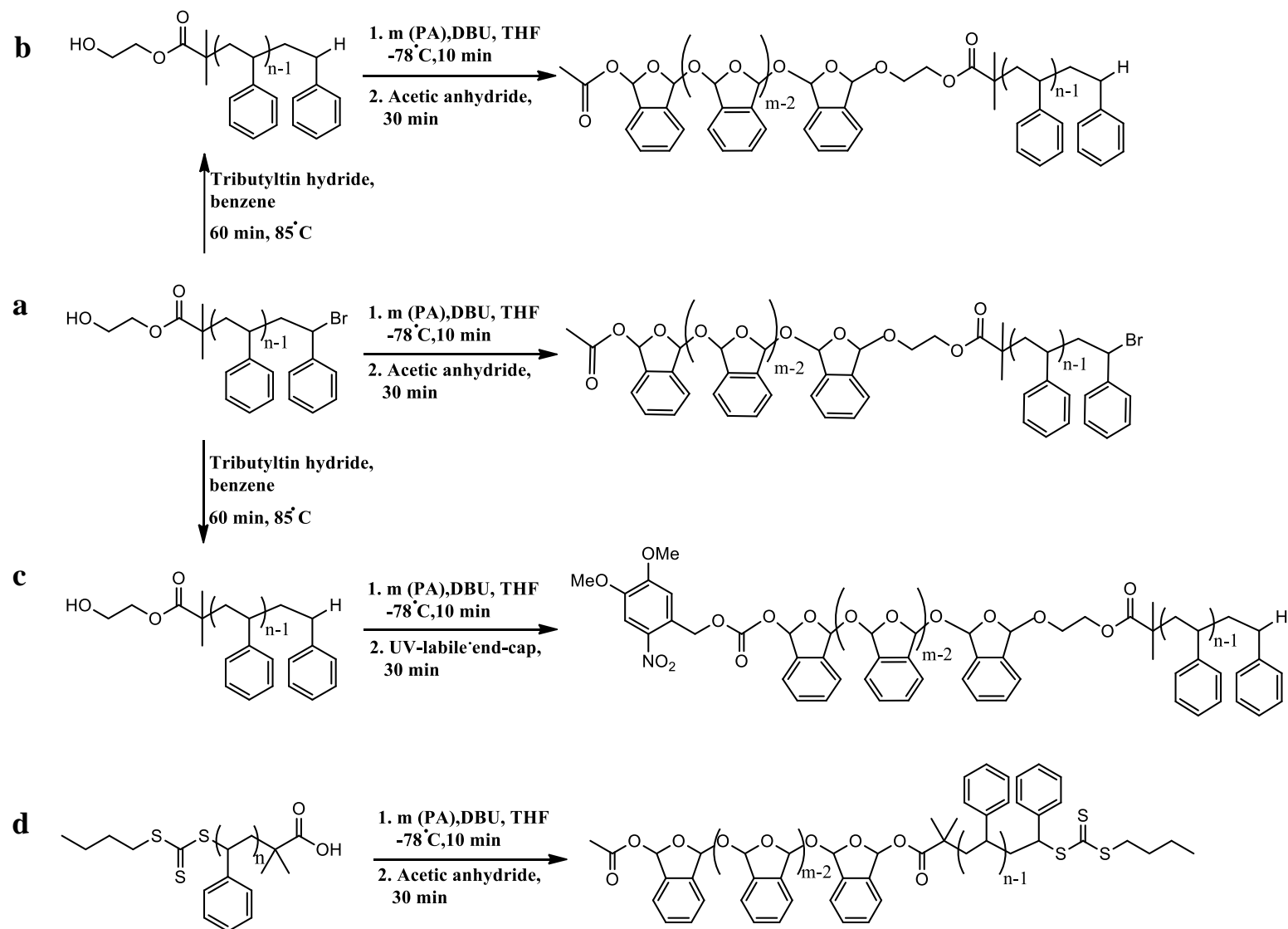
<sup>b</sup> Macroinitiator = PS prepared by ARGET ATRP with a proton chain-end-functionality

<sup>c</sup> Acetic anhydride used as quenching agent

<sup>d</sup> 4,5-dimethoxy-2-nitrobenzyl carbonochloridate used as quenching agent

<sup>e</sup> Macroinitiator = PS prepared by RAFT-mediated polymerization

## Chapter 4



Scheme 4.6. Preparation of PS-b-PPA: (a) entry 1, 2 and 7, Table 4.3, (b) entry 3, 4 and 8, Table 4.3, (c) entry 5 and 9, Table 4.3, (d) entry 6 and 10, Table 4.3.

## Chapter 4

Figure 4.5 shows an overlay of the  $^1\text{H}$  NMR spectra for the (a) PS macroinitiator (entry 2, Table 4.1), (b) PPA homopolymer and (c) the PS-*b*-PPA copolymer (entry 1, Table 4.3). Figure 4.5c clearly shows the signals representing the aromatic functional groups of both the PS macroinitiator and PPA, thereby confirming that chain extension had indeed occurred.

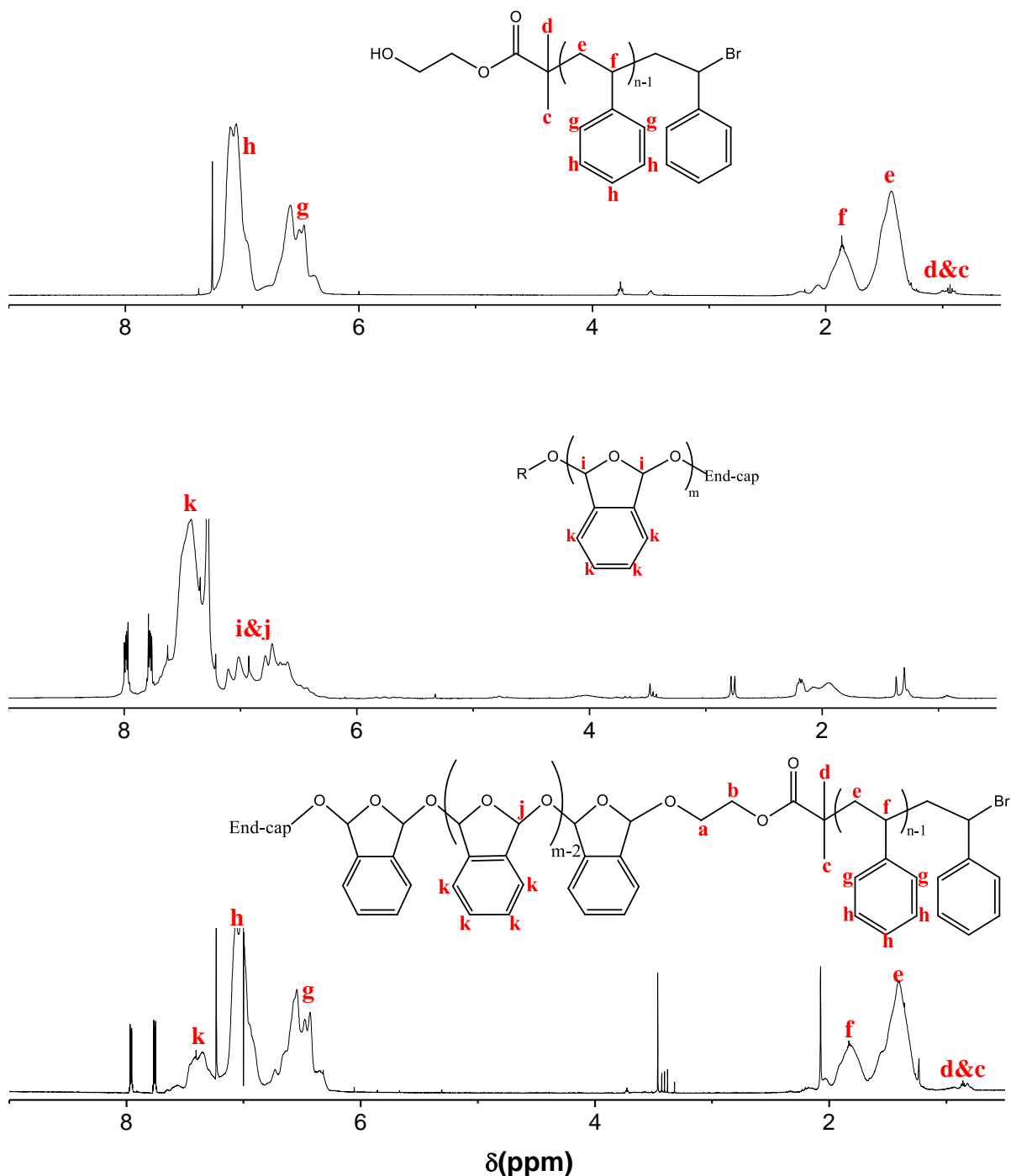


Figure 4.5. An overlay of the  $^1\text{H}$  NMR spectra (CDCl<sub>3</sub>) of the (a) polystyrene macroinitiator (entry 2 Table 4.1) following debromination, (b) polyphthalaldehyde homopolymer and (c) PS-*b*-PPA copolymer (entry 1, Table 4.3).

## Chapter 4

---

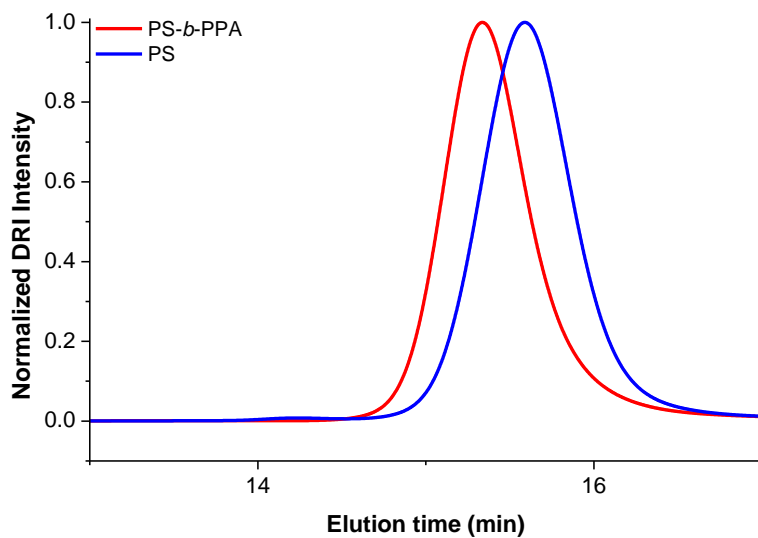
### 4.4.3.1 Control over the mole ratios of each monomer

The mole ratios of each monomer in a copolymer can be determined by using the integrated areas of the  $^1\text{H}$  NMR signals corresponding to each monomer.<sup>13</sup> In the case of PS-*b*-PPS, this can be done by comparing the integrated areas of the aromatic peaks corresponding to the phenyl ring in PS (signals assigned as g and h, Figure 4.5) and in PPA (signal assigned as k, Figure 4.5). The equation used to determine the percentage PS present in the PS-*b*-PPA copolymers is shown below (Equation 4.2) where  $A_{ph_1}$  and  $A_{ph_2}$  refers to the integrated area of the phenyl ring in PS and PPA, respectively.

$$\% PS = \frac{\frac{A_{ph_1}}{5}}{\left(\frac{A_{ph_1}}{5} + \frac{A_{ph_2}}{3}\right)} \times 100 \quad (\text{Eq 4.2})$$

Equation 4.2 was applied to entry 1 and 7 (Table 4.3). The results showed that the BCP prepared with a targeted molar ratio of  $1n_{PS}:1n_{PPA}$  (entry 1 in Table 4.3) consisted of 54 % PS and 46 % PPA. The BCP prepared with a targeted molar ratio of  $2n_{PS}:1n_{PPA}$  (entry 7, Table 4.3) was found to consist of 68% PS and 32% PPA. These results confirmed that the facile method proposed for the preparation of PS-*b*-PPA in this work resulted in the preparation of BCPs with molar ratios matching that which was targeted near perfectly.

SEC was used as a complementary technique to illustrate the shift to a higher molecular weight from that of the PS macroinitiator to that of the BCP. Figures 4.6 to 4.8 shows a comparison of the SEC traces of the PS macroinitiator and that of the PS-*b*-PPA copolymer. The figures all show a clear shift to a lower elution time from that of the macroinitiator to that of the BCP, signifying an increase in molecular weight.

**Chapter 4**

**Figure 4.6.** An overlay of the SEC trace of the PS macroinitiator (entry 2, Table 4.1) and that of the PS-*b*-PPA copolymer (entry 7, Table 4.3).

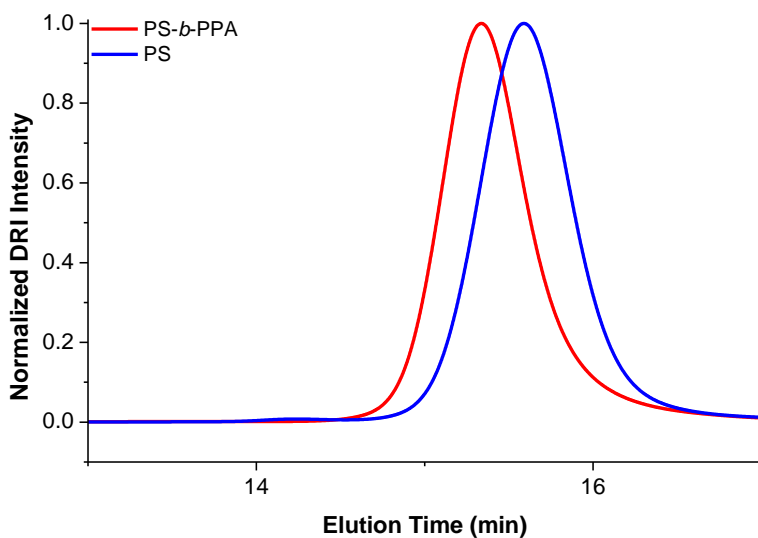


**Figure 4.7.** An overlay of the SEC trace of the PS macroinitiator (entry 2, Table 4.1) and that of the PS-*b*-PPA copolymer (entry 8, Table 4.3).

## Chapter 4

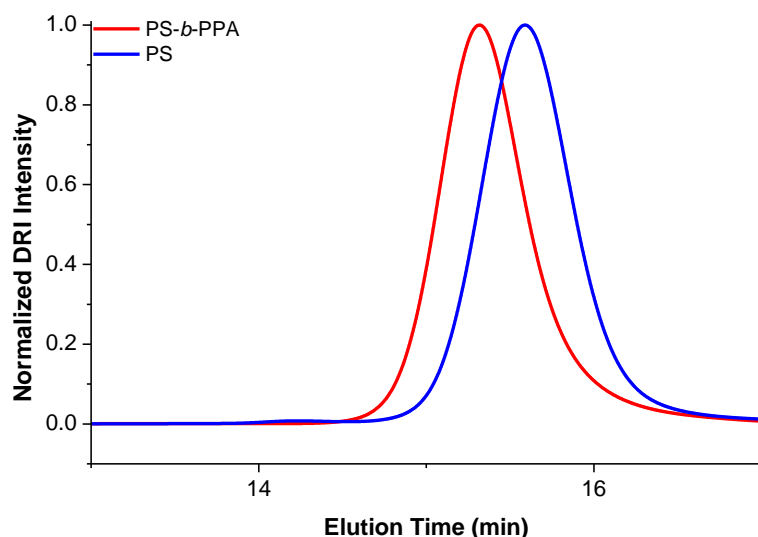


Figure 4.8. An overlay of SEC trace of the PS macroinitiator (entry 2, Table 4.1) and that of the PS-*b*-PPA copolymer (entry 9, Table 4.2).

## 4.5 Conclusions

The conditions for the DBU catalyzed anionic polymerization of PA, determined in Chapter 3, was successfully applied to the preparation of PS-*b*-PPA BCPs. PS macroinitiators were prepared by ARGET ATRP and RAFT-mediated polymerization. The hydroxyl end-functional PS, prepared by ARGET ATRP, underwent debromination to prevent the nucleophilic substitution of the bromine end-group during the anionic polymerization reaction. Carboxylic acid end-functional PS was prepared by RAFT-mediated polymerization. Analysis of the various PS macroinitiators by SEC and  $^1\text{H}$  NMR, showed that both methods had produced well-defined polymers with a good agreement between the  $M_n^{\text{Theoretical}}$ ,  $M_n^{\text{SEC}}$  and  $M_n^{\text{NMR}}$ . It was also determined that while both methods resulted in polymers with a high percentage end-group functionality, PS prepared by ARGET ATRP showed improved chain-end functionality compared to the PS prepared by RAFT-mediated polymerization.

The optimized conditions for the DBU catalyzed anionic polymerization of PA was then applied to the chain extension of the three PS macroinitiators with the aldehyde monomer. Either acetic anhydride or the UV-labile, 4,5-dimethoxy-2-nitrobenzyl carbonochloridate, were used as quenching agents. Analysis of the BCPs prepared using the hydroxyl end-functional PS showed that the method allowed for the preparation of well-defined BCPs with a good agreement between the  $M_n^{\text{Theoretical}}$ ,  $M_n^{\text{SEC}}$  and  $M_n^{\text{NMR}}$  and very low  $\text{D}$  values. The BCPs prepared using the carboxylic acid end-functional PS as macroinitiator was found to have degraded during analysis. However, the gravimetric yield, observations during the

**Chapter 4**

---

copolymerization reactions and the  $^1\text{H}$  NMR data obtained indicated that chain extension had indeed occurred. The successful application of the optimized method for the DBU catalyzed anionic polymerization of PA to the preparation of PS-*b*-PPA BCPs, shows that well-defined degradable PPA-containing BCPs can be prepared by a simple and inexpensive method that does not require multiple synthesis and purification steps.

**References**

- (1.) Jackson, E. A.; Hillmyer, M. A. *ACS Nano* **2010**, *4*, 3548–3553.
- (2.) Hillmyer, M. A. *Adv. Polym. Sci.* **2005**, *190*, 137–181.
- (3.) Jakubowski, W.; Kirci-Denizli, B.; Gil, R. R.; Matyjaszewski, K. *Macromol. Chem. Phys.* **2008**, *209*, 32–39.
- (4.) Fu, G. D.; Xu, L. Q.; Yao, F.; Zhang, K.; Wang, X. F.; Zhu, M. F.; Nie, S. Z. *ACS Appl. Mater. Interfaces* **2009**, *1*, 239–243.
- (5.) Oswald, L.; Trinh, T. T.; Chan-Seng, D.; Lutz, J. F. *Polymer* **2015**, *72*, 341–347.
- (6.) Mai, Y.; Eisenburg, A. *Chem. Soc. Rev.* **2012**, *41*, 5969–5985.
- (7.) Matsen, M. W.; Schick, M. J. *Chem. Inf. Model.* **2013**, *53*, 1689–1699.
- (8.) Olley, R.H. *Science Progress* **1986**, *71*, 17–43.
- (9.) Vogt, A. P.; De Winter, J.; Krolla-Sidenstein, P.; Geckle, U.; Coulembier, O.; Barner-Kowollik, C. *J. Mater. Chem. B* **2014**, *2*, 3578–3591.
- (10.) Pessoni, L.; De Winter, J.; Surin, M.; Hergué, N.; Delbosc, N.; Lazzaroni, R.; Dubois, P.; Gerbaux, P.; Coulembier, O. *Macromolecules* **2016**, *49*, 3001–3008.
- (11.) Köstler, S.; Zechner, B.; Trathnigg, B.; Fasl, H.; Kern, W.; Ribitsch, V. *J. Polym. Sci. A Polym Chem.* **2009**, *47*, 1499–1509.
- (12.) Matyjaszewski, K. *Polim.* **2014**, *59*, 24–37.
- (13.) Matyjaszewski, K.; Beers, K. L.; Metzner, Z.; Woodworth, B. J. *Chem. Educ.* **2001**, *78*, 547–550.
- (14.) Jia, Z. *J. Am. Chem. Soc.* **2014**, *136*, 5824–5827.
- (15.) Keddie, D. J.; Moad, G.; Rizzardo, E.; Thang, S. H. *Macromolecules* **2012**, *45*, 5321–5342.
- (16.) Moad, G.; Chong, Y. K.; Postma, A.; Rizzardo, E.; Thang, S. H. *Polymer* **2005**, *46*, 8458–8468.
- (17.) Mayadunne, R. T. a; Rizzardo, E.; Chiefari, J.; Chong, Y. K.; Moad, G.; Thang, S. H. *Macromolecules* **1999**, *32*, 6977–6980.



## **Chapter 5**

### **5.1 Introduction**

Linear Polymers with a polyacetal structure were first prepared by Staudinger in 1932 when he prepared poly(formaldehyde).<sup>1</sup> That same year Conant and Tongeberg described the preparation of amorphous poly(isoprene) and poly(butyraldehyde) under high pressures of 12 000 atmospheres.<sup>2</sup> Then in 1960, Natta and co-workers were able to prepare polyaldehydes with various side chains via a coordinative mechanism. These reactions were conducted at very low temperatures, -78 °C, at atmospheric pressure, using organometallic catalysts such as  $\text{Al}(\text{C}_2\text{H}_5)_3$ ,  $\text{Al}(\text{C}_2\text{H}_5)_2$  and  $\text{Zn}(\text{C}_4\text{H}_9)_2$ .<sup>1</sup> This process allowed for the preparation of high molecular weight, crystalline polyaldehydes.<sup>1</sup> Then in 1964 Vogl published a series of in-depth articles on the preparation of stereoregular polyaldehydes using anionic and cationic catalysts.<sup>3</sup> His publications inspired many researchers to focus their attention on the polymerization of various aldehydes and the underlying mechanisms and thermodynamics.<sup>5</sup>

Amongst the aliphatic aldehydes prepared by both Natta and Vogl, was *n*-butyraldehyde.<sup>1, 3</sup> However since these publications, the ionic polymerization of *n*-butyraldehyde has received little attention with a single in-depth study focusing on its preparation in various solvents and in bulk with cationic (Trifluoromethanesulfonic acid and Boron trifluoride diethyl etherate) and anionic (Potassium *tert*-butoxide) initiators, published in 1997 by Mohammed and co-workers.<sup>4</sup> The authors concluded that for the anionic polymerization of *n*-butyraldehyde, the best results would be obtained for polymerizations run at temperature below -50 °C and in the presence of metal alkoxide catalysts.<sup>4</sup> They also observed that initiation in polar solvents such as THF led to the appearance of side reactions, which they believed to be the formation of aldol derivatives, but that this could be avoided by using non-polar solvents such as pentane instead.<sup>4</sup>

As is the case with poly(phthaldialdehyde), poly(butyraldehyde) can also be classified as a SIP.<sup>12</sup> As a polyaldehyde it can be distinguished by a low ceiling temperature of ~ -40 °C, above which it will rapidly depolymerize.<sup>5</sup> In addition, it is susceptible to acid-catalyzed cleavage of its backbone.<sup>5</sup> In an attempt to expand the range of self-immolative polymers that can be readily synthesized by controlled chain growth processes, we investigated the non-organometallic catalyst based anionic polymerization of *n*-butyraldehyde using phosphazene

## Chapter 5

---

and amine base catalysts. This method is, to our knowledge, a novel approach for the preparation of PBA.

## 5.2 Experimental

### 5.2.1 Materials

Acetic anhydride (99 %), *n*-butyraldehyde (99 %), 1, 8-diazabicyclo [5.4.0] undec-7-ene (DBU) (98 %), 1, 5, 7-triazabicyclo [4.4.0] dec-5-ene (TBD) (98 %), *tert*-butylimino-tris(dimethylamino)phosphorane, calcium hydride anhydrous (99.5 %), *N'*-*tert*-butyl-*N,N,N',N'',N''*-hexamethylphosphorimidic triamide ( $P_1$ -*t*-Bu) (97 %), 1-*tert*-Butyl-2,2,4,4,4-pentakis(dimethylamino)-2  $\Delta^5$ ,4  $\Delta^5$ -catenadi(phosphazene) ( $P_2$ -*t*-Bu), 2 M in THF, 3-*t*-butylimino-1,1,1,5,5,5-hexakis(dimethylamino)-3-  
 {[tris(dimethylamino)phosphoranylidene]amino}-1  $\Delta^5$ ,3  $\Delta^5$ ,5  $\Delta^5$ -1,4-triphosphazadiene ( $P_4$ -*t*-Bu), 0.8 M in hexane (all Sigma-Aldrich) were used as received. Benzyl alcohol, DCM, DEE, THF and toluene were purified and stored as described in Chapter 3.

### 5.2.2 Methods

Refer to Section 3.2.2

### 5.2.3 Polymer Synthesis

#### 5.2.3.1 General polymerization procedure

All polymerizations were run at -75 °C, in pentane for ten minutes before quenching by the addition of acetic anhydride, unless specified otherwise.

##### 5.2.3.1.1 Anionic polymerization: Phosphazene base catalysts

Refer to procedure as described in Section 3.2.3.1.1

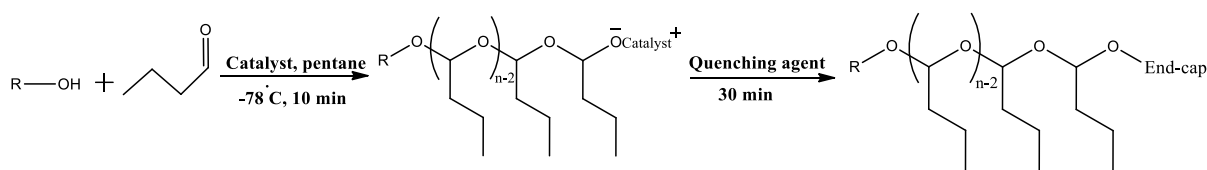
##### 5.2.3.1.2 Anionic polymerization: Amine base catalysts

Refer to procedure as described in Section 3.2.3.1.2

## Chapter 5

### 5.3 Results and discussion

Previous studies have shown the polymerization of *n*-butyraldehyde via high pressure, plasma or ionic polymerization.<sup>1</sup> Of these techniques, ionic polymerization in the presence of an organometallic catalyst is the preferred method as it allows for the simplest experimental conditions and produces well-defined polymers.<sup>3</sup> To our knowledge, the use of metal-free catalysts in the anionic polymerization of PBA (Scheme 5.1) has not yet been investigated. Following the optimization of the metal free organocatalyzed anionic polymerization of *o*-phthaldialdehyde, a similar study was applied to *n*-butyraldehyde.



Scheme 5.1. The anionic polymerization of *n*-butyraldehyde.

#### 5.3.1 Systematic study of the influence of experimental parameters

##### 5.3.1.1 Effect of the catalyst type

Following the successful application of phosphazene and amine base catalysts in the polymerization of PA, it was decided to investigate the use of these non-organometallic catalysts in the preparation of PBA. It was found however, that only the two most reactive catalysts, P<sub>2</sub>-*t*-Bu and P<sub>4</sub>-*t*-Bu, were able to catalyze the polymerization of BA. The failure of P<sub>1</sub>-*t*-Bu, TBD and DBU to do so is believed to be the result of insufficient basicity. One can therefore conclude that the anionic polymerization of BA requires a more reactive base catalyst than that of PA. This is presumably due to the aromatic stability of PA.

Table 5.1 is a summary of the results obtained for the P<sub>2</sub>-*t*-Bu and P<sub>4</sub>-*t*-Bu catalyzed polymerization of BA with varying catalyst:initiator. The polymerization reactions that were catalyzed by P<sub>4</sub>-*t*-Bu proceeded with poor control, resulting in broad *D*. As was the case with the P<sub>4</sub>-*t*-Bu catalyzed anionic polymerization of PA, a decrease in the catalyst:initiator resulted in an improved agreement between the  $M_n^{\text{Theoretical}}$  and  $M_n^{\text{SEC}}$ . A decrease in the amount of the P<sub>2</sub>-*t*-Bu catalyst relative to that of the initiator was found to also improve the agreement between the  $M_n^{\text{Theoretical}}$  and  $M_n^{\text{SEC}}$ , with a catalyst:initiator of 1:1 resulting in the best control.

## Chapter 5

**Table 5.1. Results for the anionic polymerization of BA with P<sub>2</sub>-*t*-Bu and P<sub>4</sub>-*t*-Bu phosphazene base catalysts with different catalyst:initiator.**

Catalyst	[Cat]:[Init]	$M_n^{\text{Theoretical}}$ (g/mol)	$M_n^{\text{SEC}}$ (g/mol)	$\bar{D}$	Yield (%)
P <sub>2</sub> - <i>t</i> -Bu	1:1	9 000	7 300	1.2	90
	2:1	8 800	6 500	1.6	88
	4:1	8 500	4 500	2.0	85
P <sub>4</sub> - <i>t</i> -Bu	1:1	8 600	5 900	1.8	86
	2:1	8 400	4 300	2.1	84

All reactions were run in pentane, with a [monomer] of 1.0 M for 10 min before quenching with acetic anhydride.  
 $M_n^{\text{Target}} = 10\,000 \text{ g/mol}$

Figure 5.1 and Figure 5.2 shows an overlay of the SEC traces for the P<sub>4</sub>-*t*-Bu and P<sub>2</sub>-*t*-Bu catalyzed polymerization of BA with different catalyst: initiator. The traces for the P<sub>4</sub>-*t*-Bu catalyzed polymerization reactions (Figure 5.1) show the appearance of a shoulder peak on the lower elution time/high molecular weight side of the spectrum, indicative of the appearance of side reactions. The traces for the polymerization reactions catalyzed by P<sub>2</sub>-*t*-Bu with a catalyst:initiator of 4:1 and 2:1 also show the appearance of a shoulder peak. No such peaks are present on the SEC trace for the polymerization that was run with an equimolar amount of the less reactive catalyst and initiator. These results supports the findings of Zhao *et al.* from which he concluded that the appearance of side reactions can be suppressed by using a lower catalyst to initiator ratios.<sup>7-9</sup> The results also suggests that P<sub>2</sub>-*t*-Bu, with an equimolar amount of the catalyst and initiator, is the ideal catalytic system for the anionic polymerization of PBA. Figure 5.3 shows the assigned <sup>1</sup>H NMR spectrum of PBA prepared under these conditions.

## Chapter 5

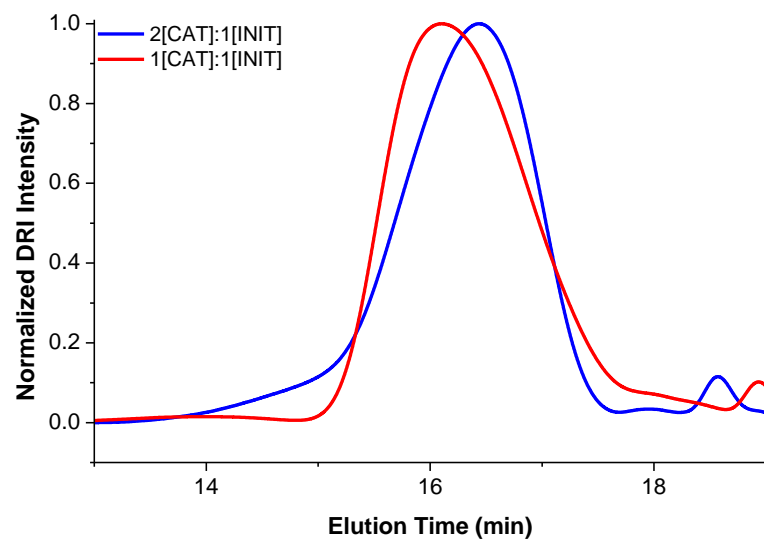


Figure 5.1. An overlay of the SEC traces of PBA prepared with  $P_4$ -*t*-Bu with different catalyst:initiator.

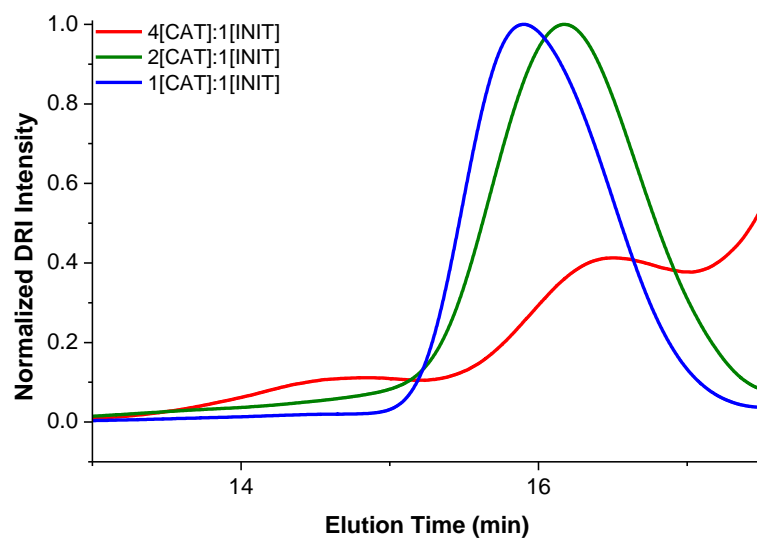
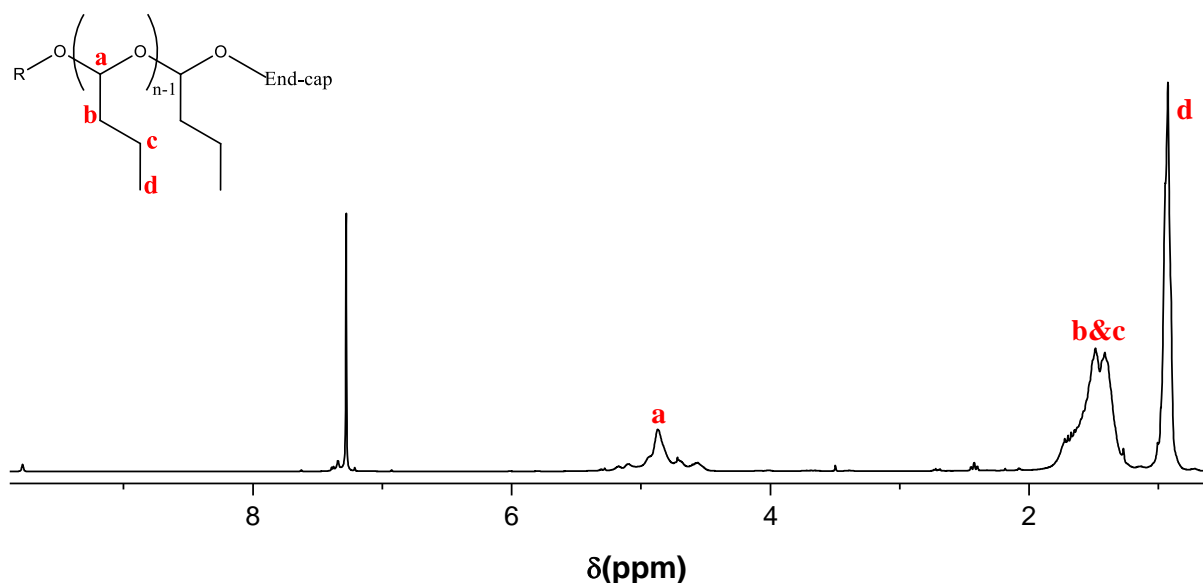


Figure 5.2. An overlay of the SEC traces of PBA prepared with  $P_2$ -*t*-Bu with different catalyst:initiator.

## Chapter 5



**Figure 5.3.** <sup>1</sup>H NMR spectrum (CDCl<sub>3</sub>) of PBA prepared with P<sub>2</sub>-*t*-Bu as catalyst, a with catalyst:initiator of 1:1, monomer concentration of 1.0 M, pentane as solvent and reaction time of ten minutes.

### 5.3.1.2 Monomer concentration

Table 5.2 is a summary of the results obtained for the anionic polymerization of BA with different monomer concentrations. As was the case with PPA, an increase in the monomer concentration had no effect on the yield but did lead to an improved agreement between the  $M_n^{\text{Theoretical}}$  and  $M_n^{\text{SEC}}$ . An overlay of the SEC traces for the P<sub>2</sub>-*t*-Bu catalyzed polymerization reactions run with monomer concentrations of 0.5 M and 1.0 M (Figure 5.4) shows a definite shift to a lower elution time, signifying an increase in molecular weight, with an increase in the monomer concentration.

**Table 5.2.** Results for the P<sub>2</sub>-*t*-Bu catalyzed anionic polymerization of PA with different monomer concentrations.

Catalyst	[Monomer] (M)	$M_n^{\text{Theoretical}}$ (g/mol)	$M_n^{\text{SEC}}$ (g/mol)	$\bar{D}$	Yield (%)
P <sub>2</sub> - <i>t</i> -Bu	0.5	8 600	4 200	1.2	86
	1.0	9 200	7 800	1.3	92

All reactions were run with a catalyst:initiator of 1:1, in pentane for 10 min before quenching with acetic anhydride.

$M_n^{\text{Target}} = 10\,000 \text{ g/mol}$

## Chapter 5

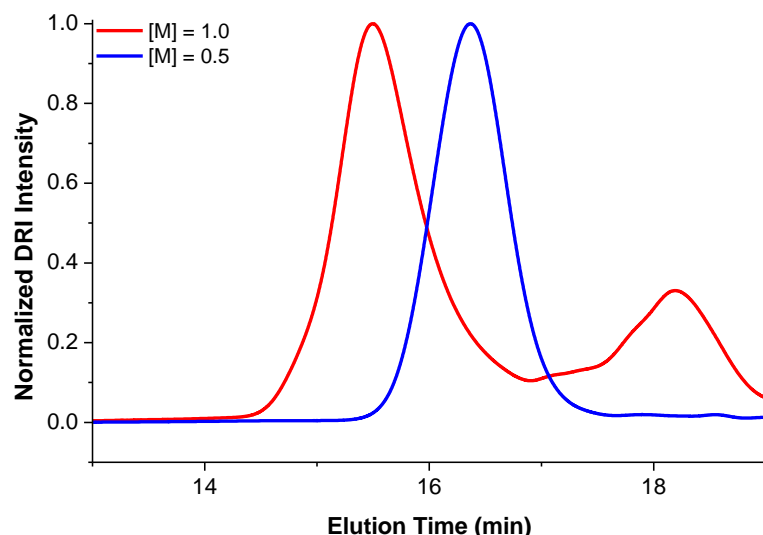


Figure 5.4. An overlay of the SEC traces for the P<sub>2</sub>-*t*-Bu catalyzed anionic polymerization of BA with different monomer concentrations.

### 5.3.1.3 Reaction Time

The anionic polymerization of BA was allowed to run for different periods of time to determine the optimum reaction time and investigate the effect of time on the polymerization. Table 5.3 is a summary of the results obtained for each reaction time.

Table 5.3. Results for the kinetic study of the P<sub>2</sub>-*t*-Bu catalyzed anionic polymerization of BA.

Catalyst	Time (min)	$M_n^{\text{Theoretical}}$ (g/mol)	$M_n^{\text{SEC}}$ (g/mol)	$\bar{D}$	Yield (%)
P <sub>2</sub> - <i>t</i> -Bu	10	8 900	7 200	1.2	89
	20	8 600	7 000	1.2	86
	30	8 300	6 900	1.2	83

All reactions were run in pentane with a catalyst:initiator of 1:1 and a [monomer] of 1.0 M. Acetic anhydride was used as quenching agent.

$M_n^{\text{Target}} = 10\,000\text{ g/mol}$

The experimental data showed that the polymerization of BA was very fast and essentially complete after just ten minutes. An increase in the reaction time did not appear to have any effect on the  $\bar{D}$  values. This is in contrast to what was found with the polymerization of PA where an increase in the reaction time resulted in higher  $\bar{D}$  values. Figure 5.5 shows an overlay of the SEC traces for each reaction time. The absence of any shoulder peaks suggests that the P<sub>2</sub>-*t*-Bu catalyzed polymerization of BA, with a catalyst:initiator of 1:1, proceeded without the appearance of any side reactions, regardless of the reaction time.

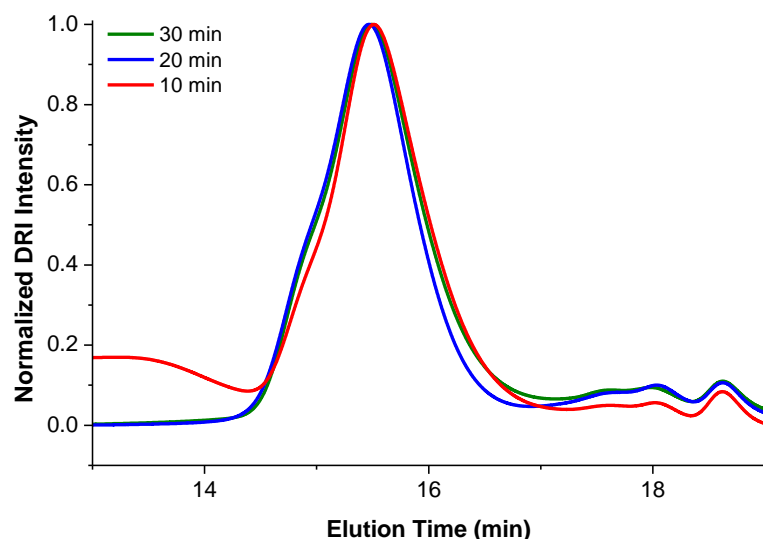


Figure 5.5. An overlay of the SEC traces for the kinetic study of BA.

#### 5.3.1.4 Solvent

*n*-Butyraldehyde was found to be soluble in a range of solvents that vary in polarity. This allowed for an investigation of its polymerizability, via metal-free organocatalysis, in a range of solvents. Table 5.4 shows a summary of the results obtained for the polymerization of *n*-butyraldehyde in a range of solvents that vary in polarity. The results show a clear trend in that the yield and the agreement between  $M_n^{\text{SEC}}$  and  $M_n^{\text{Theoretical}}$  becomes poorer as the dielectric constant of the solvent increases, with no polymer obtained in DCM. Mita *et al.* and Takida and co-workers reported similar results in their studies focusing on the ionic polymerization of aliphatic aldehydes.<sup>10, 13</sup> Both attempted to explain their findings by constructing enthalpy diagrams for a number of aldehydes, including *iso*-butyraldehyde, in THF, DEE and heptane, using an isothermally operated DSC.<sup>10, 13</sup> From the data that they recorded, they were able to determine the partial molar heat of mixing ( $H_m^{\text{mix}}$ ) for each system.<sup>10, 13</sup> The results reported by Mita *et al.* for *iso*-butyraldehyde is shown in Table 5.5 and indicates that the  $H_m^{\text{mix}}$  increases in the order of THF < DEE < *n*-heptane.<sup>10</sup>



## Chapter 5

**Table 5.4. Results for the P<sub>2</sub>-*t*-Bu catalyzed anionic polymerization of BA in various solvents.**

Solvent	$\epsilon$	$M_n^{\text{Theoretical}}$ (g/mol)	$M_n^{\text{SEC}}$ (g/mol)	$D$	Yield (%)
Pentane	1.8	8 500	7 700	1.2	85
Toluene	2.4	5 000	5 000	1.3	50
DEE	4.3	3 800	2 400	1.2	38
THF	7.6	2 800	2 000	1.2	28
DCM	8.9	No polymer			

All reactions were run in the presence of P<sub>2</sub>-*t*-Bu, with a catalyst:initiator of 1:1 and a [monomer] of 1.0 M for 10 minutes before quenching with acetic anhydride.

$M_n^{\text{Target}} = 10\,000$  g/mol

**Table 5.5. Partial molar heats of mixing for *iso*-butyraldehyde in various solvents as determined by Mita *et al.*<sup>10</sup>**

Solvent	$H_m^{\text{mix}}$
THF	-0.1
DEE	0.1
<i>n</i> -heptane	1.2

The favourable polymerization of BA in pentane can therefore be explained by the stability of the monomer in more polar solvents such as THF and DEE compared to hydrocarbon solvents such as pentane and toluene.<sup>4, 10</sup> In other words, in pentane, the solvents solvates the polymer better than the monomer and thus helps to push the equilibrium towards the polymer product.

### 5.3.1.5 Molecular Weight

The optimum conditions for the non-organometallic anionic polymerization of BA, determined in this work, were applied to the preparation of a series of PBA polymers with different  $M_n^{\text{Target}}$ . Table 5.6 shows the results that were obtained.

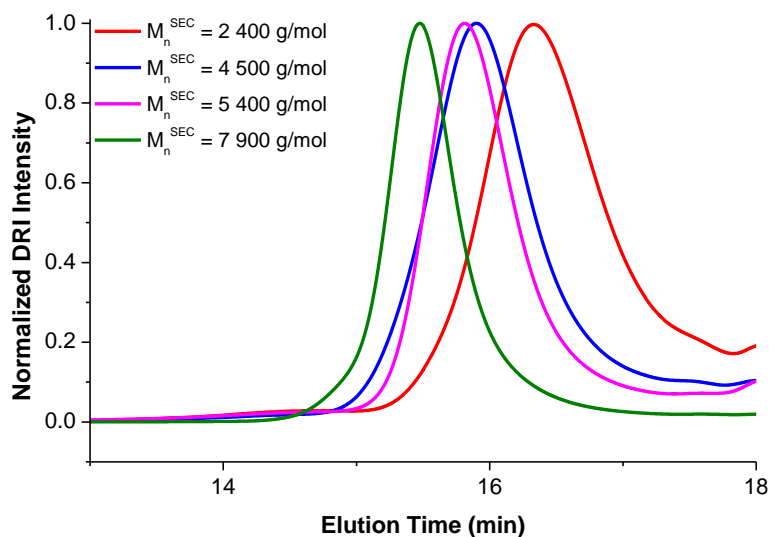
## Chapter 5

**Table 5.6. Summary of the results obtained for the preparation of PBA with different  $M_n^{\text{Target}}$ .**

$M_n^{\text{Target}}$ (g/mol)	$M_n^{\text{Theoretical}}$ (g/mol)	$M_n^{\text{SEC}}$ (g/mol)	$\bar{D}$	Yield (%)
2 500	2 400	2 400	1.2	96
5 000	4 600	4 500	1.2	92
7 500	6 100	5 400	1.3	82
10 000	9000	7 900	1.1	86

Reactions were run in the presence of  $P_2$ -*t*-Bu, with a catalyst:initiator of 1:1 with [monomer] of 1.0 M and in pentane for 10 minutes before quenching with acetic anhydride.

Figure 5.6 shows an overlay of the SEC traces of the polymers prepared for the molecular weight study. The  $M_n^{\text{SEC}}$  clearly increases with increasing  $M_n^{\text{Target}}$ . Figure 5.7 shows a comparison between the  $M_n^{\text{Theoretical}}$  and  $M_n^{\text{SEC}}$ . The figure shows that a linear relationship can be drawn between the two. The results of this study therefore confirms that the optimized  $P_2$ -*t*-Bu catalyzed system allows for the preparation of PBA with narrow  $\bar{D}$  and a good agreement between the  $M_n^{\text{Theoretical}}$  and  $M_n^{\text{SEC}}$ .

**Figure 5.6. An overlay of the SEC traces for PBA polymers prepared with different  $M_n^{\text{Target}}$ .**

## Chapter 5

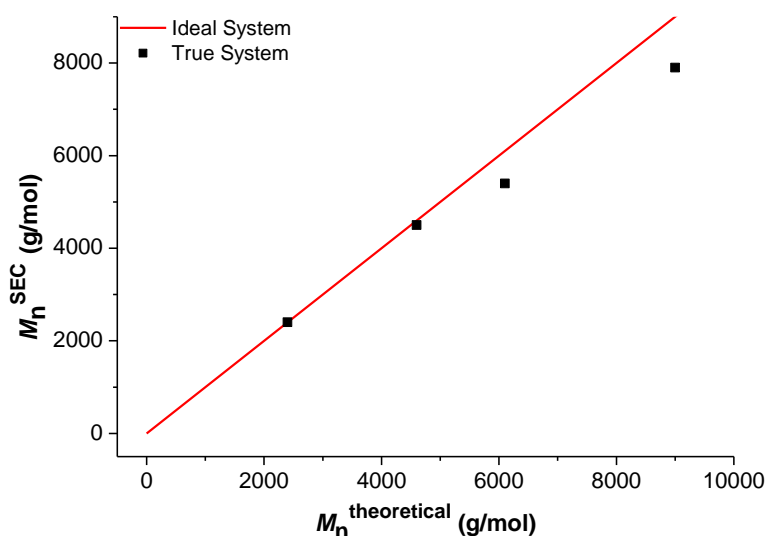


**Figure 5.7.** Graph showing the relationship between the theoretical molecular weight and that determined by SEC. The solid red line acts as a representation of an ideal system with a 100% conversion.

### 5.3.2 Investigation of polymer microstructure:

We further assessed the microstructure of PBA prepared under the optimized conditions determined in this work. The application of  $^{13}\text{C}$  NMR to study configurational sequences in polymers is well-established. The unique sensitivity of the technique means that carbons in slightly different configurational environments will result in signals with slightly different chemical shifts.<sup>11</sup>

To avoid the need for defining the absolute arrangement of each chiral centre, a simpler method is commonly used. This system is based on the relative configuration of two adjacent monomer units or dyads. If the pendant groups are in the same position, the dyad is referred to as a meso dyad (*m*). If the pendant groups are in opposite directions, the dyad is referred to as racemic (*r*). Sequences of three monomer units or triads are represented as *mm*, *mr/ rm* and *rr*, more commonly referred to isotactic, syndiotactic or atactic respectively. Figure 5.8 is an illustration of these conformational sequences. In an isotactic polymer, all pendant groups are on the same side of the polymer chain. For a syndiotactic polymer, the pendant groups are on alternating sides. When a polymer is atactic, the pendant groups are arranged randomly along the polymer chain. These configurational sequences give rise to distinguishable magnetic environments for the nuclei in the monomer units resulting in different NMR absorption frequencies.<sup>11</sup>

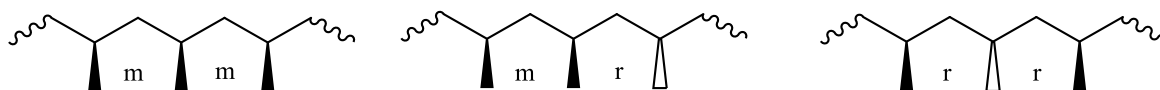


**Figure 5.8.** Triad configurational sequences of a polymer backbone.

## Chapter 5

---

Tacticity is a distributive property of a polymer. This implies that within any given polymer, configurational multiplicity will be observed. It is for this reason that tacticity is generally discussed in terms of percentage iso-, syndio- and atacticity.  $^{13}\text{C}$  spectroscopy can be used to distinguish these different configurational sequences within a polymer. A carbon in a given polymer chain will experience a different degree of shielding depending on the specific tacticity sequence. In general, the tacticity sequence that allows for a carbon to experience the highest degree of shielding will be represented by a signal that appears more upfield than the signal representing the sequence that leaves the carbon less shielded.<sup>11</sup>

Figure 5.9 shows the  $^{13}\text{C}$  spectrum of PBA prepared under the optimum conditions determined in this work. Figure 5.10 shows a closer look at the chemical shift region, 97-98 ppm, which shows the signal that represents the tertiary carbon (carbon a, Figure 5.9). The isotactic sequence of PBA leaves the tertiary carbon less shielded than the syndiotactic sequence. It can therefore be assumed that the isotactic signal will appear more downfield relative to the syndiotactic signal. Figure 5.10 shows that the main signal representing the tertiary carbon appears more downfield than the other adjacent peaks. This suggests that the  $\text{P}_2$ -*t*-Bu catalyzed anionic polymerization of BA results in high isotactic fractions.

## Chapter 5

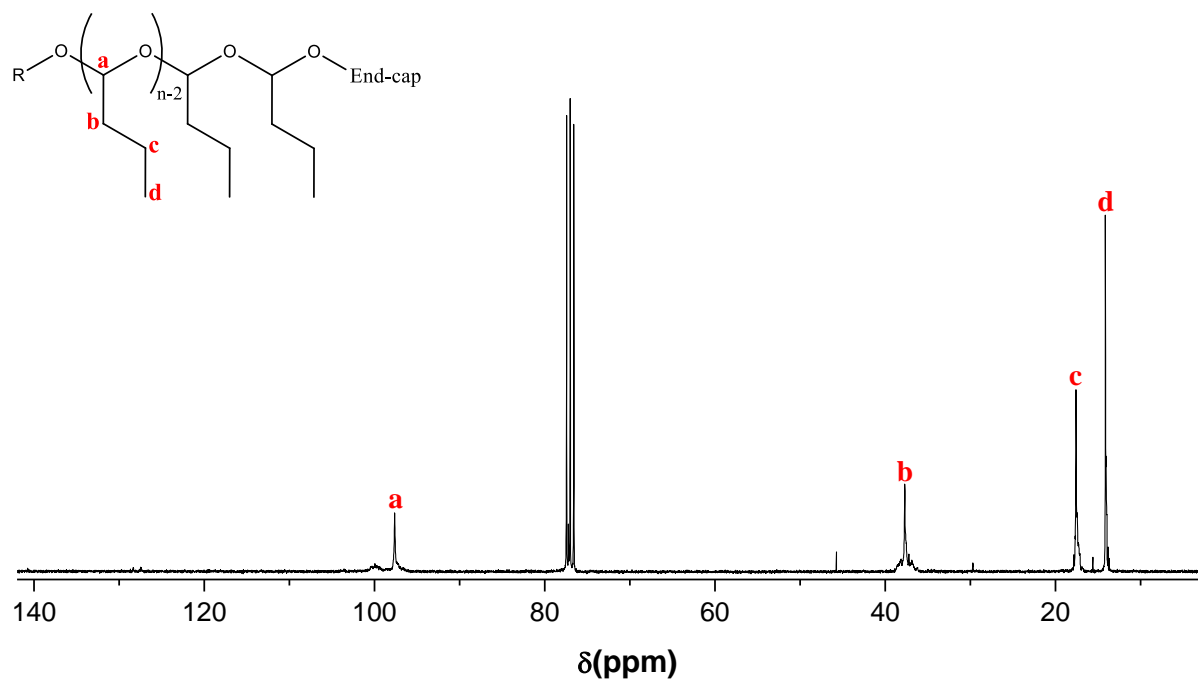


Figure 5.9.  $^{13}\text{C}$  NMR spectrum (CDCl<sub>3</sub>) of entry 1 in Table 5.4.

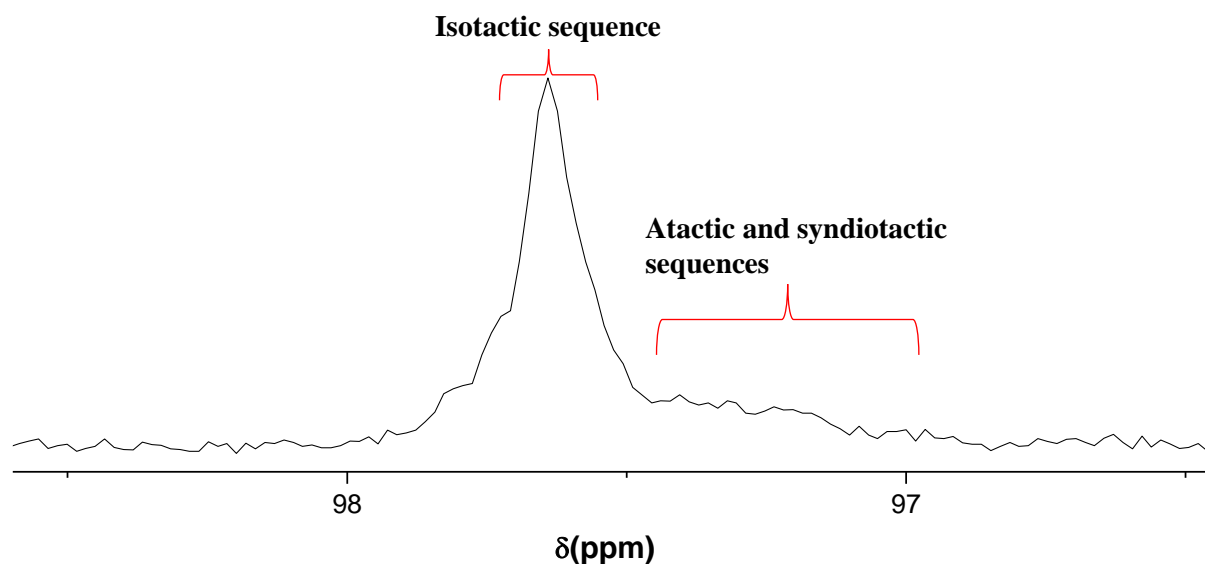


Figure 5.10.  $^1\text{H}$  NMR spectrum (CDCl<sub>3</sub>) focusing on the chemical shift region 69-96 ppm of Figure 5.10.

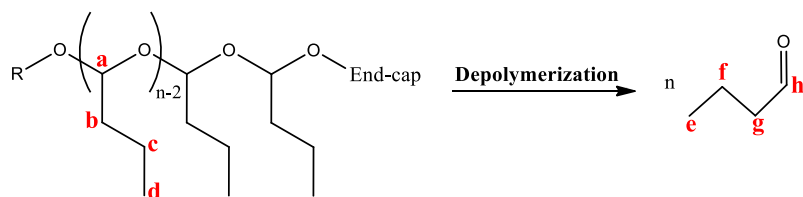
## Chapter 5

### 5.3.3 The self-immolative nature of PBA.

To demonstrate the degradability/self-immolative nature of PBA,  $^1\text{H}$  NMR spectra of the same sample left undisturbed in a deuterated solvent, was taken over a two month period.

Scheme 5.2 shows the depolymerization of PBA into its monomeric units. Figure 5.11 shows  $^1\text{H}$  NMR spectra of PBA that was taken from the same sample over a two month period. Figure 5.11a shows the  $^1\text{H}$  NMR spectrum of the sample taken shortly after the polymerization. No monomer peaks are present, indicating that no depolymerization had occurred. However, peaks representing both the monomer and polymer are clearly visible on the spectrum of the same sample taken one month later (Figure 5.11b), indicating that some degradation had occurred.

After two months the sample had undergone complete depolymerization, as indicated by the fact that only monomer peaks are present on the spectrum taken two months after the polymerization reaction (Figure 5.11c). This study affirms the self-immolative nature of PBA as it is able to degrade even when left undisturbed over a prolonged period of time.



**Scheme 5.2. Depolymerization of PBA into its monomeric units.**

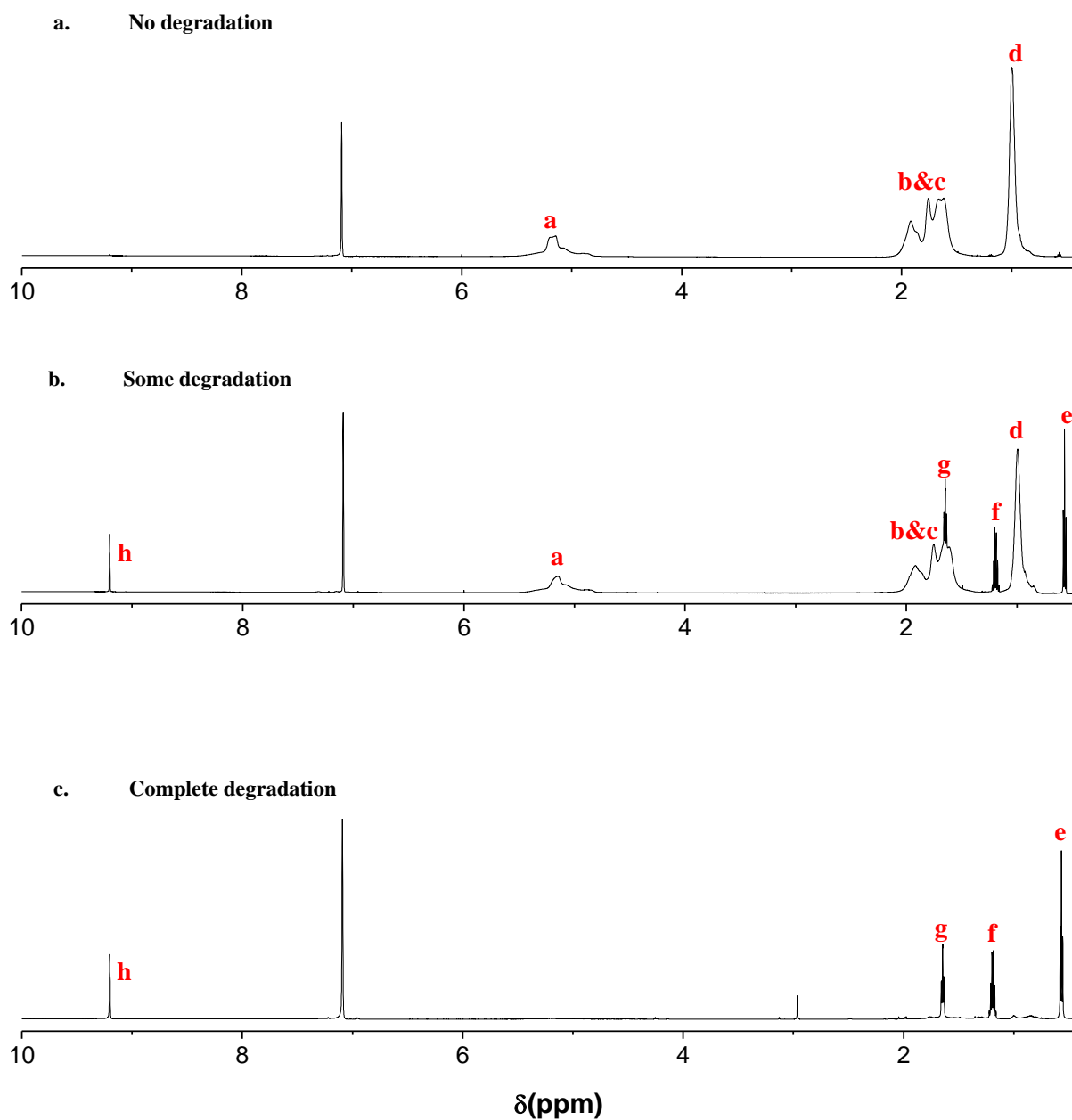
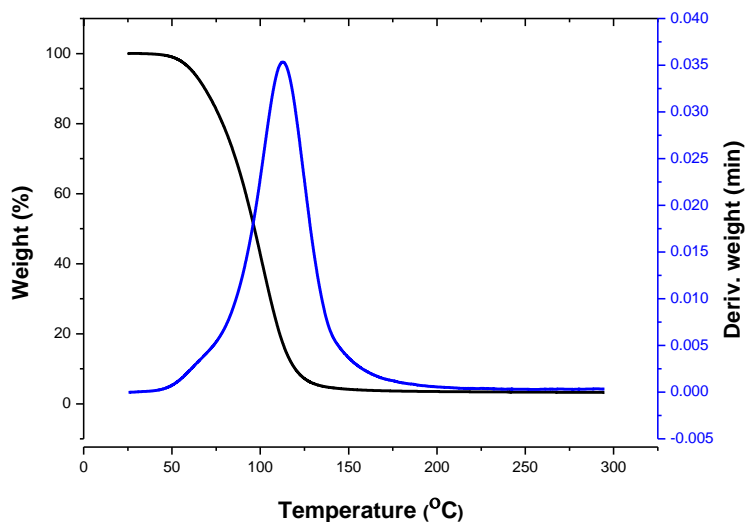
**Chapter 5**

Figure 5.11. An overlay of the  $^1\text{H}$  NMR spectra (CDCl<sub>3</sub>) of PBA, prepared under the optimum conditions determined in this work, taken over a two month period: (a) no degradation, (b) some degradation after one month, (c) complete degradation after two months.

**5.3.4 Thermal analysis**

The thermal stability of PBA, prepared under the optimum conditions determined in this work, was investigated by TGA. Figure 5.12 shows the TGA results for PBA. The derivative of the thermogravimetric curve shows that the degradation of PBA occurs in a single well-defined step in the temperature range of 50-125 °C.

## Chapter 5



**Figure 5.12.** TGA thermogram of PBA prepared with  $P_2$ -*t*-Bu as catalyst, a with catalyst:initiator of 1:1, monomer concentration of 1.0 M, pentane as solvent and reaction time of ten minutes.

### 5.4 Conclusions

A method for the non-organometallic catalyst based anionic polymerization of BA was introduced. The method was optimized by carrying out a systematic study, investigating the effect of the catalyst type, catalyst to initiator ratio, monomer concentration, solvent polarity and reaction time on the polymerization reaction. The amine base catalysts, DBU and TBD, as well as the least reactive phosphazene base catalyst,  $P_1$ -*t*-Bu, was unable to catalyze the polymerization reaction due to insufficient basicity. Both  $P_2$ -*t*-Bu and  $P_4$ -*t*-Bu was able to catalyze the reaction. Of these two catalysts,  $P_2$ -*t*-Bu allowed for the best control when used in equimolar amounts to the initiator. A monomer concentration of 1.0 M resulted in the best agreement between the  $M_n^{\text{Theoretical}}$  and  $M_n^{\text{SEC}}$  whilst still allowing for adequate control. As was the case with PPA, anionic polymerization of BA was very fast and appeared complete within 10 minutes. Finally, the polymerization of BA was found to be most favourable in the non-polar solvent pentane. The preparation of a series of PBA polymers with different  $M_n^{\text{Target}}$ , confirmed that the optimized method allowed for the preparation of PBA with narrow  $\bar{D}$  and a good agreement between the  $M_n^{\text{Theoretical}}$  and  $M_n^{\text{SEC}}$ .

The microstructure, degradability and thermal properties of PBA, prepared under the optimum conditions determined in this work, was investigated by NMR. Analysis of the polymer by  $^{13}\text{C}$  NMR showed that the polymer was predominantly isotactic.  $^1\text{H}$  NMR spectra taken of the same PBA sample over two months showed its complete degradation within this period, thereby



**Chapter 5**

---

confirming the ready degradability of the PBA. TGA of PBA showed that the polymer degraded in a single well-defined step within the temperature range of 50-125 °C.

**References**

- (1.) Natta, G.; Mazzanti, G.; Corradini, P.; Bassi, W. *Macromol. Chem.* **1960**, 37, 156–159.
- (2.) Conant, J.B.; Tongberg, C.O. *J. Am. Chem. Soc.* **1930**, 52, 1659–1669.
- (3.) Vogl, O. *J. Polym. Sci. A Polym. Chem.* **1964**, 2, 4607–4620.
- (4.) Mohammed, F.; Moreau, M.; Vairon, J.P. Thermodynamic Study of the Ionic Polymerization of *n*-Butyraldehyde. In *Cationic Polymerization*. **1997**, 50–62.
- (5.) Köstler, S. *Polym. Int.* **2012**, 61, 1221–1227.
- (6.) Ishikawa, T. *Superbases for Organic Synthesis: Guanidines, Amidines, Phosphazenes and Related Organocatalysts*; 2009, 1-326.
- (7.) Zhao, J.; Pahovnik, D.; Gnanou, Y.; Hadjichristidis, N. *Polym. Chem.* **2014**, 5, 3750–3753.
- (8.) Zhao, J.; Hadjichristidis, N.; Gnanou, Y. **2014**, No. 1. Zhao, J.; Pahovnik, D.; Gnanou, Y.; Hadjichristidis, N. *Macromolecules* **2014**, 47, 3814–3822.
- (9.) Schwesinger, R.; Schlemper, H.; Hasenfratz, C.; Willaredt, J.; Dambacher, T.; Breuer, T.; Ottaway, C.; Fletschinger, M.; Boele, J.; Fritz, H.; Putzas, D.; Rotter, H. W.; Bordwell, F. G.; Satish, A. V.; Ji, G.; Peters, E.M.; Peters, K.; von Schnering, H. G.; Walz, L. *Liebigs Ann.* **1996**, 7, 1055–1081.
- (10.) Mita, I.; Imai, I.; Kambe, H. *Macrom. Chem.* **1969**, 169–181.
- (11.) Campbell, D.; Pethrick, R. A.; White, J. R. *Polymer Characterization: Physical Characterization Techniques*, 2nd ed.; CRC Press, 2000.
- (12.) Thompson, S.A. Medical devices composed of low ceiling temperature polymers. U.S. Patent 014121, November 16 1995.
- (13.) Takida, H.; Nora, K. *Kobushi Kagaku.* **1963**, 467-472.

## Chapter 6

### Conclusions and outlook

In Chapter 3, a systematic study to determine the effect of several experimental parameters on the non-organometallic catalyst based anionic polymerization of PA was carried out. From the results of each study, it was concluded that the optimized conditions for the preparation of PPA consisted of DBU as catalyst with a catalyst to initiator ratio of 4:1, a monomer concentration of 1.0 M, THF as solvent and a reaction time of ten minutes. The optimized method was then applied to the preparation of a series of PPA polymers with different  $M_n^{\text{Target}}$ . Analysis of these polymers by SEC, showed that a linear relationship could be drawn between the  $M_n^{\text{Theoretical}}$  and  $M_n^{\text{SEC}}$ , showing that the method allowed for the preparation of PPA with tailored molecular weights. The optimized method for the non-organometallic catalyst based anionic polymerization of PA reported in this work, allows for the preparation of well-defined PPA in a way that is much simpler compared to the methods that have been reported thus far as it does not require such delicate experimental conditions or expensive reagents.

The microstructure and self-immolative nature of PPA, prepared under the optimized conditions determined in this work, was investigated by  $^1\text{H}$  NMR spectroscopy. The polymer was found to consist of a 60 % *cis* and 40 % *trans* mixture of the two stereoisomers, consistent with the theory that the anionic polymerization process favours the formation of the *cis*-stereoisomer.  $^1\text{H}$  NMR spectra taken of the same polymer sample over a two month period, showed that had maintained its degradable nature.

The optimized conditions for the DBU catalyzed anionic polymerization of PA, defined in Chapter 3, was then applied to the preparation of PS-*b*-PPA BCPs in Chapter 4. A hydroxyl end-functional PS macroinitiator was prepared by ARGET ATRP. The bromine chain-end was then replaced with a proton to prevent its interference during the chain extension reaction. Following the successful application of a carboxylic acid initiator for the preparation of PPA in Chapter 3, it was decided to attempt the chain extension of the PA monomer from a PS macroinitiator with a carboxylic chain-end functionality. RAFT-mediated polymerization was applied for the preparation of the carboxylic acid end-functional PS. Analysis of the various PS macroinitiators by SEC and  $^1\text{H}$  NMR showed that both methods had produced polymers with an excellent agreement between the  $M_n^{\text{Theoretical}}$ ,  $M_n^{\text{SEC}}$  and  $M_n^{\text{NMR}}$ , low  $D$  values and high percentages of end-group functionality. It was interesting to note however, that compared to

## Chapter 6

---

the PS prepared by RAFT-mediated polymerization, PS with improved chain-end functionality was obtained when prepared by ARGET ATRP.

Chain extension of the various PS macroinitiators with the PA monomer was then performed using the optimized conditions for the DBU catalyzed anionic polymerization of PA. Analysis of the BCPs prepared using the hydroxyl end-functional PS showed that they had been prepared with an excellent agreement between the  $M_n^{\text{Theoretical}}$  and  $M_n^{\text{SEC}}$  and between the targeted and experimentally obtained mole ratios. The BCPs prepared using the carboxylic acid end-functional PS was found to have degraded during analysis. However, the thermogravimetric yield, observations during the copolymerization reactions and the  $^1\text{H}$  NMR data indicated that chain extension had indeed occurred. In addition, 4,5-dimethoxy-2-nitrobenzyl carbonochloridate was successfully applied as quenching agent, demonstrating that the system is amendable to end-functionalization with end-groups that are desirable for applications that require UV-type triggers to induce degradation of the PPA segment. The method introduced in this work for the chain extension of a macroinitiator with the PA monomer, allows for the preparation of well-defined PPA-containing BCPs by a method that is inexpensive and much less tedious than those that have been reported thus far.

In Chapter 5, a novel method for the non-organometallic anionic polymerization of BA was introduced. The method was then optimized by carrying out a systematic study, similar to that carried out in Chapter 3, to determine the effect of various experimental parameters on the polymerization reaction. It was found that DBU, the amine base catalyst most suited for the polymerization of PA, was of insufficient basicity to catalyze the polymerization of BA. Both  $\text{P}_2\text{-}t\text{-Bu}$  and  $\text{P}_4\text{-}t\text{-Bu}$  phosphazene base catalysts were able to catalyze the reaction, with the less reactive  $\text{P}_2\text{-}t\text{-Bu}$  allowing for the best control when used in an equimolar amount to the initiator. From the results of the studies investigating the effect of the monomer concentration, polarity of the solvent and reaction time it was concluded that the optimum conditions for the  $\text{P}_2\text{-}t\text{-Bu}$  catalyzed anionic polymerization of BA consisted of a monomer concentration of 1.0 M, pentane as the solvent and a reaction time of ten minutes. These optimized conditions were then applied to the preparation of a series of PBA polymers with different  $M_n^{\text{Target}}$ . Comparing the  $M_n^{\text{SEC}}$  and  $M_n^{\text{Theoretical}}$  showed that a linear relationship could be drawn between the two, showing that the method allowed for the preparation of PBA with tailored molecular weights.

The microstructure, self-immolative nature and thermal properties of PBA, prepared under the optimum conditions determined in this work, was also investigated. Analysis of PBA by  $^{13}\text{C}$

## Chapter 6

---

NMR showed that the polymer was predominantly isotactic.  $^1\text{H}$  NMR spectra of the same sample over two months showed that the polymer had completely degraded within this time period, confirming the ready degradability of the polymer. The thermal properties of PBA was investigated by TGA. The thermogram showed that the polymer degraded in a single well-defined step within the temperature range of 50-125 °C.

Future work will entail investigating the appearance of side reactions when using more reactive non-organometallic base catalysts for the preparation of PPA and PBA. It is anticipated that by identifying these side reactions and understanding their mechanism, more knowledge will be gained as to how to prevent them from occurring. MALDI TOF will be applied for this purpose. More research will go into expanding the range of macroinitiators that can be used for the non-organometallic catalyst based polymerization of aldehydes. Finally, future work will focus on advanced applications of these SIP in BCP self-assembly.